

GEUS

Report file no.

22255

GRØNLANDS GEOLOGISKE UNDERSØGELSE
BULLETIN No. 103

THE GEOLOGY AND PETROLOGY OF
THE PRECAMBRIAN ROCKS
TO THE NORTH-EAST OF THE FJORD
QAGSSIT, FREDERIKSHÅB DISTRICT,
SOUTH-WEST GREENLAND

BY

GIORGIO RIVALENTI AND ANTONIO ROSSI

WITH 24 FIGURES AND 16 TABLES IN THE TEXT,
AND 11 PLATES

KØBENHAVN

1972

GRØNLANDS GEOLOGISKE UNDERSØGELSE

The Geological Survey of Greenland

Østervoldgade 10, DK-1350 Copenhagen K

Denmark

BULLETINS

(published in association with the series *Meddelelser om Grønland*)

- No. 93 Danian foraminifera from Nûgssuaq, West Greenland. 1970 by Hans Jørgen Hansen (*Meddr Grønland* 193, 2).
- No. 94 Paleocene Ostracoda from Nûgssuaq, West Greenland. 1971 by Janina Szczechura (*Meddr Grønland* 193, 1).
- No. 95 Contributions to the mineralogy of Ilimaussaq nos 20–21. I. On the mineralogy and paragenesis of tugtupite $\text{Na}_8\text{Al}_2\text{Be}_2\text{Si}_8\text{O}_{24}(\text{Cl},\text{S})_2$ from the Ilimaussaq alkaline intrusion, South Greenland. 1971 by H. Sørensen, M. Danø and O. V. Petersen (*Meddr Grønland* 181, 13). II. The colour and luminescence of tugtupite (beryllosodalite) from Ilimaussaq, South Greenland. 1971 by A. S. Povarennykh, A. N. Platonov, A. N. Tarashchan and V. P. Belichenko (*Meddr Grønland* 181, 14).
- No. 96 The Precambrian, Eocambrian and early Palaeozoic stratigraphy of the Jørgen Brønlund Fjord area, Peary Land, North Greenland. 1971 by Hans F. Jepsen (*Meddr Grønland* 192, 2).
- No. 97 Kaledonische Metamorphose der präekambrischen Charcot Land Serie, Scoresby Sund, Ost-Grønland. 1971 by Albrecht Steck (*Meddr Grønland* 192, 3).
- No. 98 Fossil Picrodendroid fruit from the Upper Danian of Nûgssuaq, West Greenland. 1972 by B. Eske Koch (*Meddr Grønland* 193, 3).
- No. 99 Coryphoid palm fruits and seeds from the Danian of Nûgssuaq, West Greenland. 1972 by B. Eske Koch (*Meddr Grønland* 193, 4).
- No. 100 Scleractinian corals from the Upper Cretaceous and Lower Tertiary of Nûgssuaq, West Greenland. 1972 by Søren Floris. (*Meddr Grønland* 196, 1).
- No. 101 Precambrian organic compounds from the Ketilidian of South-West Greenland. Part IV. 1972 by Jørgen Lam and K. Raunsgaard Pedersen. (*Meddr Grønland* 185, 8).
- No. 102. The Røde Ø Conglomerate of inner Scoresby Sund and the Carboniferous (?) and Permian rocks west of the Schuchert Flod. A general sedimentological account. 1972 by J. D. Collinson. (*Meddr Grønland* 192, 6).
- No. 103. The geology and petrology of the Precambrian rocks to the north-east of the fjord Qagssit, Frederikshåb District, South-West Greenland. 1972 by Giorgio Rivalenti and Antonio Rossi. (*Meddr Grønland* 192, 5).

Bulletins of the Geological Survey of Greenland are available on exchange or may be purchased from the Survey. Copies may be purchased as parts of Meddelelser om Grønland from C. A. Reitzels Forlag, Nørre Søgade 35, DK-1370 Copenhagen K, Denmark.

Printed in Denmark.

Bianco Lunos Bogtrykkeri A/S

GRØNLANDS GEOLOGISKE UNDERSØGELSE
BULLETIN No. 103

THE GEOLOGY AND PETROLOGY OF
THE PRECAMBRIAN ROCKS
TO THE NORTH-EAST OF THE FJORD
QAGSSIT, FREDERIKSHÅB DISTRICT,
SOUTH-WEST GREENLAND

BY

GIORGIO RIVALENTI AND ANTONIO ROSSI

WITH 24 FIGURES AND 16 TABLES IN THE TEXT,
AND 11 PLATES

KØBENHAVN

1972

Abstract

The area consists of migmatitic gneisses (with related pegmatites) containing small inclusions and larger concordant layers of unmigmatized rocks (mainly represented by amphibolites, metasediments and ultramafics), and a few discordant amphibolite dykes. The petrography of the various lithotypes is described and their petrogenesis discussed. The following metamorphic history is proposed: 1) an increase in metamorphic grade to the biotite–almandine–cordierite subfacies of the low hornblende–granulite facies, shown only by a few relic assemblages, followed by 2) retrogression to within the almandine–amphibolite facies. Migmatization (quartz dioritization or granodioritization) started in the low hornblende–granulite facies and reached its maximum in the upper almandine–amphibolite facies. A general microcline blastesis and formation of microcline-rich mobilisates is ascribed to the medium to low almandine–amphibolite facies. Further retrogression to epidote–amphibolite or greenschist facies is only local and weak.

Several generations of post-orogenic basic dykes intersect the gneisses.

Structurally, five phases of ductile deformation and three phases of brittle deformation are distinguished, and the relationship between deformation and metamorphism tentatively established.

The metamorphic and structural events are mostly pre-Ketilidian.

CONTENTS

	Page
Introduction	7
The migmatitic gneisses and pegmatites	9
Introduction	9
The Gneisses	9
Description	9
Veined gneiss	9
Banded gneiss	11
Homogeneous gneiss	12
Agmatitic gneiss	13
Petrography	14
Veined gneiss	14
Biotite gneiss	14
Hornblende gneiss	17
Garnetiferous gneiss	18
Banded gneiss	18
Homogeneous gneiss	19
Chemistry	19
The Pegmatites	23
Occurrence	23
Texture, mineralogy and relation to the host rock	23
Quartz pegmatites	24
Quartz-plagioclase (\pm microcline) pegmatites	24
Composition related to timing	27
Layers and inclusions in the gneisses	29
Introduction	29
Layers in the Gneisses	29
Amphibolites	29
Description	29
Petrography	30
Chemistry	37
Ultramafic rocks	37
Description	37
Petrography	38
Nucleus	38
Light-green zone	40
Amphibole-chlorite assemblage	40
Talc-chlorite assemblage	40

	Page
Anthophyllite zone	40
Hornblendite zone	42
Chemistry	42
Rusty schist	45
Description	45
Petrography	45
Biotite-garnet-sillimanite assemblage	49
Anthophyllite assemblage	50
Chemistry	51
Microgranodiorite	51
Description	51
Petrography	52
Chemistry	52
Inclusions in the Gneisses	53
Amphibolites	53
Description	53
Petrography	53
Chemistry	55
Ultramafic inclusions	55
Description and petrography	55
Calc-silicate inclusions	57
Description and petrography	57
Discordant amphibolite dykes	58
Description	58
Petrography	58
Chemistry	58
Petrogenesis	60
The Concordant Layers	60
Origin of the rocks	60
Metamorphic facies and petrogenesis	61
Inclusions in the Gneisses	67
Metamorphic facies and petrogenesis	67
Discordant Amphibolites	68
Migmatitic Gneisses and Pegmatites	68
Metamorphic facies	68
Petrogenesis	69
Conclusions	71
Post-orogenic basic dykes	73
Introduction	73
Description and petrography	73
MD ₂ dykes	73
MD ₃ dykes	74
TD dykes	75
Lamprophyres	75
Structure	77
Introduction	77
Ductile Structures	77

V	Precambrian geology north-east of Qagssit	5
		Page
	Mesosopic scale	77
	Mesosopic interference pattern	82
	Macroscopic scale	84
	Western field	84
	Eastern field	85
	Brittle Deformations	88
	Conclusions	89
	Relationships between metamorphism, petrogenesis and structure	90
	Acknowledgements	93
	Appendix	94
	Analytical methods of chemical and mineral analyses	94
	Sample localities	94
	References	95

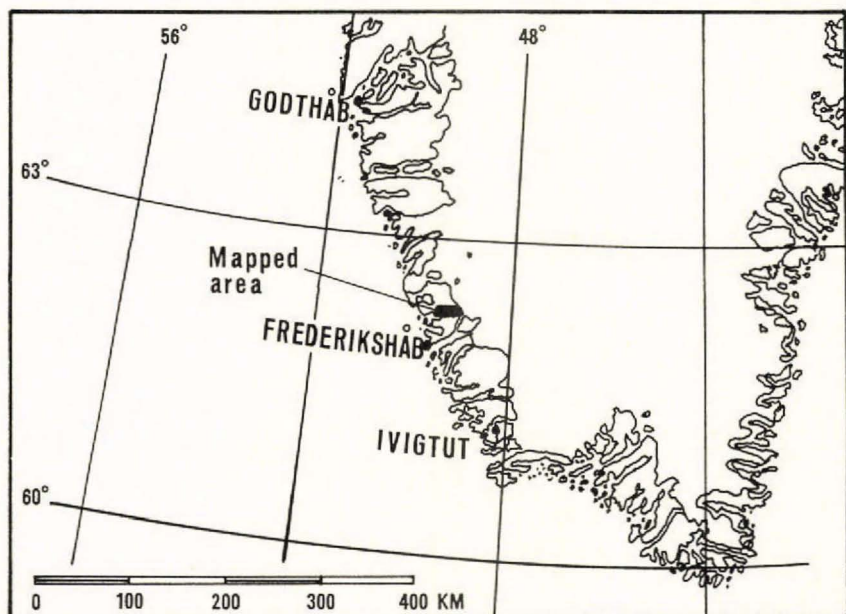


Fig. 1. Map locality in Greenland.

INTRODUCTION

During the summer months of 1967 and 1968 the authors had the chance of joining the GGU (Grønlands Geologiske Undersøgelse) geological field parties in the Mellemygd area, Frederikshåb district, southwest Greenland. The area mapped lies about 30 km NNE of Frederikshåb and consists of about 300 km², from the fjord Qagssip kangerdluarssua to the ice cap (fig. 1). Laboratory investigations were carried out at the Istituto di Mineralogia e Petrologia of the University of Modena, Italy. In 1967 the two authors mapped the northern part of the Aorngo area together; in 1968 A. Rossi mapped the southern part of the same area and G. RIVALENTI mapped the western area and the peninsula north of Sermilik avangnardleq. The chemical and some of the modal analyses were carried out by A. Rossi, while the microscopic observations, the structural interpretation, the writing and conclusions of this paper are the work of G. RIVALENTI.

The area mapped belongs to the Canadian-Greenlandic Precambrian Shield and has undergone a complicated metamorphic and structural evolution. The chronological division of the Precambrian of South Greenland can be found in BRIDGWATER (1965). The area consists of a migmatitic complex consisting of the following lithotypes: 1) migmatitic

gneisses and pegmatites, 2) concordant layers and inclusions in the gneisses, 3) discordant amphibolite dykes. These rocks are crossed by post-orogenic basic dykes which continue further south where, in the Ivigtut area, they are deformed by Ketilidian structures. Therefore, the metamorphic and structural evolution can be ascribed to the pre-Ketilidian (> 2500 m.y.).

In the following pages the field characteristics, petrography, structure, metamorphism and relationships of the various lithotypes will be described and discussed.

THE MIGMATITIC GNEISSES AND PEGMATITES

Introduction

Migmatitic gneisses and related pegmatites are the most widespread lithotypes of the area. In this paper, to avoid any misunderstandings with terminology, the gneiss classification submitted in Copenhagen at the symposium on migmatite nomenclature (BERTHELSEN, 1960) and recommended by GGU is adopted. This classification, which is based only on structural considerations, distinguishes: banded gneiss, streaky gneiss, veined gneiss, small-folded gneiss, nebulitic gneiss, homogeneous gneiss, and agmatitic gneiss. All these types are represented in this area, but the veined type predominates (plate 11). Since there is a close relationship between pegmatites and migmatisation these two subjects are considered together.

The Gneisses

Description

Veined gneiss

Veined gneisses consist of an irregular alternation of thin felsic layers, in which quartz and feldspar predominate, with more basic layers which contain a large amount of mafic minerals (biotite and hornblende). They also contain both single and branching acid veins in any attitude. The veined gneiss passes into the banded type as soon as the alternation of acid and basic layers is more regular and the single layers become more consistent along the strike. No sharp boundary can normally be traced between these two types. In many cases, the veined gneiss grades into streaky gneiss containing schlieren of amphibolite and hornblende.

In many places, such as the areas NNE of mountain 933 m, NW and NE of mountain 880 m (plate 11), this gneiss has a small-folded appearance (fig. 20). Feldspar porphyroblasts are commonly seen in the acid veins. When these porphyroblasts are the dominant characteristic of the rock, the gneiss has been indicated on the map as 'porphyroblastic gneiss' (see for instance the area of mountain 880 m in the eastern part).



Fig. 2. Migmatitic paleosome embedded in a migmatitic neosome. Border of the Nigerdlip qôrrossua homogeneous gneiss.

In some points this gneiss has a polymigmatitic character (see e.g. figs 2 and 3, which is shown by a migmatitic paleosome embedded in a migmatitic neosome).

Mineralogically, three main lithotypes can be distinguished: biotite veined gneiss, hornblende veined gneiss, and garnetiferous gneiss. Complete transitions occur between these types and in many cases the intermixing is so complete that it has foiled attempts to map them as different lithotypes. The only boundary that has been traced is of garnetiferous gneiss in the area between the fjord Qagssip kangerdluarssua and the valley Nigerdlip qôrrossua and even this is imprecise because it is gradational. In the garnetiferous gneiss layering and veining is very weakly developed and its structure is more homogeneous than that of the veined gneiss. The hornblende gneiss often represents one of the stages in the migmatisation of the amphibolites. In the field it is possible to follow the passage from a normal amphibolite to an agmatite or

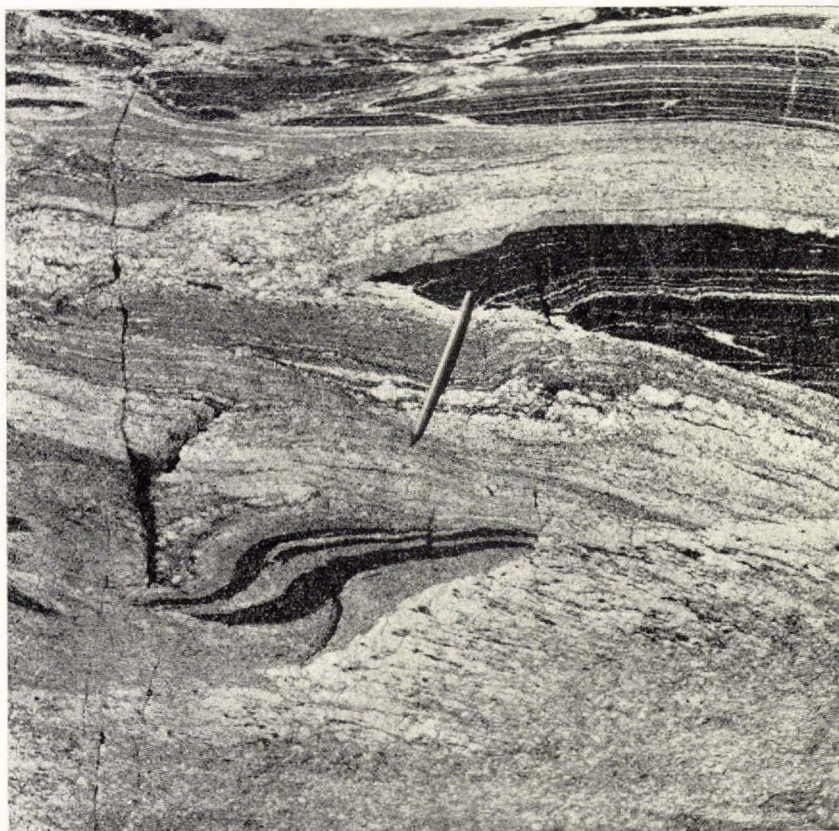


Fig. 3. Migmatitic paleosome, rich in amphibolite inclusions, passing into an inclusion-free, coarse-grained migmatitic neosome. Border of the homogeneous gneiss of the peninsula north of Sermilik avangnardleq.

streaky gneiss, and to a hornblende gneiss in which the amount of hornblende decreases and the felsic material increases; the last product of transformation may be a biotite gneiss in which no or very few relics of hornblende are present.

Banded gneiss

In general the banded gneiss consists of a regular alternation of felsic and mafic bands. Two types can, however, be distinguished on the basis of the melanocratic part: A) melanocratic bands which have a mineral assemblage similar to that of the felsic, but are enriched in biotite (and/or hornblende); B) melanocratic bands which are composed of amphibolites. *Type A* is a local, more regularly banded variety of the veined type. It is encountered sporadically all over the region; for instance the whole area between Qagssit, Qingua and mountain 825 m is formed of a gneiss with a fairly regular banded structure. The banding



Fig. 4. Homogeneous gneiss of the peninsula north of Sermilik avangnardleq. The amphibolite inclusions are almost completely transformed. 750 m east of mountain 920 m.

can vary from a few millimetres up to three metres. *Type B* commonly occurs as a transitional rock at the contact of the amphibolite horizons with the surrounding gneisses. The layering varies in thickness from a centimetre to half a metre and consists of amphibolite bands and biotite (hornblende) gneiss. The contacts are macroscopically sharp.

Homogeneous gneiss

The main fabric in this type is formed by the planar preferred orientation of mica and hornblende crystals. The small-folding present in the preceding types does not occur here. In the present area the main outcrops are represented by the garnet-bearing gneiss of the Nigerdlip qôrrossua area, by the gneiss west of mountain 780 m and by the gneiss of Sermilik avangnardleq. The first two, however, are cut by a few veins and at certain points show a faint lithological banding.

The garnet-bearing gneiss of the Nigerdlip qôrrossua area is bordered



Fig. 5. Agmatitic gneiss. 100 m east of lake 360 m.

towards the north-west by a very fine-grained nebulitic quartz-rich gneiss and towards the east by a veined gneiss. At the contact with the veined gneiss polymigmatisation phenomena have been found (fig. 2). The homogeneous gneiss completely lacks any amphibolite inclusions and major amphibolite horizons are also absent.

The homogeneous gneiss of the area west of mountain 780 m is composed of a biotitic, often hornblendic, but rarely garnet-bearing, medium-grained rock, still rich in schlieren of amphibolite and hornblendite and sporadically intersected by thin pegmatitic bodies. It has gradational contacts with the surrounding veined type.

The homogeneous gneiss of the peninsula north of Sermilik avangardleq comprises a well-defined band, up to 500 m thick, which is conformable with the veined type. It is a medium- to coarse-grained rock. In some places, inclusions are almost absent and the rock resembles a homogeneous granite. In the field it is possible to follow the passage from a migmatitic gneiss rich in mafic inclusions (veined-streaky gneiss) to the homogeneous gneiss in which the inclusions are almost completely 'digested', and the hornblende of the veined gneiss is completely replaced by biotite (see figs 3 and 4). The passage can be gradual or abrupt.

Agmatitic gneiss

Agmatites are very common all over the area. They represent one of the transitional products formed during the migmatisation of the

amphibolites. They consist of breccia-like rocks in which amphibolitic paleosome blocks are embedded in a gneissic or pegmatitic neosome (fig. 5). The characteristics of the amphibolite remnants are referred to on p. 53. The neosome presents the same characteristics as the gneisses and pegmatites described in this paper, therefore their description will not be repeated here.

Petrography

Although the various structural types have many points in common, a short description will be given for each of them to point out the differences.

Veined gneiss

The texture is generally crystalloblastic. It becomes porphyroblastic when big feldspar porphyroblasts are present. When large amounts of garnet are present it may exceptionally be granoblastic. The three main mineral assemblages are as follows.

Biotite gneiss

The only and most prominent mafic mineral is biotite. The typical assemblage is composed of quartz, plagioclase, biotite, microcline and muscovite as the major minerals with epidote, sphene, apatite, zircon and opaque minerals as accessory minerals. Modal analyses of typical rocks belonging to this group are given in Table 1.

Quartz is normally very abundant; it may be in greater or smaller quantity than the feldspar. It consists of at least two generations. The first generation is the most abundant and is replaced by the second generation which shows absorption contacts towards all the other minerals. This is particularly evident in the case of feldspar towards which it may show highly indented rims like those shown in plate 1a. The saw-like textures mainly occur when the polysynthetic feldspar twins form a wide angle to the contact with the secondary quartz. When the angle is low, the contact is usually lobate. Quartz is also present as a reaction product of some minerals (described later on) where it forms small patches in the minerals or assumes vermicular shapes, as in the case of the quartz-epidote symplectites.

Plagioclase is normally present in large amounts. Usually it is fresh, but sometimes it is altered to sericite, muscovite, calcite and epidote with the consequent formation of albite. In many instances, when this alteration is very advanced, it is possible to relate it to a local retrogression subsequent to fracturing and folding. The plagioclase compositions vary from acid to intermediate oligoclase (An 20–30 %). Frequently a normal zoning is present, with an irregular, more sodic, peripheral rim. The zoning emphasises the alteration which preferentially affects the core of the crystal. Plagioclase is almost invariably twinned. In the sections examined it has been found that the pericline law predominates over the albite law. Exceptionally, the Carlsbad, Manebach and other more complex twinings are also present. Plagioclase occurs both as equant crystals, giving the rock an interlobate, seldom amoeboidal, eugranoblastic texture, or as big porphyroblasts (porphyroblastic gneiss)

growing along the acid veins. The size of the porphyroblasts, constantly formed of oligoclase with minor amounts of microcline, may reach a maximum of several centimetres. The biotite is pushed apart and wraps around them.

Table 1. *Chemical and modal analyses of gneisses.*

GGU No	Veined gneiss							Banded gneiss 57879	
	Biotite gneiss			Hornbl. gneiss		Garnetiferous gneiss			
	57724	57873	57886	57723	57737	57738	57715		
Oxides wt. %									
SiO ₂	69.72	72.05	71.65	58.43	60.56	67.40	62.25	70.82	
TiO ₂	0.33	0.14	0.34	0.96	0.85	0.51	0.71	0.39	
Al ₂ O ₃	15.95	14.78	15.41	17.36	16.75	15.45	16.45	15.41	
Fe ₂ O ₃	0.77	0.90	0.79	1.70	1.89	0.38	1.71	1.39	
FeO	1.33	0.45	1.19	5.22	4.29	6.40	4.67	0.78	
MnO	0.03	0.01	0.01	0.15	0.10	0.16	0.21	0.01	
CaO	4.06	3.15	3.08	8.27	6.03	3.79	5.54	3.12	
MgO	1.26	0.71	0.67	3.02	4.03	1.56	2.87	1.16	
Na ₂ O	4.40	5.92	4.26	3.20	3.51	2.52	3.16	4.10	
K ₂ O	0.83	1.48	1.24	0.29	0.96	0.25	0.68	1.43	
P ₂ O ₅	0.03	0.10	0.03	0.07	0.13	0.03	0.08	0.05	
H ₂ O ⁺	0.55	0.68	0.57	0.85	0.90	0.76	1.10	0.59	
H ₂ O ⁻	0.01	0.03	0.06	0.02	0.02	0.01	0.05	0.07	
	99.27	100.40	99.30	99.54	100.02	99.22	99.48	99.32	
Mode vol. %									
quartz	11.6	28.1	26.9	6.6	16.9	40.3	16.0	31.4	28.7
plagioclase	76.1	58.2	58.9	56.4	55.7	39.2	59.6	37.3	56.1
microcline	0.4	5.2	0.3	—	—	0.1	—	27.6	0.8
biotite	8.5	7.4	9.4	3.1	13.4	1.5	9.0	2.5	12.8
garnet	—	—	—	—	—	15.1	4.0	—	—
hornblende	—	—	—	30.8	12.6	—	9.1	—	—
muscovite	1.0	0.9	4.3	—	—	0.7	—	0.2	0.6
chlorite	—	—	—	0.1	—	2.4	0.5	—	—
epidote	1.9	tr	tr	1.4	0.3	—	0.3	0.9	0.8
sphene	0.3	—	—	1.0	0.5	—	—	—	—
apatite	0.1	0.1	0.1	0.3	0.4	—	0.4	tr	0.1
zircon	tr	tr	tr	tr	0.1	tr	0.1	—	tr
calcite	—	—	—	—	—	—	0.7	—	—
opaque	0.1	—	tr	0.3	tr	0.6	0.3	—	tr
An % in plag.	29	22	22	38	35	42	35	25	25

57715: CO₂ = 0.66 %.

57879: composed of 60 % melanocratic and 40 % felsic bands, representing the ratio found in the field.

(continued)

Table 1 (continued).

GGU No.	Homogeneous gneiss					Polymigmatitic gneiss			
	73543	57756	57757	57770	57782	neo- some 73816	paleo- some 73817	neo- some 73836	paleo- some 73835
Oxides wt. %									
SiO ₂	72.77	67.21	61.23	67.61	68.43	69.35	63.64	70.17	67.92
TiO ₂	0.43	0.40	0.70	0.59	0.43	0.50	0.62	0.36	0.53
Al ₂ O ₃	14.62	15.31	18.29	16.31	16.38	15.54	16.37	16.05	16.56
Fe ₂ O ₃	0.29	1.02	3.01	0.88	0.91	0.62	0.97	0.61	0.55
FeO	2.25	2.71	1.97	1.82	1.55	2.01	3.86	0.92	2.33
MnO	0.08	0.06	0.08	0.03	0.03	0.05	0.08	0.03	0.03
CaO	4.42	4.35	6.33	5.82	4.20	4.56	5.40	4.10	4.13
MgO	1.51	2.52	1.93	0.91	1.56	1.16	2.57	0.60	1.51
Na ₂ O	3.06	3.80	4.40	3.80	4.52	4.12	3.70	4.52	4.28
K ₂ O	0.28	0.96	0.41	0.69	0.50	1.03	1.30	1.30	1.23
P ₂ O ₅	0.07	0.06	0.05	0.04	0.04	0.04	0.04	0.04	0.04
H ₂ O ⁺	0.27	0.78	0.82	0.80	0.58	0.55	0.82	1.09	0.73
H ₂ O ⁻	0.02	0.11	0.06	0.08	0.08	0.07	0.06	0.12	0.07
	100.07	99.29	99.28	99.38	99.21	99.60	99.43	99.91	99.91
Mode vol. %									
quartz	26.1	26.1	12.7	21.5	22.1	29.8	27.7	28.7	24.2
plagioclase	69.1	59.3	72.7	61.9	65.8	58.2	43.6	63.5	66.0
microcline	-	0.3	-	-	-	0.1	-	0.4	tr
biotite	1.6	11.8	3.2	8.3	7.2	10.7	16.7	5.6	8.7
garnet	3.1	-	-	0.1	-	tr	-	tr	-
hornblende	-	2.3	7.1	6.3	2.7	-	10.0	-	-
muscovite	-	-	1.2	0.8	0.2	0.4	-	-	-
chlorite	-	-	0.3	0.3	0.3	-	-	0.8	-
epidote	tr	tr	0.1	0.3	1.0	0.2	1.4	0.7	0.7
sphene	-	-	0.1	-	-	tr	0.1	-	-
apatite	tr	0.2	0.3	0.3	0.4	0.4	0.4	0.2	0.3
zircon	tr	tr	tr	tr	tr	tr	tr	tr	tr
calcite	-	-	0.9	-	-	-	-	-	-
opaque	tr	tr	1.4	0.1	0.2	0.1	tr	-	-
An % in plag.	34	35	34	35	30	29	32	30	30

73543: homogeneous gneiss of Nigerdíp qôrrossua

57756, 57757, 57770, 57782: homogeneous gneiss of the area west of mountain 880 m.

73836: homogeneous gneiss of the peninsula north of Sermilik avangnardleq

73816, 73817: neosome and paleosome respectively of fig. 2

73836, 73835: neosome and paleosome respectively of fig. 3

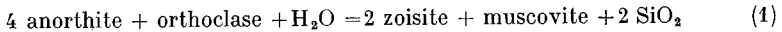
Microcline is considered a minor constituent, as it occurs often but never in large amounts. It occurs in two forms: as very thin veins running along the grain boundaries or entering the discontinuity planes of feldspar (cleavages and twinning

planes) and other minerals, or in autonomous crystals clearly showing the typical grid twinning. Microcline shows absorption contacts toward the plagioclase (plate 1b) which is clearly substituted by it, together with the second generation quartz. Sometimes microcline occurs in small patches in the plagioclase. The microcline crystallisation clearly post-dates that of the other minerals.

Biotite occurs as thin, subidiomorphic lamellae. Its pleochroism varies from α = yellow (yellowish green), $\beta = \gamma$ = deep green (greenish brown). Biotite is usually fresh, but some alteration products are highly significant from the point of view of its metamorphic history. It may be associated with muscovite, epidote or pass to chlorite. The brown or reddish biotite is fairly uncommon, though sometimes it is met with either as the only mafic mineral, or as small relics in the green biotite. When the green biotite is present, it is accompanied by a net of sagenitic rutile formed with the excess Ti, or by sphene when Ca is available. This is not seen in connection with the brown biotite, which is usually accompanied by ilmenite. This point will be reconsidered in the section concerning the chemistry of the gneisses.

Epidote is a common constituent in all the biotite gneisses, though always in small quantities. It is present mainly in two forms: 1) as very small aggregates that, together with sericite, form the usual product of the feldspar alteration; 2) more significantly, as big subidiomorphic porphyroblasts. In the latter case it is clinzoisite and pistacite. Sometimes big crystals of allanite (included with epidote in the modal analyses) are present and usually show a peripheral transformation into normal epidote. Epidote is often, though not necessarily, connected with biotite. When it occurs together, a derivation from hornblende gneiss, by means of a process to be described later on, may be suspected.

Muscovite may be present in large crystals, sometimes with a skeletal appearance. It may be formed either from biotite or from the feldspar alteration together with epidote. In the latter case a reaction similar to that suggested by MARMO (1967) seems likely:



Muscovite, though present in the majority of the samples, never attains significant proportions.

The presence of *sphene*, when hornblende is absent, is strictly controlled by the presence of green biotite and by the Ca content of the rock.

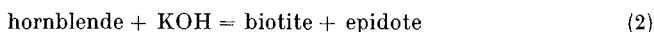
Apatite and *zircon* may occur as relatively large crystals.

Hornblende gneiss

All the transitional compositions can be found in the field between this and the biotite gneiss. The main compositional differences between the hornblende and the biotite gneisses, apart from the presence of hornblende, are the more calcic composition (up to An_{40}) of the plagioclase in the former and in a general lack of microcline, which seems to be in inverse proportion to the amount of hornblende. In Table 1 two modal analyses of samples belonging to this group are reported.

Hornblende is present in xenoblastic, sometimes porphyroblastic (up to 1 cm) crystals. Its common pleochroism is α = yellow, β = greenish, γ = greenish light blue. The slight difference of the pleochroism in the hornblende of the gneisses and of the amphibolites (Tables 1 & 5) suggests the possibility that they are chemically differ-

ent. This topic will be discussed later on (p. 21). During the migmatitic evolution of these rocks hornblende became unstable. It commonly presents lobate resorption contacts towards quartz and plagioclase. Transformation in a more or less advanced stage into biotite is general: biotite crystallises along the fractures and cleavages of the hornblende or at its border. In this transformation epidote and sphene are formed. The reaction which takes place can be represented in the following way (MARMO, 1967).



The right-hand side of the equation should be stable in lower metamorphic conditions. The equation is only approximate because it does not account for titanium present in the hornblende, which, together with some calcium and silicon forms sphene. When the transformation is very advanced the final product can be a biotite gneiss with no or very few relics of hornblende in it. The association of Ca-silicates (epidote) and Ca-Ti-silicates with biotite in biotite gneisses may indicate an original derivation from a hornblende gneiss.

Garnetiferous gneiss

The mafic minerals which accompany garnet are biotite with or without hornblende, as is shown by the two modal analyses reported in Table 1.

Garnet occurs as pink poikiloblastic crystals up to 5 cm in diameter, which contain inclusions of quartz, feldspar, biotite and opaque grains. Its relationships to the other mafic minerals are not clear: contacts with biotite and hornblende are usually sharp and no transformations seem to have taken place. Possibly garnet grew at the same time, and in equilibrium with the other minerals. Sometimes a brownish red biotite instead of the common greenish type, accompanies the garnet.

Plagioclase composition varies from An₃₅ to An₄₂. Normally no significant amounts of microcline and epidote are found.

Banded gneiss

The two types described at p. 11 have the following petrographical characteristics.

Type A: the felsic bands are enriched in quartz, plagioclase, and sometimes very strongly in microcline in respect to the melanocratic bands. (In Table 1 the large amount of microcline found in the felsic band of the examined sample is exceptionally high). The same variability in mineral assemblages described for the veined gneiss is also present in the banded gneiss.

Type B: microscopic observation reveals that the passage from the amphibolite bands to the gneissic bands is not as sharp as it appears in the field. The contact is marked by an enrichment in biotite which diminishes towards both the leucocratic bands and the amphibolite, but whereas in the leucocratic bands it remains the prominent mafic mineral, it decreases rapidly in the amphibolites to be a minor constituent. The plagioclase composition does not change much in the mafic and acid

bands: it ranges from around An_{30} in the latter and is slightly more calcic in the former. Microcline is generally limited to the felsic bands; exceptionally it may appear in small veins in the amphibolites as well. Hornblende may be present in the felsic bands, but undergoes the usual transformation into biotite, epidote and sphene. Garnet, when present in the amphibolite, may also appear in the gneiss.

Homogeneous gneiss

The garnetiferous gneiss of the Nigerdlip qôrrossua area generally has a granoblastic texture. The mineralogical composition, for the biotite variety, can be seen in Table 1 (73543). No modal determination has been made on the hornblende variety, though some thin sections of it have been studied. *Garnet* in thin section has a pinkish colour. *Biotite* is the usual green, very seldom a dark brown type already described for the veined gneisses. *Microcline* is usually lacking. The plagioclase composition seems to be independent on the presence of hornblende with a consistent composition around An_{35} . The characters of the other minerals are the same as described for the veined gneiss.

The gneiss of the area west of mountain 780 m is a medium-grained eugranoblastic rock. In Table 1 four modal analyses of samples of this gneiss are reported. The main mineralogical characters and mineral relationships in this gneiss are more or less the same as already described for the veined gneisses with a similar mineral assemblage. A few minor differences are mentioned below.

Microcline can co-exist with hornblende (as in sample 57756). It may sometimes form substitution anthiperthites, such as those shown in plate 2a. The anorthite content of the *plagioclase* ranges from 26 % to 35 %, but is most common around 30 %. *Garnet* is seldom present. *Biotite* is represented by a dark brownish type, while the green type is rare.

On the peninsula north of Sermilik avangnardleq the texture is eugranoblastic. The prominent mafic mineral is a greenish or greenish brown biotite, while hornblende is usually completely lacking or is represented by relics. The *plagioclase* composition is the same as in the preceding gneiss but *microcline* is seldom met with. A modal analysis of one sample of this gneiss is reported in Table 1.

Chemistry

A few samples for each type of gneiss have been chemically analysed (Table 1). In the same table are also reported the chemical and modal data relative to the two examples of polymigmatisation previously described p. 10 and p. 13). The following observations have been made:

i) all the gneisses have a general quartz dioritic composition, as is shown, for instance, by the triangular plot of fig. 6 regardless of the structural type they belong to.

ii) the K_2O content is always very low, but, of course, is slightly higher in the biotite (from 0.83 to 1.48) than in the hornblende gneisses (from 0.29 to 0.96). When garnet is present the K_2O content is a minimum (from 0.25 to 0.69).

iii) the Na_2O content is fairly constant, though it decreases when hornblende is present.

iv) the CaO , MgO and iron contents are higher in the hornblende than in the biotite gneiss. In the garnet-bearing samples FeO is higher than in the biotite, and of the same order as in the hornblende gneiss.

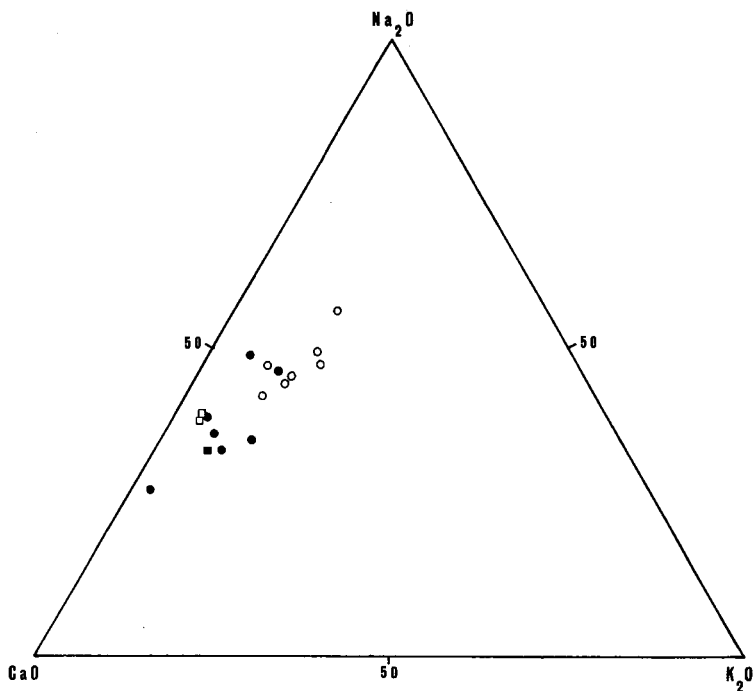


Fig. 6. Triangular plot Na_2O , CaO , K_2O (weight %) for the gneisses. Circles = biotitic gneiss; dots = hornblende gneiss, outline squares = garnetiferous biotite gneiss; black squares = garnetiferous hornblende gneiss. Analyses of Table 1.

The variations of the major oxides in relation to SiO_2 for the two polymigmatitic occurrences are shown in fig. 7.

In both the neosome samples SiO_2 increases in relation to the paleosomes. As SiO_2 increases so does Na_2O , while MgO , FeO , CaO , TiO_2 and Al_2O_3 decrease. Fe_2O_3 exhibits an opposite trend in the two examples. K_2O does not show any significant variation. The samples of paleosome were

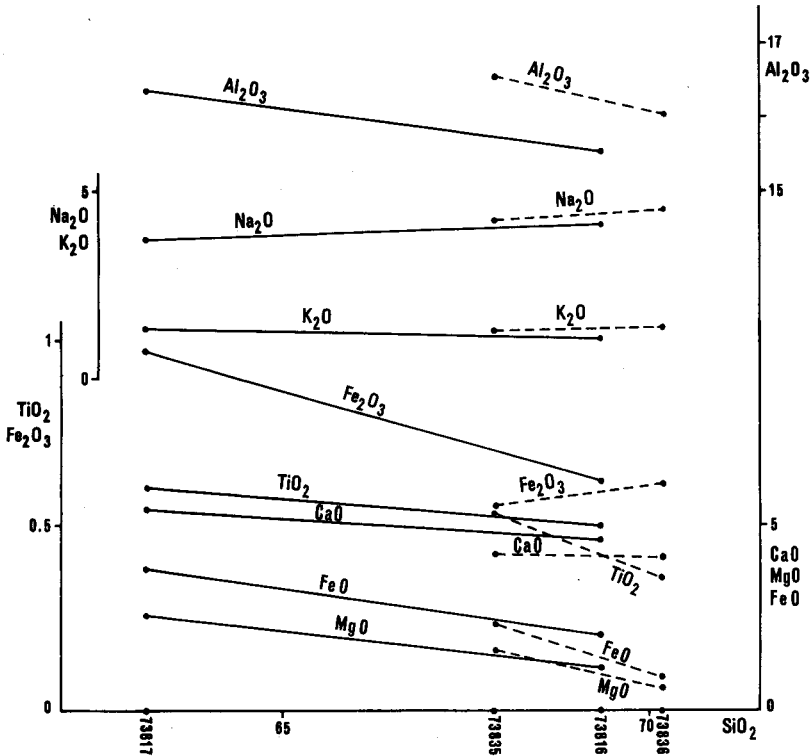


Fig. 7. Chemical variations of the major oxides against SiO_2 between migmatitic paleosomes and neosomes in the gneisses. (Samples 73816 and 73817 are the neosome and paleosome respectively of fig. 3; samples 73835 and 73836 the paleosome and neosome respectively of fig. 4).

taken from the felsic part and do not account for the amphibolite inclusions present in the gneiss. If the relative abundance of felsic and amphibolitic parts were considered when establishing the average composition of the paleosome, the chemical variation between paleosome and neosome would be much greater than appears here.

In Table 2 the chemical analyses of biotite, hornblende and garnet from the gneisses are reported. The hornblende, in spite of the different pleochroism, is chemically similar to the hornblende of the amphibolite (Table 5), except for a slightly higher total-iron and oxidation ratio in the former.

The release of titanium accompanying the crystallisation of the green biotite, so evident under the microscope as rutile needles (p. 17), cannot be demonstrated chemically, as no significant variation occurs between the green biotites and the others. This is due to the impossibility of separating the rutile from the green biotite.

Table 2. *Chemical analyses of biotite, hornblende and garnet in the gneisses.*

GGU No.	Biotites					Hornblende	Garnets	
	57782	57724	57723	73543	57738	57723	57738	73543
SiO ₂ ...	36.02	36.37	35.30	34.00	37.40	42.74	38.03	38.42
TiO ₂ ...	2.05	2.36	2.60	3.50	1.99	0.89	0.30	0.33
Al ₂ O ₃ ..	16.88	16.58	16.56	15.29	16.18	13.12	22.10	22.93
Fe ₂ O ₃ ..	3.47	5.44	6.81	9.10	6.34	4.48	0.67	—
FeO ...	13.99	13.84	10.80	14.32	15.28	12.63	27.60	28.43
MnO ...	0.18	0.21	0.20	0.06	0.05	0.31	0.68	1.54
CaO ...	0.81	0.77	1.33	0.91	0.84	11.14	4.14	5.11
MgO ...	11.74	11.03	11.39	10.03	9.32	9.80	5.95	5.74
Na ₂ O ..	0.17	0.17	0.14	0.17	0.14	1.09	tr	tr
K ₂ O ...	9.24	8.58	7.18	8.32	6.85	0.72	tr	tr
P ₂ O ₅ ...	—	0.01	tr	—	—	0.06	0.06	—
H ₂ O ⁺ ..	3.83	3.83	5.29	3.65	5.15	2.49	—	—
H ₂ O ⁻ ..	0.84	0.95	1.85	0.70	1.00	0.15	0.03	0.02
	99.22	100.14	99.45	100.05	100.54	99.62	99.56	102.52
Number of ions on the basis of 24(O)								
Si	5.475 } 8.000	5.481 } 8.000	5.244 } 8.000	5.249 } 8.000	5.510 } 8.000	6.317 } 8.000	5.952 } 6.000	5.874 } 6.000
Al	2.525 } 8.000	2.519 } 8.000	2.756 } 8.000	2.751 } 8.000	2.490 } 8.000	1.683 } 8.000	0.048 } 6.000	0.126 } 6.000
Al	0.498 } 8.000	0.428 } 8.000	0.143 } 8.000	0.029 } 8.000	0.319 } 8.000	0.601 } 8.000	4.029 } 6.000	4.008 } 6.000
Ti	0.235 } 8.000	0.266 } 8.000	0.291 } 8.000	0.406 } 8.000	0.220 } 8.000	0.099 } 8.000	0.036 } 4.144	0.039 } 4.047
Fe ³⁺ ...	0.397 } 5.588	0.616 } 5.557	0.761 } 5.082	1.056 } 5.714	0.702 } 5.176	0.497 } 4.931	0.079 } 4.144	— } 4.047
Mg	2.658 } 5.588	2.476 } 5.557	2.522 } 5.082	2.367 } 5.714	2.046 } 5.176	2.134 } 4.931	1.388 } 4.144	1.307 } 4.047
Fe ²⁺ ...	1.777 } 5.588	1.745 } 5.557	1.341 } 5.082	1.848 } 5.714	1.883 } 5.176	1.561 } 4.931	3.611 } 4.144	3.635 } 4.047
Mn	0.023 } 5.588	0.026 } 5.557	0.024 } 5.082	0.008 } 5.714	0.006 } 5.176	0.039 } 4.931	0.090 } 4.144	0.199 } 4.047
Na	0.051 } 5.588	0.051 } 5.557	0.038 } 5.082	0.052 } 5.714	0.038 } 5.176	0.313 } 4.931	— } 4.144	— } 4.047
Ca	0.132 } 1.975	0.124 } 1.824	0.212 } 1.611	0.150 } 1.841	0.133 } 1.459	1.764 } 2.213	0.694 } 5.783	0.837 } 5.978
K	1.792 } 1.975	1.649 } 1.824	1.361 } 1.611	1.639 } 1.841	1.288 } 1.459	0.136 } 2.213	— } 5.783	— } 5.978
OH	3.896 } 1.975	3.773 } 1.824	5.226 } 1.611	3.761 } 1.841	5.095 } 1.459	2.467 } 2.213	— } 5.783	— } 5.978
α	pale greenish yellow	pale yellow	pale yellow	yellow	pale yellow	yellow	62.4	60.8 almandine
α	dark green	dark green	greenish brown	dark brown	brownish red	green	0.3	1.0 andradite
γ	dark green	dark green	greenish brown	dark brown	brownish red	bluish green	24.0	21.9 pyrope
57738 biotite contains chlorite impurities.						2V -62°	11.7	13.0 grossular
						c:γ 16°	1.6	3.3 spessartite

The two garnets have a similar composition and are largely almandine in composition.

Further considerations on the metamorphic significance of some of the analysed minerals are discussed when dealing with the metamorphic facies (p. 68).

The Pegmatites

Occurrence

The area is intersected by numerous pegmatites which cut all the rock types, sometimes forming up to 70 % of the outcrop. They reach a maximum thickness of 50 m and may extend for considerable distances. In the gneisses they are represented by: a) concordant or subconcordant dykes or veins often showing a pinch-and-swell structure; b) discordant bodies sometimes pygmatically folded; c) irregular mobilisates occurring in the tensile stress area between the boudins of amphibolites or constituting the neosome of agmatites. The largest and most numerous pegmatites are found in the veined and banded gneisses. The homogeneous gneisses are also affected by pegmatitic mobilisation but their pegmatites are usually much smaller and less numerous than those of the other gneisses.

In the amphibolites there is not the abundance of pegmatites that is present in the gneisses. Nevertheless amphibolites too are cut or veined by pegmatites and some of the largest have been found to cut this rock type unconformably. In the amphibolite four types can be distinguished: a) a concordant type composed of feldspar and quartz veins, usually a few centimetres thick; b) a subconcordant, slightly discordant type; c) a completely discordant type reaching a maximum thickness of 30–50 metres; d) an irregular type wrapped around ultramafic lenses and very occasionally cutting across them. This last type is genetically identical to that occurring in the shadow pressure areas between the boudins in the gneisses.

Texture, mineralogy and relation to the host rock

All the pegmatites have a granoblastic texture, becoming locally blastomylonitic as a consequence of younger deformation and crystallisation. Locally a graphic texture may appear (P_3 pegmatites only, see p. 27). The grain size is always rather large, but very fine-grained aplitic pegmatites are present either as autonomous bodies or as a local change in the grain size near the contacts with the host rock. On the basis of the salic minerals, two main groups can be distinguished: a) quartz pegmatites; b) quartz-plagioclase (\pm microcline) pegmatites.

Quartz pegmatites

They are common in all sizes. The thickest one to be observed was an irregular body, 14 m thick, consisting of giant porphyroblasts of quartz and minor albite. Normally no calciferous mineral is associated with quartz. Very occasionally some accessory biotite may appear. In some quartz pegmatites large crystals (10 cm long) of idiomorphic epidote have been found. It is worthy of note that a few quartz pegmatites have been found to be a transformation along the strike of a zoned pegmatite. In this case the quartz pegmatite derives from a thinning of the feldspathic rims (see below), as described elsewhere, for instance by JAHNS (1955) and GRESENS (1967 a & b). As GRESENS points out, this can be due to the rate of opening of the fissures, being lower in the tails than in the centre.

Quartz-plagioclase (\pm microcline) pegmatites

These pegmatites occur either as long concordant to discordant dykes in the gneisses and amphibolites or, less commonly, as irregular bodies between boudins or around mafic lenses. They may exhibit an inward zonation which consists of: 1) a seldom seen, mafic rim of enrichment of feldspars in the host rock at the contact with the pegmatite; 2) a fine-grained, sometimes aplitic, band in the pegmatite at the contact with the host rock; 3) a coarse-grained zone consisting of quartz, feldspar and mafics; 4) a central zone of pure quartz. This zonation is not always complete and depends to some extent on the total thickness of the pegmatite.

Mineralogically, the abundance of microcline with respect to plagioclase is critical for the following reasons:

i) the largest pegmatites have been found to be microcline-rich pegmatites;

ii) if microcline is absent or accessory, the mafic minerals of the pegmatite are the same as those of the host rock. It has been seen, for instance, that the same pegmatite has biotite when crossing a biotite gneiss, and hornblende when the pegmatite passes into hornblende gneisses or amphibolites;

iii) when microcline becomes the predominant feldspar the mafic mineral of the pegmatite is always biotite regardless of the mineralogy of the host rock. In any case there is a direct correlation between the amount of biotite in the pegmatite and the amount of mafic minerals in the country rock: biotite for instance is more abundant when the pegmatite passes from a gneiss into an amphibolite.

The main characteristics of the minerals are listed as follows.

Quartz occurs either as autonomous porphyroblasts or, more rarely, in graphic intergrowth with microcline and in myrmekitic intergrowth with plagioclase.

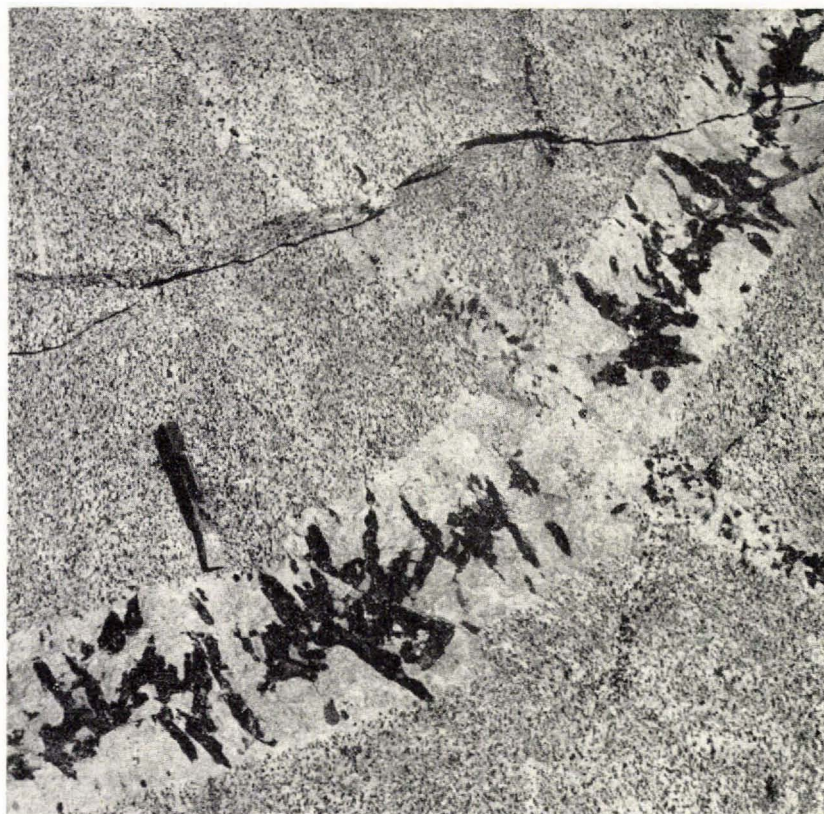


Fig. 8. Hornblende-bearing pegmatite. Hornblende has a zonal distribution and is crystallised with its axis normal to the contacts. 2000 m north-east of mountain 780 m, near the inland ice.

Plagioclase is usually oligoclase (up to An_{30}). It can either be the sole feldspar or be subordinate in amount to microcline.

Microcline, when present in appreciable amounts, can form porphyroblasts of several centimetres. Both perthites (usually microperthites) and antiperthites are common. The best examples of antiperthites occur in the pegmatites west of mountain 780 m, where they are also present in the homogeneous gneiss (see sample 57756).

Biotite is normally strongly pleochroic varying from colourless to reddish brown, and may form giant crystals up to one metre broad. It is found both inside the pegmatites (in which case it may have a random distribution or be arranged in strings parallel to the foliation of the host rock) and as a reaction product at the contact of microcline-bearing pegmatites. Small amounts of biotite are found (together with sphene and epidote) as transformation of hornblende in hornblende-bearing pegmatites.

Hornblende often forms very large crystals (up to 20 or 30 cm) which may show a random, or a zonal (fig. 8) distribution inside the pegmatite. In the latter case, hornblende crystals are mainly concentrated at the centre of the pegmatite and



Fig. 9. Pegmatite cross-cutting hornblende gneiss and a hornblende inclusion. The pegmatite contains large hornblende crystals which are more abundant when the pegmatite passes from the gneiss into the inclusion; the same locality as fig. 8.

crystallised with their major axis normal to the contacts. Hornblende is enriched in the pegmatites which cross-cuts rocks rich in this mineral (fig. 9). The relative percentages of hornblende and salic minerals in the pegmatite, as opposed to the host rock, are not very different; for instance, two estimates of the modal composition of two pegmatites, a zonal and a random (carried out by geometric measurement on projected colour slides), have given: ho 33.8 %, pl + qu 66.2 %, and ho 31.6 % pl + qu 68.4 %, respectively. The composition of the country rock is of the same order. A single hornblende crystal has been chemically analysed (Table 3), and it can be seen that it is very similar to those from the gneisses and amphibolites.

Garnet (normally a pinkish type), *epidote*, *muscovite* and *allanite* (in crystals up to 8 cm long) are accessories.

Tourmaline appears as a reaction product between microcline-rich pegmatites and amphibolites or ultramafics. Tourmaline is usually zoned, with a brownish core and green periphery and forms crystals up to 3 cm. Sometimes it forms massive aggregates with little or no feldspar or quartz.

Beryl has been found at the contact between an amoeboidal pegmatite and an ultramafic body. It consists of bluish green transparent crystals up to 4 cm long. A

Table 3. *Chemical analysis of a hornblende from a pegmatite.*

GGU No.		57766	
Oxides wt. %		Number of ions on the basis of 24 (0)	
SiO ₂	42.72	Si	6.347
TiO ₂	0.80	Al	1.653
Al ₂ O ₃	13.06	Al	0.634
Fe ₂ O ₃	4.55	Ti	0.089
FeO.....	12.39	Fe ³⁺	0.508
MnO.....	0.33	Mg	2.434
CaO.....	10.44	Fe ²⁺	1.539
MgO.....	10.99	Mn	0.040
Na ₂ O.....	1.17	Na	0.338
K ₂ O.....	0.54	Ca	1.662
H ₂ O ⁺	2.08	K	0.103
H ₂ O ⁻	0.13	OH	2.037
99.20			
c:γ 14°		α pale yellow	
2V -65°		β light green	
		γ light blue	

few crystals are present in the pegmatite reaching a maximum size and concentration in the biotite reaction zone and rapidly decrease in the hornblendite zone of the ultramafic lens (p. 42).

Composition related to timing

There is good field evidence that pegmatites were formed in several episodes during the evolution of the area. A key sub-area, shown in fig. 10, enabled us to establish the following age relationships: the first pegmatites (P₁) are a consequence of metamorphic differentiation and are conformably folded together with the biotite-rich layers by F₃ folds (p. 80); the second pegmatites (P₂) are represented by subconcordant to completely discordant bodies whose emplacement took place during the F₃ deformation, as is shown by the fact that the pegmatites have suffered only partially from the folding (see also RAMSAY, 1967, p. 344 for a similar example). P₃ pegmatites are represented by sills and dykes that, in the examples shown by fig. 10, are undeformed; the youngest pegmatite swarm, P₄, consists of quartz-veins which occur in the tension areas of F₅ folds (p. 82).

The field data and samples are not sufficient to give unambiguous relationships between the composition and the relative ages of the pegmatites, but the following observations can be made.

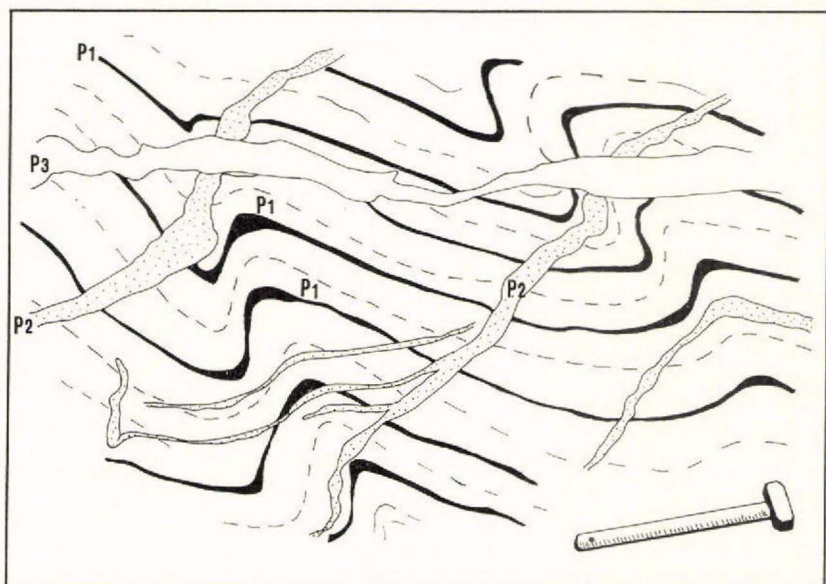


Fig. 10. Pegmatite network in the gneisses. Three generations of pegmatites can be distinguished (P_1 , P_2 , P_3). P_1 (black) are concordant pegmatites conformably folded in a F_3 fold. P_2 pegmatites (dots) were emplaced during the F_3 deformation as they have suffered only partially from the folding. P_3 (white) are undeformed and cross all the other pegmatites. 2500 m north-east of mountain 933 m. (Drawn from a series of photographs).

The P_1 swarm, concordant with the foliation, contains a little microcline which post-dates plagioclase (see p. 17). The pegmatites of the P_2 swarm have either plagioclase as the only feldspar or microcline subordinate to plagioclase, and this only when the pegmatite cuts biotite gneisses. The P_3 pegmatites, parallel to F_4 axial surfaces (p. 82), contain more microcline than plagioclase, and biotite as the only mafic mineral. The mobilisates connected to F_5 deformation (p. 82) are quartz-rich.

LAYERS AND INCLUSIONS IN THE GNEISSES

Introduction

Layers of unmigmatized rocks are interbanded with the gneisses and form long, thin horizons which can be traced for many kilometres. These are of great assistance in explaining some of the intricate structures of the area. They consist of four intimately associated lithotypes: 1) amphibolites, which largely predominate; 2) ultramafic lenses; 3) rusty schists; 4) micro-granodioritic rock. The layers formed by these lithotypes are concordant with the gneiss foliation for many kilometres and suggest that the foliation in these places is concordant with a primary bedding. It is possible however that in parts of the area where the amphibolites are lens-shaped, younger foliations may have obliterated the primary orientation through transposition. Discordance between foliation and lithology is seen in the closures of both F_1 and F_2 folds (see p. 78). All these layers tend to fade out along the strike. At first processes of boudinage, conforming with the pattern described by RAMBERG (1956), and of agmatitisation transform the amphibolites into streaky gneisses and agmatites. The final transformation product can be a hornblende gneiss or even a biotite gneiss with few or no relics of amphibolite.

Small lens-shaped or angular inclusions of unmigmatized rocks are also found in the gneisses. They consist of amphibolites, ultramafic rocks, and calc-silicate rocks. Amphibolites and ultramafic rocks occur as both lenses and layers whilst calc-silicate rocks occur only as lenses.

Layers in the Gneisses

Amphibolites

Description

It has been mentioned that the lateral passage from an amphibolite horizon to the country gneisses often takes place through an alternation of felsic gneisses and amphibolite bands. Sometimes, however, the contact is sharp. When unaffected by macroscopic signs of migmatitisation, the amphibolites are concordant layers which in some places, such as in

the amphibolites of mountain 933 m, possess a strong F_2 cleavage. In many cases the amphibolites possess either continuous or discontinuous compositional layering which has been divided into 3 types:-

- i) thin (up to 10 cm thickness) discontinuous but concordant quartz-feldspar or quartz layers with hornblendite rims;
- ii) layering expressed by an alternation of either grain size or the abundance of the main minerals;
- iii) alternating layers having different mineral assemblages which give the various layers different colours (colour-layering).

In the colour-layering the typical alternation consists of the following types:

a) *dark-green layers* of almost pure hornblendite with a maximum thickness of 20 cm grade both laterally and along the strike into normal plagioclase amphibolites. They may contain sporadic crystals of clinopyroxene and traces of epidote and feldspar.

b) *green layers* are the dominant type of amphibolite. They are characterised by the predominance of hornblende over feldspar and by the lack of significant amounts of other minerals.

c) *light-green layers* are characterised by the presence of epidote and/or clinopyroxene. They have a maximum thickness of 50 cm and are fairly continuous but thin out along the strike.

d) *garnet-bearing layers*. Garnet is associated with both the dark-green layers and the green layers. When it is present in large amounts, quartz is also abundant. Garnet is either concentrated in irregular pods uniformly distributed within the banding, or is limited to acid veins which cut the amphibolite.

Petrography

The following petrographic description mainly refers to the colour-layering.

The texture of the normal amphibolites is crystalloblastic and is characterised by a planar arrangement of elongated hornblende prisms with intergranular feldspar. The epidote, pyroxene and garnet-bearing layers often possess an imperfectly developed granoblastic texture. The texture of the hornblendite layers is characterised by the parallel arrangement of the hornblende crystals, which impart either a planar or linear fabric to the rock.

The modal analyses of samples belonging to the different bands are shown in Table 4. No point counting has been carried out on hornblendites, but their hornblende content has been estimated at over 90 %.

Table 4. *Chemical and modal composition of amphibolites of the concordant layers.*

GGU No.	green layers								
	57731	57821	57849	58821	73518	73820	73841	75839	75895
Oxides wt. %									
SiO ₂	48.00	47.68	48.68	50.38	46.97	46.89	48.56	48.38	49.99
TiO ₂	1.00	0.67	0.37	0.97	0.90	1.04	1.04	0.70	0.66
Al ₂ O ₃	15.28	13.00	15.29	14.97	15.92	14.91	14.94	15.93	14.33
Fe ₂ O ₃	1.69	2.14	1.07	1.57	1.75	2.24	1.87	1.90	2.14
FeO	8.93	8.99	9.58	9.40	8.56	9.96	9.67	10.14	10.01
MnO	0.20	0.19	0.18	0.20	0.20	0.20	0.17	0.01	0.18
CaO	13.70	12.61	10.59	9.88	12.06	11.78	11.57	10.59	11.71
MgO	8.04	11.03	9.48	8.06	8.97	8.06	6.80	7.56	6.55
Na ₂ O	1.82	1.50	2.80	2.54	2.01	2.44	2.80	2.72	2.10
K ₂ O	0.56	0.56	0.20	0.30	0.27	0.55	0.54	0.22	0.28
P ₂ O ₅	0.02	0.03	0.05	0.01	0.04	0.01	0.02	0.03	0.02
CO ₂	—	—	—	0.53	—	—	—	—	0.61
H ₂ O ⁺	1.23	1.75	1.25	0.99	1.50	1.34	1.23	1.32	1.29
H ₂ O ⁻	0.04	0.04	0.05	0.05	0.19	0.05	0.03	0.03	0.04
	100.51	100.19	99.59	99.85	99.34	99.47	99.24	99.53	99.91
<i>mg</i>	0.57	0.64	0.61	0.57	0.61	0.54	0.51	0.53	0.49
<i>ti</i>	1.61	1.03	0.60	1.69	1.46	1.69	1.78	1.18	1.15
Mode vol. %									
quartz	1.3	—	1.0	2.9	0.7	1.2	3.6	1.2	2.7
plagioclase	28.0	20.8	27.0	29.8	40.6	27.0	42.8	32.1	27.5
biotite	0.1	—	—	3.7	—	tr	0.9	—	—
chlorite	—	0.1	—	1.1	—	—	tr	0.1	2.9
garnet	—	—	—	—	—	—	tr	—	—
hornblende	70.3	76.9	68.0	60.8	58.4	68.0	51.5	61.5	61.2
clinopyroxene	—	—	—	—	—	—	—	—	—
epidote	0.1	1.3	0.2	0.1	0.1	1.3	tr	2.3	2.8
sphene	—	0.3	3.4	—	—	1.4	tr	2.1	1.3
apatite	—	0.2	tr	0.2	0.1	0.1	0.1	0.1	—
zircon	—	0.3	tr	0.1	tr	0.1	0.1	tr	tr
calcite	—	—	—	1.0	—	—	—	—	0.4
tourmaline	—	—	—	—	—	—	—	—	—
zeolites	—	—	—	—	—	0.7	—	—	—
opaque	0.1	0.1	0.3	0.3	0.1	0.1	1.0	0.6	1.1
An % in plagioclase	49	51	38	35	43	39	35	41	63-43
hornblende { 2V	-78°	-84°	-78°	-76°	-77°	-77°	-77°	-75°	-76°
{ <i>c:γ</i>	14°	15°	13°	16°	15°	14°	13°	14°	14°
clinopyroxene { 2V	—	—	—	—	—	—	—	—	—
{ <i>c:γ</i>	—	—	—	—	—	—	—	—	—

57821: 16.2 % of altered plagioclase.

75839: 1.67 % of altered plagioclase.

75895: 11.3 % of altered plagioclase.

(continued)

Table 4 (continued).

GGU No.	garnet-bearing green layers							
	73517	73519	73520	73846	73863	75815	75833	75838
Oxides wt. %								
SiO ₂	51.42	47.50	48.29	54.28	53.72	51.72	52.98	59.77
TiO ₂	2.40	2.59	1.00	0.92	1.86	0.45	0.81	0.86
Al ₂ O ₃	12.29	12.54	14.33	14.27	12.33	16.63	15.67	15.03
Fe ₂ O ₃	3.17	4.44	4.13	2.80	2.96	1.48	0.87	2.17
FeO.....	14.04	14.24	12.72	10.54	16.25	8.87	11.38	6.38
MnO.....	0.28	0.28	0.23	0.24	0.31	0.18	0.23	0.16
CaO.....	9.46	9.92	9.39	7.64	6.80	10.41	8.13	6.52
MgO.....	3.93	5.47	5.59	5.29	3.53	6.27	5.54	3.58
Na ₂ O.....	1.46	1.56	2.14	2.39	0.41	1.60	1.98	2.62
K ₂ O.....	0.20	0.34	0.26	0.31	0.19	0.52	0.35	0.32
P ₂ O ₅	0.05	0.04	0.02	0.01	0.13	0.02	0.06	0.03
CO ₂	—	—	—	—	—	—	—	—
H ₂ O ⁺	1.24	1.36	1.70	0.86	1.20	1.77	1.36	1.72
H ₂ O ⁻	0.10	0.12	0.19	0.07	0.03	0.06	0.03	0.09
	100.04	100.40	99.99	99.62	99.72	99.98	99.39	99.25
<i>mg</i>	0.29	0.34	0.37	0.41	0.25	0.52	0.44	0.43
<i>ti</i>	4.61	4.49	1.75	1.82	3.84	0.83	1.57	2.08
Mode vol. %								
quartz.....	15.5	7.3	5.4	5.0	36.7	11.7	4.5	13.7
plagioclase.....	33.6	14.2	27.7	49.6	5.5	10.3	44.7	54.3
biotite.....	0.6	—	—	0.6	0.2	0.7	tr	4.3
chlorite.....	—	—	—	—	0.9	2.2	0.4	2.0
garnet.....	13.9	4.7	8.1	1.1	26.9	10.6	5.1	0.2
hornblende.....	31.8	69.9	57.0	41.7	25.4	62.5	43.0	23.7
clinopyroxene.....	—	—	—	—	—	—	—	—
epidote.....	—	—	tr	—	—	0.7	0.3	—
sphene.....	—	2.0	0.1	—	—	tr	tr	tr
apatite.....	0.5	0.2	tr	0.1	0.9	0.3	tr	0.2
zircon.....	tr	—	0.1	tr	0.1	0.1	tr	0.1
calcite.....	—	—	tr	—	—	—	—	—
tourmaline.....	—	—	—	—	—	—	0.1	0.1
zeolites.....	—	—	—	—	—	—	—	—
opaque.....	4.1	1.7	1.5	1.8	3.4	0.9	1.8	1.4
An % in plagioclase.....	36	39	41	40	20	69	45	42
hornblende { 2V.....	-56°	-61°	-63°	-73°	-67°	-79°	-79°	-78°
{ <i>c</i> : <i>γ</i>	14°	11°	14°	14°	14°	15°	14°	12°
clinopyroxene { 2V.....	—	—	—	—	—	—	—	—
{ <i>c</i> : <i>γ</i>	—	—	—	—	—	—	—	—

75838: modal garnet probably underestimated because of its irregular distribution.

(continued)

Table 4 (continued).

GGU No.	light-green layers			garnet-bearing light-green layers		
	57872	73858	75904	57748	57794	75910
Oxides wt. %						
SiO ₂	48.28	50.40	56.98	46.28	48.39	48.18
TiO ₂	0.70	0.28	0.60	1.35	3.60	0.50
Al ₂ O ₃	14.84	15.03	15.67	14.90	12.60	13.38
Fe ₂ O ₃	4.15	1.64	1.65	2.63	6.84	3.27
FeO.....	8.48	8.25	6.87	9.34	14.65	8.95
MnO.....	0.22	0.19	0.24	0.22	0.23	0.21
CaO.....	12.69	12.90	8.34	12.48	8.88	12.90
MgO.....	7.21	7.91	4.23	10.58	2.89	8.01
Na ₂ O.....	1.76	1.29	2.07	1.18	1.02	2.05
K ₂ O.....	0.14	0.22	1.38	0.19	0.07	0.20
P ₂ O ₅	0.04	0.01	0.03	0.05	0.09	0.03
CO ₂	0.53	0.26	—	—	0.10	0.92
H ₂ O ⁺	0.99	0.97	1.41	1.12	0.97	1.73
H ₂ O ⁻	0.05	0.04	0.09	0.04	0.05	0.10
	100.08	99.39	99.56	100.36	100.38	100.43
mg.....	0.51	0.59	0.47	0.61	0.20	0.54
ti.....	1.16	0.48	1.31	2.07	6.79	0.82
Mode vol. %						
quartz.....	3.1	2.4	7.7	0.1	12.2	1.2
plagioclase.....	19.7	32.0	32.6	29.7	29.0	11.1
biotite.....	—	—	8.2	0.6	0.1	—
chlorite.....	—	—	2.7	—	—	0.7
garnet.....	—	—	0.4	8.6	8.6	4.0
hornblende.....	61.2	53.7	35.9	40.7	20.8	63.9
clinopyroxene.....	—	5.5	—	15.7	13.5	0.5
epidote.....	13.4	4.3	10.0	3.3	0.3	15.5
sphene.....	1.6	0.5	1.2	0.1	tr	1.4
apatite.....	0.1	0.2	0.5	0.1	0.7	0.3
zircon.....	tr	tr	0.1	—	—	tr
calcite.....	0.6	1.1	—	—	0.1	1.2
tourmaline.....	—	—	0.7	—	—	—
zeolites.....	—	—	—	—	—	—
opaque.....	0.3	0.3	tr	1.0	14.7	0.2
An % in plagioclase	68–36	78	45	53	40	71
hornblende { 2V ..	-73°	-77°	-76°	-77°	-49°	-76°
{ c:γ ..	15°	15°	15°	13°	13°	14°
clinopyroxene { 2V	—	+59°	—	+61°	+62°	—
{ c:γ	—	41°	—	39°	46°	—

75910: 0.34 % of altered plagioclase.

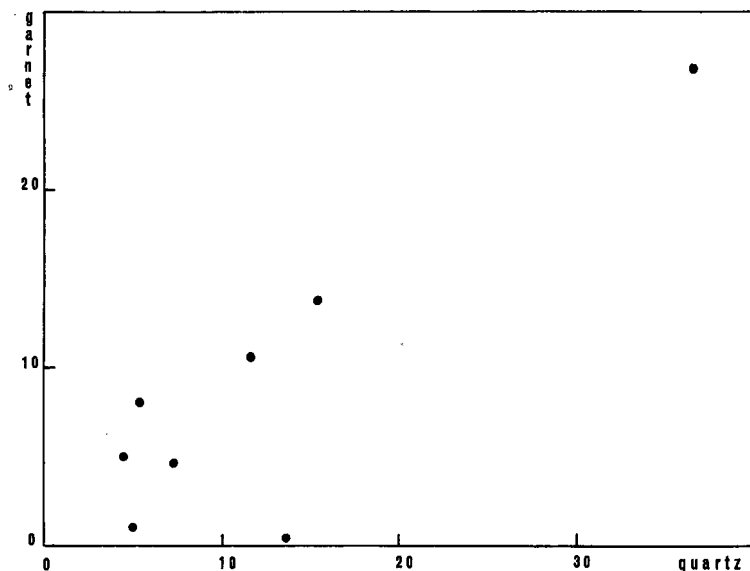


Fig. 11. Plot of modal quartz against modal garnet in the amphibolites of the garnet-bearing light-green layers (Table 4). A good positive correlation can be seen.

The following observations have been deduced from the modal analyses:

1) quartz is present in the majority of the samples. It reaches a maximum level when garnet is present in the hornblende-plagioclase-bearing layers. In these layers its increase is proportional to that of the garnet (fig. 11).

2) the normal amphibolites contain between 51–77 % hornblende; the light-green layers contain between 36–61 % hornblende; the green layers which possess garnet contain between 23–70 % hornblende, while the light-green layers which possess garnet contain 21–64 % hornblende.

3) the anorthite content in plagioclase is higher in the pyroxene-epidote (-garnet)-bearing layers than in the other types.

4) biotite occurs only in very small amounts in the various layers, regardless of their mineralogical composition.

As many of the mineralogical features are similar in the different layers, their mineralogy will be discussed together to avoid repetition; differences will be pointed out as they occur.

Hornblende is normally green with α = yellow, β = green (greyish, brownish green), γ = brownish green (green, bluish green). The $2V\alpha$ in the examined hornblendes is generally 70° , with a maximum of 84° . A good correlation exists between Niggli *mg* of the rocks and $2V$ of hornblende (fig. 12). Therefore, as the *mg* of the rock depends mainly on hornblende, it can be inferred that the $2V$ in hornblende largely depends

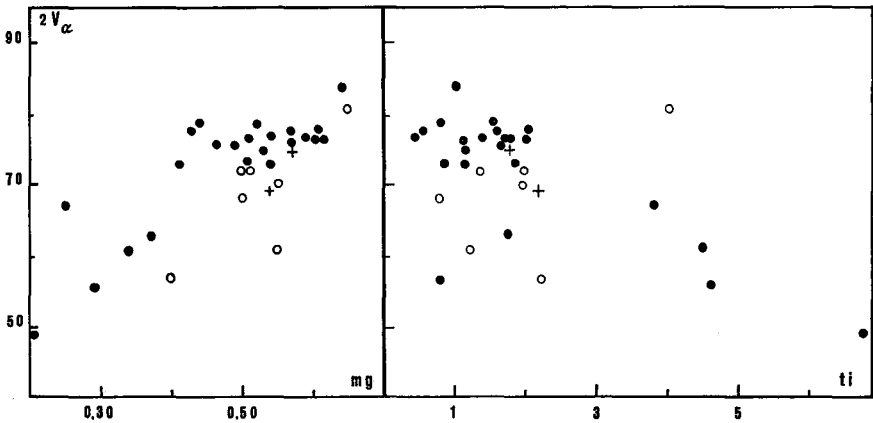


Fig. 12. Plot of Niggli *mg* and *ti* of the rocks against 2V of hornblendes. (Circles = amphibolite boudins in the gneisses; dots = major amphibolite layers, crosses = discordant amphibolite dykes).

on its magnesium content, in agreement with what was observed by WINCHELL & WINCHELL (1951, p. 434) and TRÖGER (1952, p. 77). A poorer correlation also exists between the 2V of hornblende and Niggli *ti* (fig. 12), but this is to be expected because the titanium in the rock does not depend only on hornblende, but also on the presence of titanium minerals such as ilmenite, sphene and rutile. Nevertheless, it is likely that titanium also influences the 2V in the sense that as titanium increases, the 2V decreases.

Secondary transformations to actinolite are often present. The chemical composition of a hornblende can be seen in Table 5.

Plagioclase has a wide range of composition with an average of An₄₀ and more than half the samples have an anorthite content between 35% and 45%.

Plagioclase is usually fresh but may possess some alteration to sericite and epidote. In the vicinity of a fault, plagioclase is completely recrystallised as albite. In one case the plagioclase was microantiperthitic (plate 2b), which is unusual because the antiperthites co-exist with an An content of 78%. A similar phenomenon, antiperthites on calcic plagioclase, was found by CAPEDE (1968) on high-grade metamorphic basic rocks of the Ivrea-Verbano zone in Italy. Sometimes an irregular zoning is present, with a core of An content between 60% and 70% rimmed by An between 35% to 45%.

Clinopyroxene occurs in the light-green layers as pale green (rarely colourless) pleochroic crystals, together with epidote. It is normally a diopsidic salite or augite. The optical data on pyroxene occurring in the analysed samples are reported in Table 4.

Pyroxene seems to be an unstable phase; it shows rounded resorption contacts towards the other minerals and is often substituted by alteration products such as saussuritic aggregates, iron oxides and epidote (which may replace it completely). Its relationship to hornblende is not clear; sometimes they seem to co-exist in equilibrium, while at other times it is partially replaced by hornblende either marginally or along cleavage planes. Actinolite is also seen replacing pyroxene. The relationship between pyroxene and hornblende can be represented by the following equation:

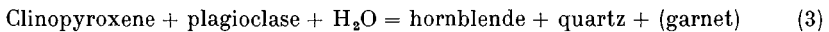


Table 5. *Chemical analyses of hornblende and garnet from amphibolites.*

GGU No.	Oxides wt. %		Number of ions on the basis of 24 (0)			
	57731 hornblende	57794 garnet	57731 hornblende		57794 garnet	
SiO ₂ ...	44.09	37.72	Si	6.496	Si	6.013
TiO ₂ ...	0.93	0.47	Al	1.504	Al	-
Al ₂ O ₃ ..	12.23	19.94	Al	0.619	Al	3.746
Fe ₂ O ₃ ..	2.81	2.14	Ti	0.104	Ti	0.056
FeO ...	11.88	26.32	Fe ³⁺ ...	0.311	Fe ³⁺ ...	0.257
MnO ...	0.23	0.68	Mg	2.541	Mg	0.839
CaO ...	11.64	8.17	Fe ²⁺ ...	1.464	Fe ²⁺ ...	3.509
MgO ...	11.57	3.53	Mn	0.029	Mn	0.092
Na ₂ O ..	1.11	0.06	Na	0.316	Na	0.016
K ₂ O ...	0.94	0.02	Ca	1.838	Ca	1.396
P ₂ O ₅ ...	0.10	-	K	0.176	K	0.003
H ₂ O ⁺ ..	2.02	-	OH	2.020		
H ₂ O ⁻ ..	0.15	0.17				
	99.70	99.22	2V	-78°	almandine	60.1
			c:γ	14°	andradite	8.0
			α	yellow	pyrope	14.4
			β	brownish green	grossular	15.9
			γ	dark green	spessartite	1.6

Clearly, the right-hand side of the equation represents lower metamorphic conditions or at least conditions in which the increase in the water pressure has led to disequilibrium between pyroxene and plagioclase.

Garnet occurs as pink poikiloblastic crystals, rich in inclusions of all the other minerals. In some thin sections it can be observed that the development of garnet either followed equation 3 above or equation 4 described later, by replacement of pyroxene (plate 3a).

The chemical composition of one garnet is reported in Table 5. It is rich in almandine, but an appreciable amount of grossular and pyrope are present.

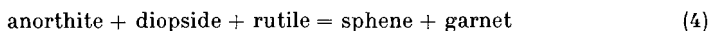
Quartz is present in small amounts in the majority of the samples. It occurs as both primary, irregular-shaped crystals and as small porphyroblasts derived from the reaction pyroxene-hornblende or hornblende-epidote.

Biotite occurs as brownish red pleochroic flakes which are frequently altered to chlorite (notably in shear zones). Sometimes biotite occurs in the cracks of garnets. Biotite was the last mafic, except for chlorite and epidote, to crystallise.

Epidote usually occurs as porphyroblasts of pistacite ($2V = -78^\circ$) but optically positive clinozoisite and allanite also occur. The formation of epidote is related to the calcium content of the rock.

Titanium minerals are represented either by ilmenite or by sphene. Rutile is absent because of the high iron content of the amphibolites. The ilmenite content may in some cases reach 15% (see for instance sample 57794, Table 4). It is unstable

and is partially replaced by sphene with the release of iron oxides. Sometimes sphene is the only titanium mineral in the rock. In some cases it is associated with garnet which suggests that the reaction



(RAMBERG, 1952, p. 73) has occurred. According to RAMBERG, the lower grade of metamorphism is represented by the right-hand side. This reaction is very clear in sample 73819 (plate 3a).

Accessory minerals are apatite, zircon, tourmaline, calcite, zeolites, pyrrhotite, calcopyrite and pyrite.

Chemistry

Chemical and modal analyses of amphibolites are reported in Table 4. These analyses are representative of the principal amphibolites of the area and are arranged in accordance with the different paragenetic bands to which they belong. RIVALENTI (1971) has undertaken a special study of the amphibolites and it is only noted here that the amphibolites generally have a non-alkaline composition which may be seen by plotting SiO_2 against $\text{Na}_2\text{O} + \text{K}_2\text{O}$.

Ultramafic rocks

Description

Ultramafic rocks occur as discontinuous lens-shaped bodies in the concordant amphibolites. They are easily recognisable in the field, even from a long distance, because of their rounded erosion surface which is red or grey in colour. A single lens may reach a maximum length of several hundred metres and a maximum thickness of 200 metres. The elongation of the lenses in a single amphibolite horizon is roughly parallel to the foliation of the amphibolite, which indicates that formerly the lenses were connected in a single horizon and their actual shape may be a tectonic phenomenon, such as boudinage. The untransformed ultramafics do not generally show any foliation except an occasional closely-spaced set of parallel fractures, and are fine- to medium-grained, equigranular rocks. Foliation is, however, present when serpentinite or talc rock replaces a peridotite. Contacts with amphibolites are always marked by a rim of pure hornblendite which rapidly grades into the amphibolite by enrichment with feldspar. The ultramafic lenses possess concentric zonation. Four zones can be distinguished which are from core to rim: a) nucleus; b) light-green zone; c) anthophyllite zone; d) hornblendite zone. It is worth noting that a similar zoning was found in ultramafic rocks by DAWES (1970), while working on J. A. D. Jensens Nunatakker and Dalagers Nunatakker north of the present area and by MISAŘ (in press) in the area north of Sermilik, see also WALTON (1966).

The transitions among the different zones, although appearing abrupt in the field, are gradational when observed under the microscope.

Petrography

Nucleus

The nucleus generally consists of peridotite, partially transformed outwards into serpentinite. When the transformation is very advanced serpentinite alone may form the nucleus. When untransformed, the peridotite core is massive, equigranular (seldom heterogranular) fine- to medium-grained with a composition that varies from pure dunite (90–100% olivine, STRECKEISEN, 1967) to amphibole-(mica-) peridotite which is normally an amphibole saxonite.

The *olivine* composition (Table 6) varies from Fo₇₀ (sample 57874, amphibole-mica saxonite) to a maximum Fo₉₈ (sample 73840, amphibole saxonite). Olivine occurs both as fresh subidiomorphic grains and partially altered to chrysotile and talc. In

Table 6. *Composition of olivines and orthopyroxene co-existing in ultramafic rocks.*

GGU Sample Nos.	olivine Fo %	orthopyroxene	
		2V	100 Mg Mg + Fe ²⁺ + Fe ³⁺ + Mn
57753.....	95	-72°	77
57786.....	93	+83°	93
57806.....	81	-	-
57814.....	88	-	-
57858.....	93	+85°	90
57860.....	90	-	-
57866.....	83	-83°	83
57870.....	87	-64°	71
57874.....	70	-	-
57888.....	91	-	-
58856.....	90	-	-
73566.....	89	-	-
73591.....	94	-	-
73809.....	87	-	-
73826.....	84	-86°	86
73839.....	94	+55°	100
73840.....	98	+85°	90
75813.....	83	-85°	85
75853.....	81	-80°	82

The Fo % in olivine has been determined by X-ray diffractometry (YODER & SAHAMA, 1957).

The composition of orthopyroxene has been optically determined (DEER, HOWIE & ZUSSMAN, 1963, vol. 2, p. 28).

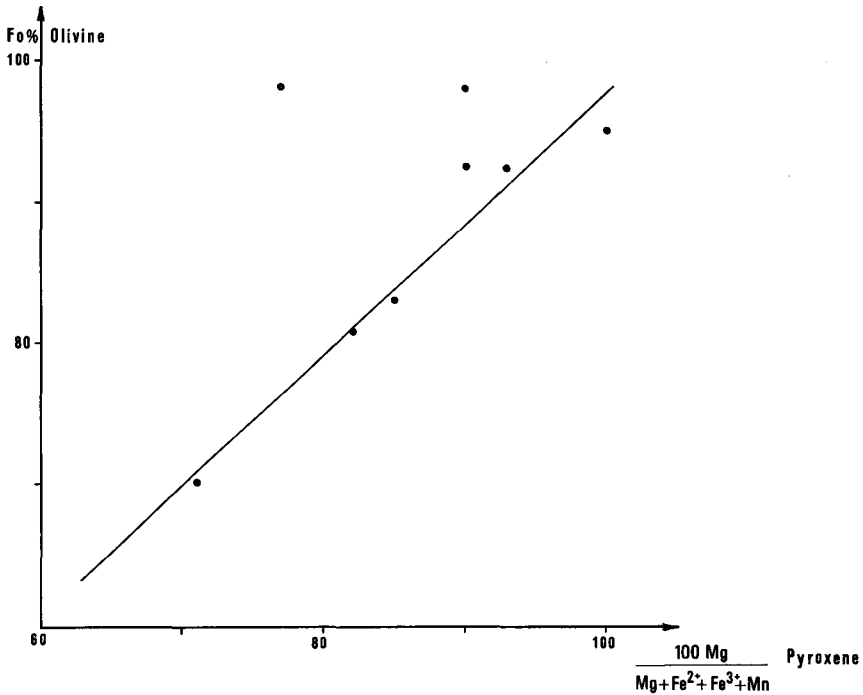
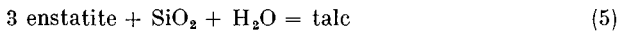


Fig. 13. Plot of Fo % in olivine against $100 \text{ Mg} / \text{Mg} + \text{Fe}^{2+} + \text{Fe}^{3+} + \text{Mn}$ in orthopyroxene from peridotites. The samples plot on a line at approximately 45° . Samples 57753 and 73840, which plot far from the line, are of orthopyroxene from monomineralic veins or masses.

some cases olivine (and the co-existing orthopyroxene and amphibole) appear to be derived from the recrystallisation of a former serpentinite. The serpentinite consists of large lamellae of chrysotile completely different in form and shape from those derived from the transformation of the peridotite nucleus (described in more detail below).

Orthopyroxene occurs in variable amounts but occurs in two forms: i) normally as crystals of the same size as olivine, and uniformly distributed in the rock; ii) rarely as monomineralic pegmatitic veins or masses in the ultramafic rock. The orthopyroxene composition varies from pure enstatite to hypersthene. The variations of Mg and Fe content in the pyroxene is directly correlated with the variation in olivine (see fig. 13). All the analysed samples plot on a line at approximately 45° , except two (57753 and 73840) in which pyroxene is present as monomineralic veins or masses cutting a dunite. The slope of the correlation line between pyroxene and olivine indicates that the two minerals have crystallised in equilibrium (RAMBERG & DEVORE, 1951; MEDARIS, 1969). Pyroxene has often been almost completely transformed into talc and in smaller amounts into amphibole and serpentinite. Talc probably developed by the reaction



(suggested by DEER, HOWIE & ZUSSMAN, 1963, vol. 2, p. 25).

Amphibole normally consists of a colourless or faintly pleochroic (pale green) magnesian hornblende. It has a 2V around 90° , and is sometimes positive and some-

times negative. Amphibole is present in the majority of the samples. Its relationship to olivine and orthopyroxene is not clear; in some cases amphibole seems to be a later transformation product, indicating disequilibrium, but in most cases no transformation contacts exist and amphibole exhibits a polygonal form (plate 3b) with 120° junctions indicating equilibrium (RAST, 1965).

Chlorite, identified by X-ray diffractometry, is constantly present as large colourless lamellae.

Carbonate is a minor, but common, constituent. Large xenoblasts of dolomite or magnesian calcite have crystallised among the other minerals. Carbonate may be related to the transformation of amphibole shown by plate 4a.

Accessory minerals are *phlogopite*, *clinopyroxene*, *spinel* and *opaque minerals*.

The serpentinite which forms the outer transformation zone of the peridotite consists of *chrysotile* and subordinate *antigorite*, with few relics of olivine, orthopyroxene or amphibole. The serpentinite is usually richer in carbonates than the peridotite and may contain some talc.

Light-green zone

This zone, not always present, occurs adjacent to either the serpentinite or the peridotite. It consists of a fine-grained rock with two main mineral assemblages. They are: 1) *amphibole-chlorite* (*-phlogopite*) (*-anthophyllite*) and 2) *talc-chlorite* (*-anthophyllite*). The former usually occurs as an inner shell, while the latter is more common as an outer zone.

Amphibole-chlorite assemblage.

The *amphibole* is very similar to that found in the nucleus. It is a faintly pleochroic type, sometimes replaced by talc, carbonates and chlorite. Its chemical composition can be seen in Table 7. An amphibole having a similar composition and classified as 'hornblende' has been reported by DEER, HOWIE & ZUSSMAN (1963, vol. 2, p. 276) as occurring in a hornblende-mica peridotite. Other occurrences of magnesian hornblendes have been described by several authors (see ESKOLA, 1952; LOSCHI GHITTONI, 1968). By comparing the present hornblende with that analysed by LOSCHI GHITTONI from a peridotite in granulite facies, it may be seen that the hornblende of sample 57867 has lower hexacoordinate Al and higher Mn and Fe.

Phlogopite occurs as small flakes. Its analysis is presented in Table 7. It has been classified as a phlogopite because the Mg/Fe ratio is higher than 2:1 (DEER, HOWIE & ZUSSMAN, 1963, vol. 3, p. 42).

Anthophyllite occurs rarely as prismatic crystals which cut across all other minerals.

Talc-chlorite assemblage.

Talc, with subordinate *chlorite* is predominant. *Anthophyllite* is more abundant than in the amphibole-chlorite assemblage but it is still scarce and may replace both talc and chlorite.

Anthophyllite zone

This is a peculiar shell which occurs towards the rim of the ultramafic body. The same association of minerals has also been found to cut

Table 7. *Chemical analyses of minerals of ultramafic lenses.*

GGU No.	Light-green zone		Anthophyllite zone	Hornblendite zone
	57867 amphibole	57867 phlogopite	57896 anthophyllite	57898 hornblende
Oxides wt. %				
SiO ₂	47.64	39.78	56.68	46.07
TiO ₂	0.70	0.90	tr	0.55
Al ₂ O ₃	8.54	14.94	1.33	10.51
Fe ₂ O ₃	1.35	1.50	1.08	5.10
FeO	6.53	6.40	10.20	7.48
MnO	0.12	0.04	0.26	0.22
CaO	9.73	0.60	0.42	12.09
MgO	19.55	21.92	28.15	15.42
Na ₂ O	1.14	0.18	tr	0.80
K ₂ O	0.67	9.00	tr	0.34
P ₂ O ₅	—	—	tr	0.05
H ₂ O ⁺	2.79	4.53	2.26	1.85
H ₂ O ⁻	0.45	0.75	0.21	0.13
	99.21	100.54	100.59	100.61
Number of ions on the basis of 24 (0)				
Si	6.770 } 8.000	5.660 } 8.000	7.746 } 7.959	6.623 } 8.000
Al	1.230 } 8.000	2.340 } 8.000	0.213 } 7.959	1.377 } 8.000
Al	0.200 } 5.351	0.166 } 5.835	— } 7.099	0.403 } 5.213
Ti	0.075 } 5.351	0.097 } 5.835	— } 7.099	0.060 } 5.213
Fe ³⁺	0.144 } 5.351	0.161 } 5.835	0.110 } 7.099	0.522 } 5.213
Mg	4.140 } 5.351	4.646 } 5.835	5.732 } 7.099	3.303 } 5.213
Fe ²⁺	0.777 } 5.351	0.761 } 5.835	1.166 } 7.099	0.898 } 5.213
Mn	0.015 } 1.919	0.004 } 1.771	0.029 } 7.099	0.027 } 2.144
Na	0.316 } 1.919	0.048 } 1.771	— } 7.099	0.221 } 2.144
Ca	1.481 } 1.919	0.091 } 1.771	0.062 } 7.099	1.862 } 2.144
K	0.122 } 1.919	1.632 } 1.771	— } 7.099	0.061 } 2.144
OH	2.626	4.324	2.036	1.799
2V	+88°	nd	+89°	-81°
<i>c</i> : <i>γ</i>	18°			18°
<i>α</i>	nd (colourless)	nd (light yellow)	1.622 (colourless)	1.646 (yellow)
<i>β</i>	nd (colourless)	nd (light brownish red)	1.644 (colourless)	1.659 (green)
<i>γ</i>	nd (colourless)	nd (light brownish red)	1.649 (colourless)	1.672 (bluish green)

nd = refractive index not determined.

the ultramafic mass as an irregular network of veins. It consists of a zone, from 1 to 20 cm wide, of asbestos crystals of anthophyllite in a radial arrangement. According to WALTON (1966), this feature indicates a post-tectonic crystallisation. Its chemical composition can be seen in Table 7. Anthophyllite replaces talc with which it is often associated, but subsequently it is itself partially transformed into talc.

Hornblendite zone

This is the outermost zone of the ultramafics and is directly enclosed by the amphibolite. The passage from hornblendite to amphibolite takes place within a few centimetres by progressive enrichment in salic minerals. The inner contact of the hornblendite zone is separated from the anthophyllite zone by a thin shell of a talc-amphibole assemblage in which the green hornblende appears. The hornblendite shell has a fairly constant thickness of about 20 or 30 cm regardless of the total size of the ultrabasic body of which it forms part. Normally it consists of more than 90 % hornblende. Small amounts of ilmenite, sphene, quartz, biotite and apatite may also be present. More rarely the hornblende is accompanied by large amounts of clinopyroxene.

The *hornblende* is greenish to greenish brown in colour. Its chemical composition is represented in Table 7. Pyroxene is present in only two of the examined samples. It is an augite or a faintly pleochroic diopside varying from colourless to pale green. Hornblende seems to have crystallised later than, and as a transformation product from, clinopyroxene, because it occurs as a rim around the pyroxene or along its cleavages.

When in contact with pegmatites, the hornblendite rim is partially transformed into biotite. Sometimes tourmaline, and in one case even beryl, occur in conjunction with biotite.

Chemistry

Seven samples of ultramafics have been chemically analysed and the results are reported in Table 8. Some of them represent zones of the same lens. In the diagram of fig. 14 the various oxides are plotted against SiO_2 to show the variations between the different zones of the same lens. Passing from the nucleus to the green zone, there is an increase in SiO_2 , Al_2O_3 , FeO , CaO , Na_2O and a decrease in Fe_2O_3 , MgO , K_2O . In the hornblendite zone, SiO_2 , Al_2O_3 , CaO and Na_2O increase further whilst Fe_2O_3 also increases, and FeO and MgO decrease in respect to the green zone. The variations between the nucleus and the green zone, although

Table 8. *Chemical composition and mineral assemblages of ultramafic rocks.*

GGU No.	57858	57862	57866	57867	57888	57889	57890
Oxides wt. %							
SiO ₂	41.75	39.36	45.07	49.13	41.90	46.71	47.65
TiO ₂	0.49	0.49	0.58	0.70	0.34	0.42	0.48
Al ₂ O ₃	2.93	3.69	6.25	6.85	5.22	9.30	11.08
Fe ₂ O ₃	2.55	7.94	2.16	1.23	2.75	0.35	1.10
FeO	9.88	7.17	6.39	8.22	6.67	9.28	8.83
MnO	0.21	0.17	0.21	0.16	0.16	0.18	0.20
CaO	2.66	3.61	5.96	7.67	5.02	7.43	10.97
MgO	38.15	30.59	28.02	22.26	30.95	21.67	16.27
Na ₂ O	0.01	0.17	0.48	0.78	0.28	0.81	1.28
K ₂ O	0.01	0.01	1.08	0.75	0.56	0.05	0.13
P ₂ O ₅	0.05	0.06	0.03	0.02	0.03	0.03	0.03
CO ₂	—	0.34	—	—	0.45	0.20	—
H ₂ O ⁺	1.19	6.89	3.84	2.09	5.02	3.02	1.36
H ₂ O ⁻	0.07	0.14	0.11	0.05	0.09	0.08	0.08
	99.95	100.63	100.18	99.91	99.44	99.53	99.46

Mineral assemblages

- 57858: Amphibole saxonite. Olivine (70–80 %), orthopyroxene (5–10 %), amphibole (5 %), chlorite (5 %), opaque.
- 57862: Serpentinite. Chrysotile (70 %), amphibole (10–20 %), chlorite (5–10 %), carbonates, opaque.
- 57866: Amphibole saxonite. Olivine (30–40 %), orthopyroxene (10–20 %), amphibole (30–40 %), talc, chrysotile, chlorite.
- 57867: “Green zone”. Amphibole (80–90 %), phlogopite (5 %), chlorite, opaque.
- 57888: Amphibole peridotite. Olivine (40–50 %), amphibole (30–40 %), chlorite, chrysotile (10–20 %), opaque, carbonate.
- 57889: “Green zone”. Colourless Mg-amphibole (40–50 %), green hornblende (40–45 %), chlorite (10–20 %), opaque, carbonates.
- 57890: Hornblendite. Pale green hornblende.

57866, 57867: nucleus and “green zone” respectively of the same ultramafic.

57888, 57889, 57890: nucleus, “green zone”, hornblendite zone respectively of the same ultramafic.

having different absolute values, are similar in both the occurrences examined.

It is reasonable to believe that the chemical variations shown above are a consequence of metasomatic exchanges with the country rock.

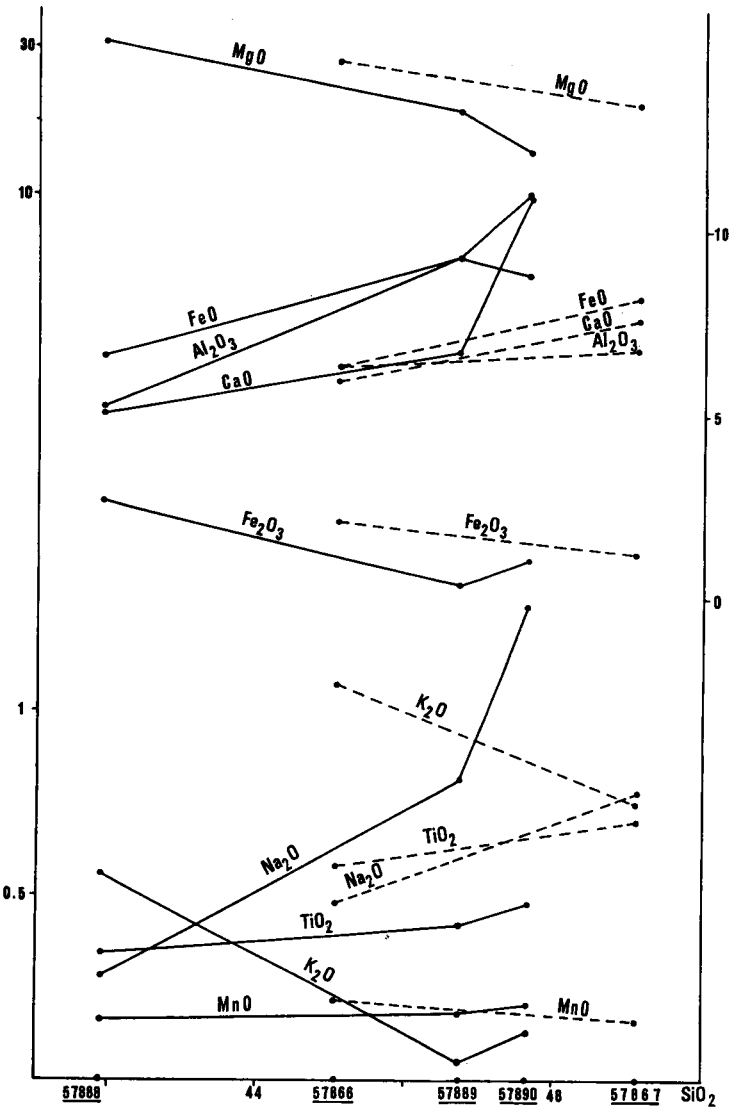


Fig. 14. Chemical variations of the major oxides against SiO_2 in ultramafic lenses. Samples 57888, 57889 and 57890 are the nucleus, green zone and hornblende zone, respectively, of the same lens. Samples 57866 and 57867 are the nucleus and green zone of the same lens.

Rusty schist

Description

Rusty coloured rocks are frequently seen in the field. This coloration is most often due to a superficial alteration of mafic rocks: amphibolites, ultramafics and sometimes dykes. But in one case the rusty-brown colour helps one to recognise a lithological type: the rusty schist. The colour is in this case mainly due to the weathering of biotite. However, small amounts of sulphides such as pyrite, chalcopyrite and pyrrhotite, have been found, and their alteration contributes to the colour of the rock surface. The rusty schist forms thin, normally single, layers of rock which lie conformably within the concordant amphibolites. These rusty horizons are, in spite of being thin, very continuous; in the amphibolite complex which passes north of mountain 933 m, rusty schist is found inside the amphibolite for a distance of several tens of kilometres with a maximum thickness of only 20 m. Thus it provides a good marker horizon. In other cases the thin rusty schist band is limited to an intercalation a few centimetres or tens of centimetres wide.

The importance of the rusty schist arises also from the fact that it shows the best preserved primary lithological contacts in the area: those between rusty schist and amphibolite, and between quartzite layers and more pelitic layers within the rusty horizons. These lithological distinctions, whose primary origin can hardly be doubted, are preserved because the enclosing, comparatively resistant, amphibolite has protected the schist from the affects of migmatisation and consequently metamorphism of the schist has taken place in a closed system. Where the protective amphibolite layer is lacking, the rusty schist passes gradually into a normal biotite and garnet-bearing gneiss.

Petrography

There are several pointers to the metasedimentary origin of the rusty schist. The rock consists of a regular alternation of beds whose composition varies from pure quartzite to argillaceous sandstone. Graphite is common, mainly in the beds which closely approach pelite in composition. The mineral assemblages are varied, reflecting both original differences and metamorphic differentiation. The most important assemblages, excluding the almost monomineralic quartzites, are: 1) a *biotite-garnet-sillimanite assemblage* consisting of quartz, plagioclase, biotite, garnet, \pm sillimanite, (K-feldspar, muscovite, epidote, rutile); and 2) an *anthophyllite assemblage* with quartz, plagioclase, anthophyllite (or hornblende), (muscovite, epidote, rutile). The first assemblage, which

best reflects the original composition, is found in layers regularly alternating with quartzites and is by far the most common. The second, which is rare, is derived from the first through transformations described later.

Table 9. *Chemical and modal composition of rusty schists.*

GGU No.	biotite-garnet-sillimanite assemblage						
	57820	57856	58884	73590	73859	75805	75842
Oxides wt. %							
SiO ₂	60.24	61.77	64.70	56.85	65.82	66.11	67.39
TiO ₂	1.15	2.20	0.51	1.11	0.49	0.69	0.40
Al ₂ O ₃	17.01	18.03	16.56	19.75	16.94	17.20	16.43
Fe ₂ O ₃	0.02	1.01	2.50	1.27	0.89	1.35	0.81
FeO	8.03	7.11	1.62	8.32	2.40	3.87	1.79
MnO	0.18	0.23	0.07	0.24	0.04	0.03	0.03
CaO	4.20	3.71	2.59	4.10	4.98	3.36	4.84
MgO	3.53	2.17	1.96	2.85	1.97	1.81	1.91
Na ₂ O	2.36	2.11	4.12	2.16	3.69	2.51	2.54
K ₂ O	1.23	0.24	1.36	1.12	1.23	0.83	1.20
P ₂ O ₅	0.02	0.09	0.01	0.02	0.03	0.03	0.03
H ₂ O ⁺	1.69	0.67	3.04	1.50	0.72	1.43	1.82
H ₂ O ⁻	0.12	0.13	0.20	0.13	0.12	0.13	0.13
	99.78	99.47	99.24	99.42	99.32	99.35	99.32
Mode vol. %							
quartz	12.5	21.8	16.3	11.1	23.7	20.8	29.0
plagioclase	56.4	57.2	42.6	50.1	61.6	50.2	54.4
K-feldspar	0.4	0.1	0.1	—	—	—	0.2
biotite	15.6	6.0	17.6	20.1	13.1	13.8	5.7
garnet	12.0	10.7	12.2	11.7	0.6	4.9	—
sillimanite	—	3.4	7.6	4.0	—	5.5	—
staurolite	—	0.1	0.2	tr	—	—	—
amphibole	—	—	—	—	—	—	—
cordierite	—	—	tr	—	—	—	—
kyanite	—	—	—	—	—	—	—
muscovite	—	—	0.3	1.0	0.1	3.6	1.0
chlorite	tr	—	1.2	tr	0.2	—	5.7
epidote	0.3	—	0.4	—	0.2	—	2.9
calcite	—	—	—	—	—	—	—
rutile	0.1	0.1	0.1	0.2	—	—	0.1
tourmaline	tr	tr	tr	—	—	—	—
zircon	tr	tr	tr	0.1	tr	tr	tr
apatite	0.2	—	—	—	0.1	—	0.1
opaque	2.4	0.5	1.3	1.6	0.4	1.2	0.8
An % in							
plagioclase	39	38	31	36	31	31	50

(continued)

Table 9 (continued).

GGU No.	biotite-garnet-sillimanite assemblage				anthophyllite assemblage	
	75880	75884	75892	75898	75899	75900
Oxides wt. %						
SiO ₂	64.71	58.93	57.22	67.00	59.05	59.53
TiO ₂	0.50	1.26	0.70	0.43	1.45	1.59
Al ₂ O ₃	15.06	18.47	18.00	14.84	18.25	18.41
Fe ₂ O ₃	0.55	0.29	1.72	1.22	0.28	0.49
FeO	5.03	5.46	10.21	2.73	3.58	2.67
MnO	0.27	0.18	0.53	0.12	0.09	0.06
CaO	5.68	6.03	4.07	5.75	9.74	9.95
MgO	3.12	3.43	5.14	2.37	5.24	5.04
Na ₂ O	0.86	3.00	0.31	1.04	0.58	0.34
K ₂ O	1.62	1.11	0.25	1.96	0.07	0.06
P ₂ O ₅	0.04	0.06	0.01	0.04	0.02	0.04
H ₂ O ⁺	1.80	1.06	1.65	1.55	1.12	1.08
H ₂ O ⁻	0.14	0.08	0.23	0.13	0.08	0.08
	99.38	99.36	100.04	99.18	99.55	99.34
Mode vol. %						
quartz	39.3	14.4	a	37.8	30.8	32.2
plagioclase	34.5	59.3	va	36.7	47.7	39.2
K-feldspar	0.1	—	—	—	1.1	—
biotite	21.0	16.0	a	17.5	8.9	—
garnet	2.3	5.0	a	1.4	—	—
sillimanite	—	—	a	—	—	—
staurolite	—	0.2	—	—	—	—
amphibole	—	—	—	—	2.8	23.4
cordierite	—	—	tr	—	0.3	—
kyanite	—	—	tr	—	—	—
muscovite	0.2	0.1	—	2.1	—	—
chlorite	—	1.6	—	—	5.9	1.1
epidote	—	1.5	—	2.9	0.9	3.1
calcite	—	—	—	0.4	—	—
rutile	—	0.2	tr	tr	1.1	0.7
tourmaline	0.1	—	a	—	—	—
zircon	tr	tr	—	tr	tr	—
apatite	0.6	0.4	—	tr	0.4	—
opaque	1.9	1.2	—	1.1	—	0.2
An % in plagioclase ...	80-60	48	89	80-62	89	89

75892: modal analysis not made owing to the irregular grain size and distribution of the minerals, (va = very abundant; a = abundant; tr = traces).

75899: anthophyllite. $2V = + 79^\circ$.

75900: hornblende. $2V = 90^\circ$; $c: \gamma = 16^\circ$.

75880 and 75898: zoned plagioclase. The zones with An 80 % are micro-antiperthitic.

Table 10. *Chemical analyses of co-existing garnets, biotites and of an amphibole from the rusty schists.*

GGU No.	Garnets				Biotites				Amphibole
	57820	57856	75880	75884	57820	57856	75880	75884	75900
Oxides wt. %									
SiO ₂	37.32	39.16	38.01	39.78	35.40	35.73	38.05	37.90	47.96
TiO ₂	0.67	0.25	0.15	0.50	2.61	1.70	1.65	2.00	1.36
Al ₂ O ₃	22.74	20.57	25.99	21.72	17.84	18.41	18.38	18.22	14.09
Fe ₂ O ₃	1.59	0.26	1.61	1.74	2.37	2.77	2.31	1.92	1.79
FeO	26.50	28.96	19.27	23.48	11.45	13.32	11.89	13.09	6.45
MnO	1.25	1.04	10.40	0.98	tr	tr	0.36	0.06	0.15
CaO	2.73	3.15	3.64	2.84	0.77	0.67	0.95	1.26	10.61
MgO	7.21	5.64	1.41	8.84	13.81	11.62	12.10	12.50	12.23
Na ₂ O	0.07	0.05	0.09	0.03	0.18	0.31	0.12	0.28	0.69
K ₂ O	0.07	0.04	0.13	0.05	8.00	7.90	8.64	7.94	0.17
H ₂ O ⁺	-	-	-	-	5.26	4.58	4.59	4.56	2.68
H ₂ O ⁻	0.33	0.12	0.25	0.04	1.58	1.00	0.40	0.70	0.69
	100.48	99.24	100.95	100.00	99.27	98.01	99.44	100.43	98.87

Number of ions on the basis of 24(0)

Si	5.794	6.172	5.885	6.067	5.220	5.401	5.573	5.523	6.780
Al	0.206	-	0.115	-	2.780	2.599	2.427	2.477	1.220
Al	3.957	3.822	4.629	3.905	0.320	0.680	0.746	0.651	1.129
Ti	0.077	0.045	0.018	0.058	0.289	0.194	0.182	0.220	0.145
Fe ³⁺	0.186	0.030	0.188	0.200	0.263	0.315	0.255	0.210	0.190
Mg	1.669	1.324	0.326	2.008	3.035	2.529	2.642	2.714	2.578
Fe ²⁺	3.440	3.816	2.495	2.994	1.412	1.683	1.455	1.594	0.762
Mn	0.165	0.139	1.365	0.126	-	-	0.045	0.008	0.017
Na	0.020	0.016	0.027	0.007	0.050	0.091	0.034	0.080	0.189
Ca	0.453	0.531	0.604	0.464	0.121	0.079	0.150	0.196	1.607
K	0.036	0.008	0.026	0.009	1.505	1.524	1.614	1.475	0.031
OH	-	-	-	-	5.186	4.596	4.452	4.430	2.528
almandine	60.1	65.7	52.1	53.5	α	pale yellow	pale yellow	pale yellow	colourless
andradite	6.9	1.9	6.5	6.9	β = γ	reddish	reddish	reddish	pale greyish
pyrope	29.1	22.8	6.8	35.9		brown	brown	brown	brown
grossular	1.0	7.2	7.1	1.4					2V 90°
spessartite	2.9	2.4	28.5	2.3					c:γ 16°

Biotite-garnet-sillimanite assemblage.

Modal analyses of samples belonging to this group are reported in Table 9. The minerals have the following characteristics:

Quartz is always abundant and consists of crystalloblasts which show undulose extinction.

Plagioclase occurs in variable amounts usually as fresh, twinned crystals. Its composition varies between An_{31} and An_{89} . The CaO content of the rock does not vary with increasing An content but there is a significant decrease in Na_2O (Table 9). The more anorthitic feldspars present an irregular recrystallisation with zones of An_{80} and An_{60} (see samples 75880 and 75898, Table 9, plate 4b). The parts with 80 % An are micro- (almost crypto-) antiperthitic (plate 4b) which is unusual in such calcic plagioclases. A similar phenomenon (anthiperthites in calcic plagioclases) has been described in granulite facies rocks of the Alps (CAPEDRI, 1968). Rusty schists with plagioclases containing 80 % An are limited to the amphibolite of mountain 933 m, at the zone between mountain 880 m and mountain 760 m in the eastern part of the area.

K-feldspar is normally rare and occurs as microcline. But small, roundish patches of orthoclase occur, however, inside the microperthitic plagioclase described above.

Biotite is the commonest mafic mineral. It is pleochroic from α = yellow or colourless, to $\beta = \gamma$ = reddish brown. Analyses of four biotites co-existing with garnet are reported in Table 10. Biotite has complex relationships with garnet and sillimanite (described below under the sections on garnet and sillimanite). It is sometimes altered to chlorite in association with the alteration of garnet and plagioclase as a consequence of local retrogression due to faulting. It may also be associated with large flakes of muscovite.

Garnet presents some interesting features. It occurs both as deformed porphyroblasts (elongated in the plane of the foliation) that are strongly poikilitic and corroded by quartz and feldspar, and as crystals that are much more compact and poor in inclusions and look undeformed, yet which still have corroded rims. The two types may occur together in the same thin section. The compact, more idioblastic, garnet may occur as an outer zone around the strongly poikilitic type. Moreover atoll structures, such as those described by RAST (1965), are sometimes present (plate 5a). Biotite presents complex relationships to garnet. The following observations have been made:

a) garnet has grown without pushing aside the biotite matrix, whereas the biotite laminae are interrupted without any deformation by garnet: b) biotite occurs as inclusions inside garnet, which should not be expected since, according to RAMBERG (1952, p. 134), the interfacial energy between garnet and (001) in biotite is high; c) biotite occurs as veins cutting across garnet; d) biotite is pushed apart and wraps around the growing garnet.

Of particular interest are the inclusions found in garnet. They consist of quartz, plagioclase, biotite, staurolite, sillimanite, rutile and opaque minerals. The quartz grains forming the inclusions are smaller than both the quartz grains of the matrix and of the quartz which corrodes the garnet. The same holds good for feldspar. Sometimes quartz and feldspar, both singly and as aggregates, may present a pseudo-idioblastic hexagonal or polygonal shape inside garnet (plate 5b). Sillimanite is a rare inclusion, but in one case, biotite, sillimanite and fibrolite occur in the inner part of an atoll garnet (plate 7a). In this case fibrolite is clearly formed on biotite and after

sillimanite. Opaque minerals are represented by granules of ilmenite either orientated in planes which are parallel to the foliation of the rock, indicating that garnet crystallisation post-dates the development of the S-surface (TURNER & WEISS, 1963, p. 208), or having a concentric arrangement (plate 6a & b).

Analyses of garnets are reported in Table 10.

Sillimanite occurs in variable amounts. It may be associated with biotite, muscovite, or with sericite. The association with sericite is clearly due to low metamorphic grade, possibly deuteric transformation, but the association with muscovite has important metamorphic implications which will be discussed later on (page 64). Fibrolite is uncommon, but in a few cases has been derived from large crystals of sillimanite (plate 7a).

Staurolite has been observed in small amounts in only three of the samples examined (Table 9). It always occurs as irregular, corroded crystals inside garnet and it therefore appears to be an unstable relic phase.

Kyanite has been observed in only one sample as a small crystal. It has not been possible to establish its relation to sillimanite which occurs in the same sample and its significance is therefore doubtful.

Muscovite may be present in large amounts. It is always secondary after biotite or sillimanite. Its significance will be discussed later on.

Rutile is common as large crystals in most of the samples studied and, apart from ilmenite, represents the sole titanium mineral. It plays an important role in determining the pressure to which these rocks have been subjected.

Accessory minerals include tourmaline (sometimes very abundant), epidote, zircon, apatite and in one case a very small amount of calcite. Opaque minerals include small grains of graphite, pyrrhotite, pyrite, ilmenite and in one case marcasite (57820).

Anthophyllite assemblage.

A rusty schist with this assemblage has only been found between the mountains 880 m and 760 m in the eastern part of the area (plate 11). Two samples have been taken, one (75899) from the limb and the other (75900) from the hinge of a F_4 fold. Their modal analyses are reported in Table 9. They deserve two separate descriptions because of the different significance of their mineral assemblage.

Sample 75899 is a greyish rock consisting of the following minerals: *Plagioclase* is very fresh, twinned and with An_{30} . *Quartz* shows undulose extinction. *Anthophyllite* occurs as altered porphyroblasts and is clearly secondary after biotite. K-feldspar is formed during this reaction and remains either as small inclusions or as crystals wrapped around the anthophyllite. A reaction giving these products is reported by RAMBERG (1952, p. 152):



The 2V is approximately $+80^\circ$ indicating that iron is present in this amphibole.

Biotite is a relic phase. It is represented by the reddish brown type typical of the rusty schist. *Cordierite* is very difficult to identify because it occurs sporadically and is almost completely transformed into a pinite aggregate. *Rutile* forms large crystals. Some apatite, epidote, and chlorite are present as accessory minerals.

Sample 75900 differs from sample 75899 owing to the presence of an *amphibole* which in a hand sample is yellowish and in thin section is pleochroic, ranging from

colourless (α) to pale greyish brown ($\beta = \gamma$). It forms lineations with the same trend as the F_4 fold axis. Its analysis is reported in Table 10. This hornblende is formed by the reactions

$$\text{anorthite} + \text{anthophyllite} = \text{hornblende} + \text{SiO}_2 \quad (7)$$

Quartz is released during this reaction and remains poikilitically included in the hornblende or forms porphyroblasts at its border.

Biotite is completely absent. The other characteristics are the same as in sample 75899.

Chemistry

Thirteen chemical analyses of rusty schists, representing all lithological varieties except quartzite, are presented in Table 9. Eleven analyses are of rocks with a biotite-garnet-sillimanite assemblage and two have an anthophyllite assemblage. Analyses of co-existing biotite and garnet in four samples of rusty schist are presented in Table 10 and discussed together with the metamorphism (p. 62).

The original rocks were sandstone, represented now by quartzites, and more pelitic rocks, represented now by rocks with high Al_2O_3 content and with sillimanite. The low alkalis, especially K_2O , indicate, however, that little clay was present in the original rock, and therefore the analyses suggest an original greywacke composition; in particular the analyses are comparable with those of certain rare aluminous greywackes (PETT-JOHN, 1957, p. 306).

There is no correlation between the anorthite content of the plagioclase and the CaO content of the rock. There is, however, a negative correlation between the anorthite content of the plagioclase and the Na_2O content of the rock.

The anthophyllite(-cordierite)-bearing rocks have the lowest alkali content and their composition does not correspond with that of any sedimentary or igneous rock.

Microgranodiorite

Description

This is a lithotype seldom met with in the area. It is usually granodioritic or quartz dioritic in composition. It outcrops in the form of small, thin, lenticular bodies, which are normally too small to be mapped, concordantly inside the amphibolites. Only in two cases, in the hinge zones of F_4 folds near mountain 933 m and between mountains 880 and 760 m, were they sufficiently large to be indicated on the map. The microgranodiorite is a fine-grained generally homogeneous rock which in some places possesses nebulitic structures.

Table 11. *Chemical and modal composition of microgranodiorite.*

GGU No.	57813	58887	75835		57813	58887	75835
	Oxides wt. %				mode vol. %		
SiO ₂	58.36	67.41	70.19	quartz	6.1	30.8	33.2
TiO ₂	0.74	0.49	0.40	plagioclase	68.5	57.1	49.0
Al ₂ O ₃	19.11	15.99	15.49	microcline	—	0.4	3.2
Fe ₂ O ₃	1.33	0.86	0.62	biotite	14.2	7.0	10.4
FeO	5.88	2.76	1.60	garnet	0.8	—	—
MnO	0.22	0.10	0.03	hornblende	9.1	0.4	—
CaO	5.54	5.22	2.80	muscovite	—	—	3.8
MgO	2.02	2.02	1.31	chlorite	tr	—	tr
Na ₂ O	3.70	3.64	4.52	epidote	—	tr	—
K ₂ O	1.06	0.83	2.16	sphene	tr	4.0	—
P ₂ O ₅	0.11	0.02	0.01	apatite	0.3	0.1	0.2
H ₂ O ⁺	1.03	0.66	0.67	zircon	0.1	tr	0.1
H ₂ O ⁻	0.13	0.09	0.06	rutile	—	tr	—
	99.23	100.09	99.86	opaque	0.9	0.2	0.1
				An % in plag. . .	39	39	29

Petrography

The three modal analyses (Table 11) of this rock indicate that the association quartz, plagioclase, (microcline), biotite, garnet, (hornblende) is the commonest; some of the more interesting mineralogical characteristics are as follows:

Biotite is always a reddish brown colour, identical to that of the rusty schist. *Microcline* occurs in variable amounts. *Plagioclase* varies in composition from An₂₉ to An₃₉. *Garnet* only occurs in one sample where it forms pink, idioblastic crystals poor in inclusions. *Hornblende* is the usual bluish green type similar to that encountered in the gneisses. *Rutile* occurs as large crystals as a primary mineral associated with ilmenite. *Epidote* and *muscovite* are common as secondary minerals.

A general retrogression is present in the area of the large N-S fault near the large lake between the mountains 880 and 760 m. Signs of recrystallisation are evident, such as indented rims to some of the minerals, substitutions by microcline, formation of albite, chlorite and epidote.

Chemistry

Three samples have been chemically analysed and the results are reported in Table 11. Their composition varies from granodiorite to quartz diorite. The chemistry of these rocks is similar to that of migmatitic gneisses bearing the same minerals.

In Table 12 the chemical analyses of co-existing garnet and biotite of one sample are reported. Its significance will be considered later (p. 66).

Table 12. *Chemical composition of co-existing garnet and biotite in a microgranodiorite.*

GGU No.	57813		Number of ions on the basis of 24 (0)				
	Oxides wt. %		garnet		biotite		
	garnet	biotite					
SiO ₂	37.16	36.18	Si	5.869	} 6.000	5.443	} 8.000
TiO ₂	0.57	1.60	Al	0.131			
Al ₂ O ₃	20.70	18.54	Al	3.724	} 4.152	0.730	} 5.611
Fe ₂ O ₃	3.03	4.03	Ti	0.067			
FeO	25.92	16.19	Fe ⁺³	0.361	} 5.820	0.457	} 1.528
MnO	2.35	0.12	Mg	0.983			
CaO	6.31	1.47	Fe ⁺²	3.424	} 5.820	2.036	} 1.528
MgO	4.17	9.78	Mn	0.314			
Na ₂ O	0.10	0.22	Na	0.028	} 5.820	0.063	} 1.528
K ₂ O	0.02	6.40	Ca	1.068			
P ₂ O ₅	0.03	0.06	K	0.003	} 5.820	1.228	} 1.528
H ₂ O ⁺	—	3.94	OH	—			
H ₂ O ⁻	0.17	0.72					
	100.53	99.25	almandine	59.2		α pale yellow	
			andradite	11.1		β brownish red	
			pyrope	17.0		γ brownish red	
			grossular	7.3			
			spessartite	5.4			

Inclusions in the Gneisses

Amphibolites

Description

The boudins and schlierens of amphibolite which occur in the gneisses can be divided into two categories: 1) those which have been migmatized and are fringed by a marginal zone of hornblende gneiss and 2) boudins which have arisen by the deformation of an amphibole, without evident introduction of new material. The layering which was present in the continuous amphibolite horizons can often be recognised in the boudins.

Petrography

In the first type, quartz, biotite and feldspar increase progressively from the centre to the rim of the amphibole inclusions. Biotite forms from hornblende, epidote and sphene are other products of this reaction (see p. 18) and the anorthite content of the plagioclase decreases from the

Table 13. *Chemical and modal composition of inclusions in the gneisses.*

GGU No.	Amphibolites							Calc-silicate inclusion 57759
	Type 1			Type 2				
	57787A	57787B	57891	57721	57759	58805A	58805B	
Oxides wt. %								
SiO ₂	45.90	52.87	57.16	47.87	48.35	44.55	50.23	51.29
TiO ₂	1.23	0.38	1.95	0.81	0.72	1.30	1.21	0.75
Al ₂ O ₃	15.71	21.47	13.47	14.27	15.68	14.08	17.68	15.19
Fe ₂ O ₃	3.99	1.52	2.11	4.12	4.23	4.43	5.51	3.20
FeO.....	8.62	3.77	5.76	8.63	7.63	10.20	3.98	7.39
MnO.....	0.20	0.09	0.16	0.21	0.20	0.30	0.22	0.33
CaO.....	10.97	8.94	7.71	12.62	10.67	12.35	14.62	14.93
MgO.....	8.50	2.94	8.27	7.46	7.94	8.04	3.48	3.43
Na ₂ O.....	2.40	5.40	1.00	1.35	2.46	2.04	2.10	0.44
K ₂ O.....	0.28	0.21	0.53	0.33	0.58	1.00	0.47	0.23
P ₂ O ₅	0.04	0.02	0.05	0.06	0.04	0.02	0.02	0.07
CO ₂	0.57	1.10	nd	nd	nd	nd	nd	1.35
H ₂ O ⁺	0.78	0.65	1.17	1.70	0.99	1.27	1.05	0.80
H ₂ O ⁻	0.04	0.05	0.06	0.09	0.11	0.02	0.02	0.03
	99.23	99.41	99.40	99.52	99.60	99.60	100.59	99.43
<i>mg</i>	0.55	0.50	0.65	0.51	0.55	0.50	0.40	
<i>ti</i>	1.99	0.79	4.03	1.35	1.20	2.03	2.21	
Mode vol. %								
quartz.....	0.9	0.7	20.1	1.7	1.9	0.2	6.4	
plagioclase.....	23.0	70.1	50.9	15.3	33.5	12.8	12.3	
biotite.....	0.3	0.7	4.9	-	-	0.1	-	
garnet.....	-	-	-	tr	-	-	-	
hornblende.....	72.0	26.0	23.9	67.6	60.5	84.8	34.8	
clinopyroxene.....	-	-	-	4.6	1.4	-	0.5	
epidote.....	0.4	-	-	9.7	2.1	0.1	42.1	
sphene.....	0.4	tr	tr	0.6	-	1.9	3.1	
apatite.....	0.2	0.2	tr	0.2	0.1	tr	tr	
zircon.....	0.1	0.1	tr	0.1	0.5	0.1	0.1	
calcite.....	1.4	1.7	-	-	-	-	-	
opaque.....	1.2	0.5	0.1	0.2	-	tr	0.7	
An % in								
plagioclase.....	45	38	36	43	38	39	35	
hornblende	{ 2 V -70°	-68°	-81°	-72°	-61°	-72°	-57°	
	{ <i>c</i> : γ 15°	15°	15°	16°	16°	14°	15°	
clinopyroxene	{ 2 V -	-	-	+67	+63°	-	+64°	
	{ <i>c</i> : γ -	-	-	38	47°	-	48°	

57787 A and B: the inner and outer zone respectively of the same inclusion.

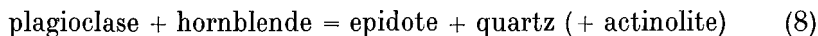
57891: the outer zone of an inclusion.

58805 A and B: different bands of the same inclusion.

57759: analysis carried out on a strip across all the zones of the calc-silicate inclusion.

nucleus to the transformed rim. Modal analyses of samples belonging to this type are reported in Table 13.

The second type of amphibolite inclusion is characterised by the presence of quartz-epidote and quartz-actinolite symplectites (plate 7b). They always occur at the contact between hornblende and plagioclase and are possibly formed by a reaction of the type:



Actinolite is formed by the excess of Mg and Fe and sphene by the Ti present in the reacting hornblende. These symplectites never occur in the major amphibolite horizons, only in the inclusions. This is most probably a consequence of the different environmental conditions ($P_{\text{H}_2\text{O}}$ and P_{CO_2} , higher in the migmatitic environment) which caused an instability between calcic plagioclase and hornblende. Modal analyses of samples belonging to this group are reported in Table 13.

Chemistry

Chemical analyses of the two types of amphibolite inclusions are shown in Table 13.

First type. If two samples (57787 A & B) of the same boudin are compared, it can be seen that the more highly transformed one is characterised by an increase of Si, Al and Na and a decrease of Ti, Fe^{3+} , Fe^{2+} , Ca and Mg while K does not vary appreciably. An introduction of salic elements is evident.

Second type. The chemical composition of the boudins is quite similar to that of the layers of major amphibolites. The boudins therefore acted as a closed system during migmatisation, at least for the major elements.

Ultramafic inclusions

Description and petrography

The ultramafic inclusions are serpentinites and hornblendites. The former are very rare, but the latter are quite common. The serpentinite inclusions are small ball-shaped bodies whose occurrence shows that they were closely associated with amphibolites. The serpentinites acted as resisters and have survived even when the amphibolite has been completely transformed by migmatisation. Towards the gneisses they show reaction zones similar to those described for the zoned ultramafic lenses (p. 37) except that the innermost part is here always constituted of serpentinite.

Hornblendite inclusions are very common both in agmatite zones and as isolated boudins in the gneisses. The size of single inclusions varies from a few centimetres to a maximum of 150 centimetres. They have no counterpart in the lithologies of the major layers. They cannot correspond to the uniformly narrow hornblendite layer (30 centimetres thick) found around the ultramafic lenses because the hornblendite inclusions are up to 150 centimetres thick and never enclose a core of different composition. They cannot correspond to the thin hornblendite layers intercalated with amphibolites because there is normally no intercalation in the inclusions and they are much thicker.

The hornblendite inclusions are equigranular, medium- to coarse-grained, and are composed of hornblende (more than 90 %). This hornblende is dark green in a hand sample and is pleochroic in thin section from colourless or yellowish (α) to bluish green (γ). It is sometimes accompanied by significant amounts of diopsidic pyroxene and minor amounts of biotite. Quartz, plagioclase, sphene and opaque minerals are

Table 14. *Chemical composition of a hornblende and a clinopyroxene from a hornblendite inclusion.*

GGU No.	57720					
	Oxides wt. %		Number of ions on the basis of			
	hornblende	clinopyroxene	24(0)		6(0)	
			hornblende		hornblende	clinopyroxene
SiO ₂	50.69	52.70	Si	7.284	8.000	1.933
TiO ₂	0.65	0.24	Al	0.716		0.055
Al ₂ O ₃	4.71	1.27	Al	0.081	5.131	-
Fe ₂ O ₃	0.78	2.72	Ti	0.070		0.006
FeO	9.61	4.31	Fe ³⁺	0.085	0.075	0.941
MnO	0.23	0.29	Mg	3.713	0.835	
CaO	12.34	23.41	Fe ²⁺	1.155	0.132	0.941
MgO	17.34	15.27	Mn	0.027	0.009	
Na ₂ O	0.48	0.28	Na	0.136	0.020	0.941
K ₂ O	0.35	0.02	Ca	1.900	0.920	
H ₂ O ⁺	2.25	0.15	K	0.064	0.001	0.941
H ₂ O ⁻	0.12	0.07	OH	2.141	0.043	
	99.55	100.73				
2V	-73°	+57°				Mg 58.93
c:γ	18°	40°				Fe 39.22
						Ca 1.84
α	pale yellow	colourless				
β	green	pale green				
γ	bluish green	pale green				

accessories. Analyses of co-existing hornblende and pyroxene in one sample (Table 14) show that the hornblende is actinolitic, with low Al_2O_3 , and that the pyroxene is salite.

Calc-silicate inclusions

Description and petrography

Small inclusions of calc-silicate skarns are sometimes present within the gneisses. Inclusions of this kind have already been described in the Frederikshåb district (WALTON, 1966 and BRØGGER SØRENSEN, 1968) both in the gneisses and in the hornblende schists. In the area described here these lenses occur up to tens of centimetres wide. They are characterised by a zonation similar to that described by BRØGGER SØRENSEN. When complete, the zonation comprises (with reference to sample 57769) from the centre of the lens outwards:

i) *garnet zone* characterised by the presence of a poikilitic pink garnet with inclusions of pink calcite, salitic green diopside, epidote, sphene and quartz,

ii) the garnet zone gradually passes outwards to a shell in which plagioclase (An 50 %) and scapolite predominate. Scapolite replaces plagioclase. The mafics are green diopside, bluish green hornblende, epidote, and minor amounts of garnet,

iii) an *outer zone* is composed of plagioclase–diopside–hornblende–epidote-bearing amphibolite.

This complete threefold zonation is rarely seen. In many cases the calc-silicate inclusions consist of only an epidote-rich nucleus sheathed by amphibolite.

The chemical analysis of a calc-silicate skarn is reported in Table 13.

DISCORDANT AMPHIBOLITE DYKES

Description

Only two examples of discordant amphibolites have been found and these occur in the eastern part of the area. They have the form of discontinuous dykes, which reach a maximum thickness of one metre and are dark green in colour with a fine-grained, massive texture. However, sometimes inhomogeneities are present as a weak foliation or garnet clusters.

Petrography

Two thin sections have been examined (73843 and 73844) of samples taken from a discordant amphibolite on the peninsula north of Sermilik avangnardleq. Sample 73843 contains a relic igneous texture, while sample 73844 has a granoblastic texture. In both samples there is a small amount of quartz with undulose extinction. The plagioclase of sample 73843 shows normal zoning (nucleus An_{11} ; periphery An_{33}) while in sample 73844 plagioclase is not zoned and has an anorthite content of 45 %. Hornblende in both samples has pleochroism α = yellow; β = deep green; γ = greenish blue, but the former has a 2V of -75° and $c:\gamma$ angle of 16° whilst the latter has a 2V of -69° and $c:\gamma$ angle of 17° . A secondary transformation into actinolite is present. Biotite is present in both samples as an accessory mineral. Porphyroblasts of garnet occur in sample 73844. Apatite, zircon and ilmenite are accessories.

It can be seen that there is no substantial difference in mineral assemblage between these rocks and the normal amphibolites (see p. 29 et seq.).

Chemistry

The chemical analyses of samples 73843 and 73844 are reported in Table 15. These discordant amphibolites have the same chemical composition as the concordant amphibolites.

Table 15. *Chemical composition of discordant amphibolites.*

GGU No.	73843	73844
SiO ₂	50.55	50.11
TiO ₂	1.00	1.25
Al ₂ O ₃	14.65	14.52
Fe ₂ O ₃	2.40	3.20
FeO	9.01	8.69
MnO	0.17	0.17
CaO	9.96	9.92
MgO	8.42	7.71
Na ₂ O	1.80	2.34
K ₂ O	0.15	0.21
P ₂ O ₅	0.01	0.01
H ₂ O ⁺	1.18	1.21
H ₂ O ⁻	0.06	0.06
	99.36	99.40
<i>mg</i>	0.57	0.54
<i>ti</i>	1.74	2.19

PETROGENESIS

The petrography shows that the concordant layers in the migmatitic gneisses are the most useful indicators of the metamorphic history. These layers will therefore be discussed first and followed by a discussion of the migmatitic gneisses and the inclusions found in them.

The Concordant Layers

Origin of the rocks

It has already been shown that the rusty schist is a metasedimentary rock, whose composition approaches that of sandstones and greywackes.

Field and petrographic observations do not help us to understand the origin of amphibolites, as has been demonstrated by several authors (e.g. LEAKE, 1964; RIVALENTI, 1966; RIVALENTI & SIGHINOLFI, 1969). The origin of their banding is also uncertain: if the banding of type i (p. 30) was formed by early metamorphic differentiation, then the banding of types ii and iii could either represent a pre-metamorphic feature, or be of metamorphic origin (RIVALENTI, 1971).

Many theories have been proposed to explain the origin of ultramafic rocks (e.g. SØRENSEN, 1953; VUAGNAT, 1954). The ultramafics of the present area are in most cases continuous single layers intercalated with the other lithotypes. There is a striking similarity between this pattern and that described by TURNER & VERHOOGEN (1960, p. 307) as "Peridotites and serpentinites of the 'alpine type' occurring in folded geosynclinal sediments of orogenic belts". This similarity seems to be more than accidental and in this case the layers as a whole could represent remnants of an old geosynclinal series. The amphibolites could therefore represent the volcanics (basalts, spilites, etc.) which are usually present in the geosynclinal sediments.

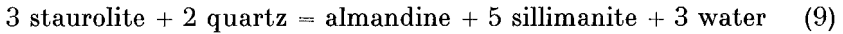
The microgranodiorite appears to have been derived by migmatization from either the rusty schist or from amphibolite because its contacts are concordant with the foliation of the other rocks and its composition is similar to that of the gneisses. When large crystals of rutile are present they suggest a derivation from rusty schist which is the only other rock

in which rutile occurs; but when hornblende is present, it suggests a derivation from amphibolite.

Metamorphic facies and petrogenesis

The best indicators of metamorphic petrogenesis are the mineral assemblages which occur in the rusty schist. These indicate that the rusty schist is a pelitic rock metamorphosed in the almandine-amphibolite facies of regional metamorphism. Several phenomena throw light on the metamorphic history of this rock.

i) Garnet sometimes contains inclusions of staurolite, which has never been found elsewhere. A similar phenomenon has been described by LAL & MOORHOUSE (1969) who consider it indicative of a progressive metamorphism starting from the staurolite-almandine subfacies. Staurolite may have disappeared through a reaction of the type:



(WINKLER, 1965, p. 90).

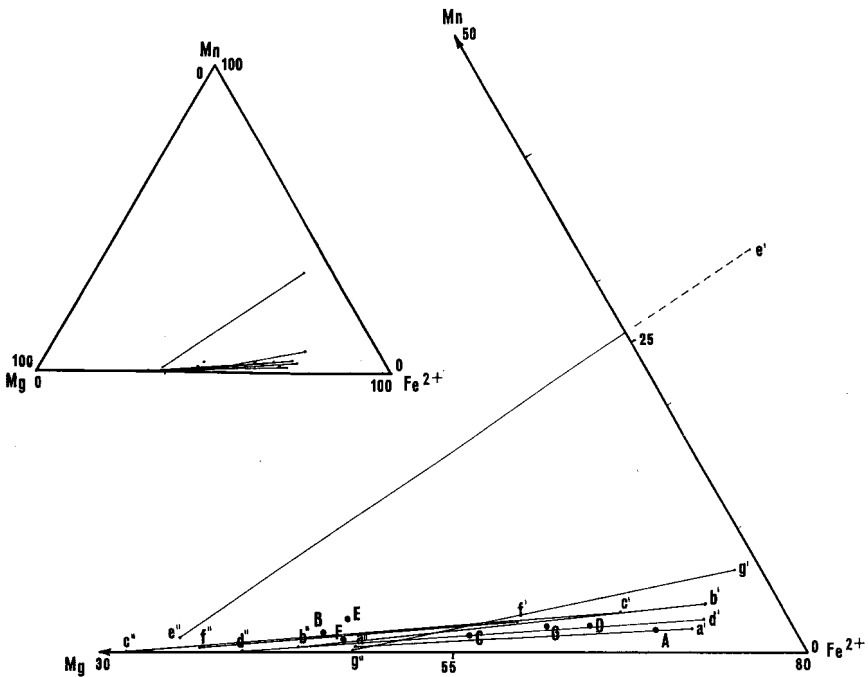


Fig. 15. Triangular Mn-Fe²⁺-Mg plot of co-existing garnets and biotites and their host rocks. A represents the whole rock sample A; a' the garnet in sample A and a'' the biotite in sample A. The samples A-G correspond with GGU sample A = 57738, B = 73543, C = 57820, D = 57856, E = 75880, F = 75884 and G = 57813. A and B are gneisses, C-F are rusty schists and G is microgranodiorite. See text p. 62 for discussion of the results.

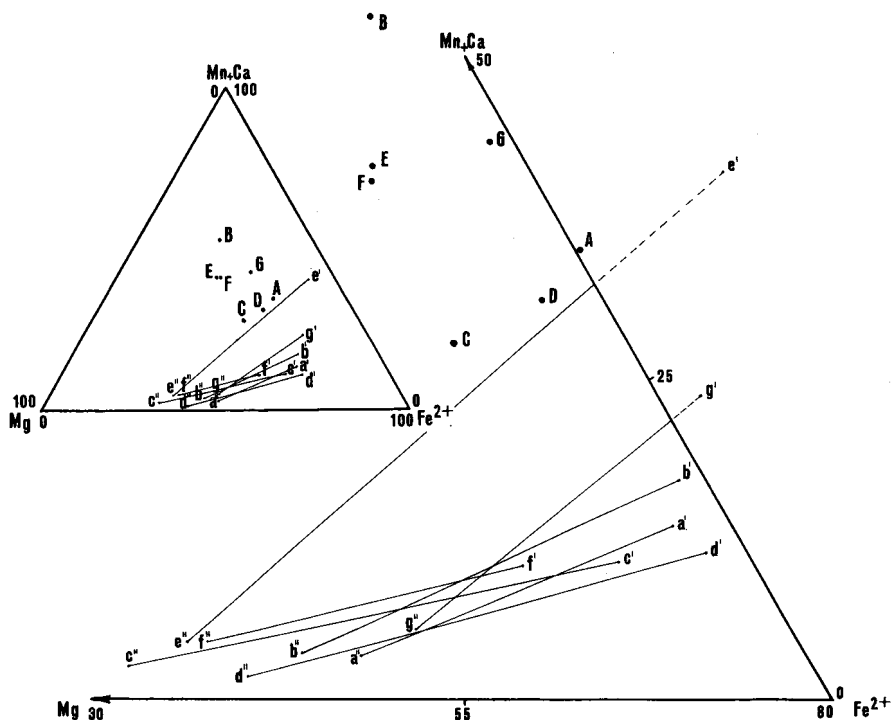
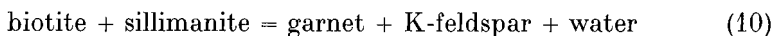


Fig. 16. Triangular (Mn + Ca) - Fe^{2+} - Mg plot of the same co-existing garnets and biotites and their host rocks as fig. 15. Explanation of the letters the same as that in fig. 15.

ii) The atoll structure of garnet indicates that it crystallised in two periods of metamorphism (RAST, 1965); this is also suggested by the relationship between garnet and other minerals, mainly to biotite. The older generation is pre- or syntectonic, while the later one exhibits post-tectonic features. In order to ascertain the relationship between garnet crystallisation and metamorphic grade, co-existing garnets and biotites (Table 10) have been examined following the method described by ATHERTON (1965). The tie-line pattern is shown in figs 15 and 16. Samples 57820, 57856 and 75884 (mainly syntectonic garnet) have parallel tie-lines, while that of sample 75880 (mainly post-tectonic garnet) has a completely different slope, showing that this garnet grew under different metamorphic conditions. Since the Mn content increases sharply in the garnet of sample 75880, it can be assumed that it crystallised under a lower grade of metamorphism than the garnets in other samples (MIYASHIRO, 1953; SIGHINOLFI, 1967).

iii) The occurrence of sillimanite inside garnet possibly indicates a reaction of the type:



occurring at the amphibolite-granulite facies border.

iv) According to RAMBERG, the transformation of biotite into anthophyllite and K-feldspar (reaction (6), p. 50) indicates conditions approaching granulite facies.

v) The association anthophyllite–cordierite. GRANT (1968) has suggested that anthophyllite–cordierite-bearing rocks formed from assemblages of the type feldspar–plagioclase–biotite–sillimanite–quartz by partial melting, filter pressing and recrystallisation, phenomena which suggest a high-grade environment. LAL & MOORHOUSE (1969) suggest that gedrite–cordierite assemblages may have originated by partial anatexis and removal of the melted granitic fraction. An anatectic process would clearly fit the rusty schist too, because a derivation from a normal biotite–sillimanite–garnetiferous schist is evident. Our assemblages differ from other known assemblages, however, in that they contain a fairly high amount of CaO, which entered the plagioclase and did not primarily form calcic amphibole. DE WAARD (1966) puts the anthophyllite–cordierite assemblage in the biotite–cordierite–almandine subfacies of the low hornblende–granulite facies.

vi) Rusty schists with a biotite–garnet–sillimanite assemblage have a chemical composition that corresponds only to that of rare aluminous greywackes (see p. 51). An anatectic process, with partial removal of a granitic melt (BROWN & FYFE, 1970) affords the best explanation of their composition.

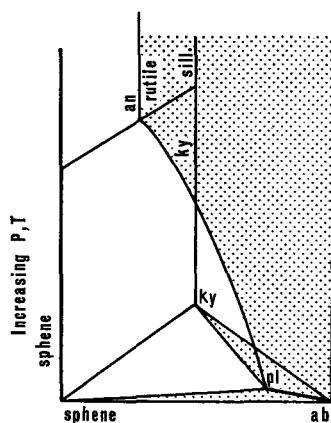


Fig. 17. Equilibrium diagram plagioclase–sphene–kyanite (from RAMBERG, 1952, p. 74).

vii) The widespread occurrence of large crystals of rutile, which together with ilmenite are the only titanium minerals, is also significant. Sphene is completely absent. In the several reactions leading to the formation of rutile reported by RAMBERG (1952, p. 73), the side of the equations where rutile is formed is considered to represent higher P – T conditions. It is

worth noting that rutile remains unchanged even when plagioclase is very calcic (Table 9). According to RAMBERG's diagram of equilibrium between sphene, plagioclase and kyanite (fig. 17) this again represents high P - T conditions. Similar significance is attached to rutile by DEER, HOWIE & ZUSSMAN (1962, vol. 5, p. 34). Several occurrences of rutile have been found in granulite facies rocks (BERTOLANI, 1968). The latter author has also discovered that rutile, once formed, is not easily re-transformed with decreasing metamorphism (personal communication).

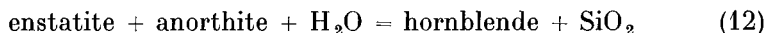
viii) The more calcic plagioclase is micro- (crypto-)antiperthitic. A similar phenomenon has been described in granulite facies rocks (CAPEDRI, 1968). Its replacement by more sodic plagioclase indicates a decrease in metamorphism.

ix) Sillimanite is retrogressively transformed into muscovite. Possibly this transformation takes place through a reaction of the type:



(RAMBERG, 1952, p. 151) which occurs at the boundary between granulite and amphibolite facies.

x) The transformation of anthophyllite and plagioclase into hornblende (reaction (7) p. 51) indicates instability due to the decreasing metamorphism. There is a similarity between reaction (7) and that reported by RAMBERG (1952, p. 54):



RAMBERG points out that the right-hand side of the equation is stable at lower temperatures and that enstatite can be substituted by anthophyllite, depending on the water pressure.

xi) The transformation biotite-chlorite and possibly biotite-muscovite, the pinitisation of cordierite and the formation of epidote indicate low-grade transformations.

All these phenomena show that the metamorphic evolution of the rusty schist was complex. A possible interpretation is given below.

i) Very early regional metamorphism took place in the staurolite-almandine subfacies of the almandine-amphibolite facies (recognised by the presence of staurolite enclosed by garnet).

ii) Increasing conditions of T and P gave rise to the formation of sillimanite and garnet. This phase must have reached the uppermost part of the almandine-amphibolite facies or the lowest part of the

granulite facies. During the culmination of this phase anatectic conditions were created and a granitic melt was mobilised. The overall effect of anatexis was weak, although at certain points (cordierite–anthophyllite assemblages) it was more pronounced owing to tectonic factors. This high-grade environment was characterised by high water pressure because anthophyllite occurs instead of enstatite and suggests that the rocks were metamorphosed in the lower part of the almandine–biotite–cordierite subfacies of the hornblende–granulite facies (DE WAARD 1966). Relics of high-grade assemblages are scattered throughout the rusty schist but are more commonly seen between the mountains 880 m and 760 m in the eastern part of the area.

iii) The peak of progressive metamorphism was followed by retrogression. The main evolution must have occurred within the almandine–amphibolite facies. On the whole, the mineral assemblages fit well with those found in the sillimanite–almandine–muscovite subfacies of Barrovian metamorphism (TURNER & VERHOOGEN, 1960, p. 548), but the lowest grade attained by these rocks extends to the lowest part of the almandine–amphibolite facies (staurolite–almandine subfacies again?). The widespread occurrence of large crystals of epidote associated with muscovite and chlorite indicates that in some cases even lower metamorphic grades were attained. Garnet probably recrystallised during this phase and so did plagioclase, becoming less calcic and more sodic. The equilibrium anthophyllite–anorthite was upset and consequently hornblende was formed.

Sometimes even sillimanite recrystallised in the form of fibrolitic aggregates.

iv) Some of the lowest grade transformations are connected with faulting and are only locally important.

The amphibolites also show signs of disequilibrium and polymetamorphism. Titanium minerals are as usual one of the most important indicators of metamorphic petrogenesis. Ilmenite, which in these iron-rich rocks has the same significance as rutile in the rusty schist, shows instability and partial transformation into sphene which clearly represents retrogression (see for instance reaction (4)). Reaction (3) has a similar meaning. The presence of microantiperthites probably indicates high-grade metamorphism (p. 35). The recrystallisation of normally zoned plagioclase indicates that the more calcic plagioclase became unstable. The widespread occurrence of large crystals of epidote indicates a retrograde transformation. Therefore, although it is difficult to assign an exact subfacies to these mafic assemblages, the amphibolites would

appear to have undergone a metamorphic evolution, from a high to a lower grade of the almandine–amphibolite facies, similar to that of the rusty schist.

The ultrabasic rocks also conform to this general picture. If the peridotite nucleus recrystallised from a former serpentinite (which is not certain, see p. 39) this should have occurred with decreasing P_{H_2O} and increasing metamorphism, which could correspond to the first relic phase of increasing metamorphism in the rusty schist.

The peridotite mineral assemblage of the nucleus would have been stable from the granulite facies to the almandine–amphibolite facies. But when chlorite occurs in the nucleus in equilibrium with olivine, orthopyroxene and amphibole, this assemblage is stable in a medium amphibolite facies (TROMMSDORF & EVANS, 1969).

On page 40 it has been shown that the amphibole of this assemblage is characterised by lower hexacoordinate Al and higher Mn and Fe than amphiboles occurring in peridotites in granulite facies rocks.

The transformation of the nucleus into serpentine and talc does not necessarily indicate greenschist facies conditions. BOWEN & TUTTLE (1949) and RAMBERG (1952) have pointed out that the appearance of these minerals is controlled by the partial P_{H_2O} of the environment: if P_{H_2O} is high, then talc and serpentine are stable up to 700°C and 500°C respectively. In our occurrences a high water pressure is indicated by the crystallisation of anthophyllite instead of enstatite (p. 64) in the rusty schist. The formation of talc and serpentine may thus have occurred in the almandine–amphibolite facies. As regards anthophyllite, HINRICHSSEN (1967) has shown experimentally that Fe-rich anthophyllites are stable above $520^\circ \pm 10^\circ$ at a constant P_{H_2O} of 1000 bar. In our case anthophyllite substitutes talc. This may be the result of a decrease in water pressure occurring in the almandine–amphibolite facies. The petrogenesis of the ultramafic rocks is complicated by metasomatic exchanges with the country rock and redistribution of elements within the body (see p. 43). A metasomatic mechanism has probably produced the rim of hornblendite. The ultramafic rocks also underwent low-grade transformations such as a weak chloritisation of hornblende and the partial transformation of anthophyllite into talc.

The microgranodioritic rock does not present any interesting metamorphic features. The presence of large crystals of rutile probably means that this rock has undergone high-pressure metamorphism. Its mineral assemblages, when not downgraded to the epidote–amphibolite or greenschist facies by local faulting, conform with those of the almandine–amphibolite facies. A garnet–biotite tie-line for a microgranodiorite (sample 57813) is reported in figs 35 and 36. It intersects

the high-grade tie-lines of the rusty schist couples and therefore the garnet in the microgranodiorite might have crystallised in a medium to low almandine–amphibolite facies, but the presence of some hornblende makes the interpretation doubtful.

Inclusions in the Gneisses

Metamorphic facies and petrogenesis

All the inclusions possess mineral assemblages which are stable in the almandine–amphibolite facies. Assemblages indicating an upper almandine–amphibolite facies are found in the calc-silicate inclusions. Some transformations (for instance, the biotitisation of hornblende or that shown by reaction (8)), have clearly occurred by decreasing the metamorphic grade.

It has been shown that most of the inclusions correspond to lithologies found in the major layers and are formed through boudinage or agmatization with or without chemical exchanges with the migmatites. A possible explanation of the hornblendite inclusions which cannot correspond to the hornblendites found in the layers (p. 56) is that they could have originated through basification, either by the subtraction of salic elements or by the introduction and fixation of mafic elements (RAMBERG, 1952, p. 262). As RAMBERG points out, basic elements may become fixed in remnant inclusions in zones of general quartz-feldspathisation such as that under consideration.

Many theories have been proposed for the origin of the calc-silicate lenses. In another part of the Frederikshåb district, WALTON (1966) considers that they developed from pillow lavas. This theory has been criticised by BRØGGER SØRENSEN (1968) who proposed a derivation from original Ca-rich rocks. HENTSCHEL (1943), BACKLUND (1953) and MEHNERT (1968, p. 304) consider similar skarns to be a product of metamorphic–metasomatic transformation of limestones and marbles, while SHAW *et al.*, (1962) describe calc-silicate skarns which they interpret as altered amphibolites and metagabbros.

Although it is possible that the skarns described in this paper are derived from marbles, it is considered probable that they formed by the metamorphism of amphibolites for the following reasons: 1) they only occur in connection with agmatites; 2) epidote–pyroxene–hornblende-bearing layers (p. 30) with the same mineral composition as the inclusions occur in major amphibolites; 3) the chemical composition of the inclusions is similar to that of amphibolites (compare the analysis of sample 57769 (Table 13) with those of Table 4).

Discordant Amphibolites

The discordant amphibolites possess almandine–amphibolite facies assemblages which are similar to those of other rocks and therefore they probably represent mafic dykes which were emplaced early in the history of the region.

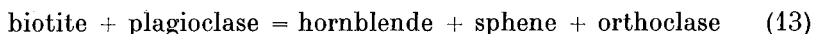
Migmatitic Gneisses and Pegmatites

Metamorphic facies

The gneisses possess almandine–amphibolite facies assemblages but they lack critical minerals, such as Al-silicates, which would enable the subfacies to be established exactly. However, indications are found also in the gneisses of retrogression from the sillimanite–almandine muscovite subfacies to the almandine–amphibolite facies. This retrogression is shown by the following transformations:

i) Biotite is often recrystallised as a green type, with release of titanium in the form of sagenitic rutile. It is well known that, as metamorphic grade decreases, the titanium content in biotite also decreases (ENGEL & ENGEL, 1960; AOKI, 1961; SIGHINOLFI, 1968);

ii) The transformation of hornblende into biotite is accompanied by the formation of epidote and sphene. MEHNERT (1968, pp. 52 and 262) observed that the titanium content of biotite is higher than that of hornblende and suggested the reaction:



This equation is correct if the transformation takes place at a high metamorphic grade. But if, as in the present case, potash is added with decreasing metamorphism, it may happen that biotite takes up less titanium than is present in hornblende, because the amount of titanium in biotite decreases with decreasing metamorphism.

iii) Muscovite and epidote formed by the reaction (1).

Two co-existing garnets and biotites from gneisses with the same composition as that of the rusty schist have been analysed (Table 2) to obtain information on the metamorphic grade under which garnet crystallised. The tie-lines are reported in figs 15 and 16.

Fig. 16 shows that both the gneiss tie-lines intersect those of rusty schists whose garnet was formed during high-grade metamorphic conditions, but they do not cross that of sample 75880, whose garnet was formed under lower metamorphic conditions (p. 62). In fig. 15 one

gneiss conforms to this pattern, but the tie-line of the other is subparallel to those of rusty schists with high-grade garnet. The difference in behaviour may reflect the influence of host rock composition upon the garnet. However, according to ATHERTON (1965), Ca in garnets plays a role similar to that of Mn during retrogressive metamorphism. Although unambiguous conclusions cannot be based on the analyses of only two couples, it seems that garnet in the migmatitic gneisses crystallised in low almandine–amphibolite facies.

All the mineral transformations and assemblages considered so far are consistent and seem to have occurred during retrogression from high to low almandine–amphibolite facies. Further transformations into epidote–amphibolite and greenschist facies assemblages are sometimes found. These are indicated by the chloritisation of mafics and the transformation of plagioclase into albite and epidote.

The facies of the pegmatites generally reflects that of the country gneisses as is shown by the similarity of their mineral composition and reactions (see p. 23). Only the quartz and epidote-bearing mobilisates (P_4) can represent a low grade hydrothermal mobilisation.

Petrogenesis

Interpretation of the origin and evolution of polymigmatitic gneisses and related pegmatites is a difficult subject (MEHNERT, 1968) which requires much more detailed work than it was possible to carry out in the present area. However, a few comments can be made here. There are three main possible explanations of the origin of the gneisses: a) they represent the product of an isochemical metamorphism of pre-existing rocks (an explanation proposed, for instance, by KALSBECK (1970) for gneisses exposed 50 km south of Frederikshåb); b) they were formed by anatexis; or c) they were formed by metasomatism.

The phenomena which we have observed which are relevant to a discussion of these three hypotheses are summarised below.

i) Layers (the concordant layers, p. 29) of a pre-migmatitic series are scattered throughout the migmatitic gneisses. We therefore consider that the gneisses were chiefly derived by migmatitisation from the lithotypes of the layers because most of the relic inclusions in the gneisses correspond to lithotypes found in the layers.

ii) Amphibolite boudins in the gneisses are often enclosed within a sheath of hornblende gneiss.

iii) during retrogressive metamorphism microcline crystalloblasts developed by replacement in the gneisses; hornblende was replaced by biotite (p. 18), and epidote and muscovite formed from plagioclase (p. 17).

iv) The composition of the older pegmatites (P_1 and P_2) is strictly related to that of the host rock, while the younger P_3 are richer in K-feldspar, irrespective of the country-rock composition.

v) The pegmatites appear to have been formed by several mechanisms. The concordant pegmatites and veins sometimes have dark rims, and are most likely to be the product of metamorphic differentiation. When the composition of discordant pegmatites is the same as that of the host rock, and the host-rock structures continue as shadows in the pegmatite, they are considered to be replacement bodies. Pinch-and-swell structure and zoning were considered by RAMBERG (1956) to be proof that pegmatite had grown by metasomatism in a solid state, while GRESENS (1967a & b) believes that zoned pegmatites formed by the migration of hydrothermal intergranular fluids under tectonic influence. Dilatational intrusive pegmatites have also been found: for instance the P_3 K-feldspar-rich pegmatites which cross-cut the amphibolites.

vi) Feldspar porphyroblasts occur which have grown by forceful shouldering aside of biotite (p. 15).

No single theory can explain all these phenomena. The hypothesis of isochemical crystallisation, however, can be completely rejected because the hornblende gneiss has no counterpart in the pre-migmatitic series and it is statistically unlikely that, if such a lithotype existed, it would have been completely migmatitised in all cases.

Both intracrystalline and intercrystalline metasomatism (MEHNERT, 1968, p. 285) has been experimentally demonstrated to be effective only on a small scale (BLACKBURN, 1968). Nevertheless, phenomena generally accepted as metasomatic occur in the present migmatites.

As far as anatexis is concerned the composition of an anatectic mobilisate should be granitic according to the experimental works of several authors (see e.g. BROWN & FYFE, 1970), while our gneisses have a dioritic composition. An evolution towards a dioritic composition has only been experimentally obtained in unnatural conditions (for instance with very high T and P_{H_2O} , JAMES & HAMILTON, 1969). However, anatexis cannot be completely excluded for the following reasons: 1) laboratory conditions do not correspond to natural ones; 2) many anatectic migmatites have leucosomes of non-granitic composition (see for example MEHNERT, 1962); 3) if anatectic phenomena are repeated after the formation of a primary granitic melt the following melts must trend towards a more dioritic composition because the primary granitic melt might migrate (see BROWN & FYFE, 1970; SIGHINOLFI, 1971); 4) the melting

of biotite by anatexis depends on the water pressure and thus, if water pressure is sufficiently high and other K-bearing minerals are absent, then the composition of the melt must tend towards diorite.

To conclude, neither anatexis nor metasomatism can be excluded in the present area and a mechanism which might be proposed is a combined activity of both: i.e. an anatectic mobilisate metasomatically reacting with basic rocks.

The sequence of events which led to the formation on the migmatites is considered to be:

1. High-grade (possibly low granulite facies) metamorphism of a series of rocks similar to those which now form the concordant layers.
2. The rocks were deformed and reacted in different ways depending on their composition; the metasediments behaved plastically whilst the amphibolites were boudinaged.
3. Partial anatexis occurred with migration of a granitic melt. This phenomenon is suggested by the anthophyllite–cordierite assemblage in the rusty schist (pp. 63 and 65). Migmatitisation may have begun here, with the formation of concordant leucosomes (P_1) and the reaction of the mobilisates with the amphibolites to give hornblende gneisses. It continued with increase in P_{H_2O} , in high almandine–amphibolite facies where it reached its maximum. The mobilisates were always granodioritic to quartz dioritic (quartz dioritisation) and there was a tendency towards general homogenisation, because the amphibolites were transformed by reaction with material coming from felsic gneisses. The process reached completion (probably under the influence of tectonic factors) at certain points where homogeneous gneisses were found (diatexites of MEHNERT, 1968, p. 253).
4. Retrogressive metamorphism took place in low almandine–amphibolite facies and the last stages of migmatitisation occurred forming microcline crystalloblast, microcline-rich pegmatites and the biotitisation of hornblendes. This last phase might have followed immediately after quartz dioritisation, but the possibility of a gap cannot be excluded.

Conclusions

The gneisses of the area were formed from a geosynclinal series, which first underwent prograde metamorphism from the staurolite–almandine subfacies to the low hornblende granulite facies (almandine–biotite–cordierite subfacies, p. 64). At the highest stage of metamorphism partial anatexis occurred (p. 65) and the period of migmatitisation began. Subsequently, there was a period of retrograde metamorphism from the upper (sillimanite–almandine–muscovite subfacies) to the lower al-

mandine–amphibolite facies. The effects of migmatization were most marked during the period of decreasing metamorphism. The general “quartz (grano-) dioritization” can be ascribed to the high almandine–amphibolite facies, and microcline blastesis to the medium and low part of the same facies. Epidote–amphibolite facies and greenschist facies metamorphism were late phenomena locally associated with brittle deformation. Mafic dykes (now discordant amphibolites) were intruded at some stage before the almandine–amphibolite facies metamorphism.

POST-OROGENIC BASIC DYKES

Introduction

The basic dykes are the subject of a paper by RIVALENTI & SIGHINOLFI, (1971) and therefore they will only be briefly described here. The whole area is intersected by basic dykes whose thicknesses vary from a few centimetres up to 300 metres. All the dykes weather to a reddish brown colour and, with the exception of the TDs which always lie in erosional hollows, they stand out in relief with respect to the gneisses. The most widespread dykes are the first dolerite generations which are typically covered by several metres of an alteration gravel. The following generations of dykes have been established in the southern part of the Frederikshåb district (JENSEN, 1966).

MD₁—the oldest, with a general strike north-south.

MD₂—general strike north-east.

MD₃—general strike south-east or east-south-east.

BD (brown dolerites)—general strike east-south-east or north-east.

TD (trap dolerites)—the youngest, with a strike parallel to the coast (i.e. south-south-east).

Lamprophyres—irregular strike.

The first three generations are thought (JENSEN, 1966) to be pre-Ketilidian (> 2500 m.y.) since, farther south, in the Ivigtut area, they are deformed by Ketilidian structures. BDs are considered to be of Gardar age (c. 1250 m.y.), while TDs are much younger with ages of 138 and 164 m.y. (LARSEN & MØLLER, 1968; WATT, 1969) indicating a Mesozoic age. The age of the lamprophyres in our area is not well defined. This dyke terminology is used in the present description because all these generations of dykes have been found, except MD₁ and BD. No Gardar dyke has been found west of the present area (CHADWICK, 1969).

Description and petrography

MD₂ dykes

The thickest dykes of the area belong to this generation. The maximum thickness observed is 300 m (in the dyke crossing the area from Aorngo to the inland ice and forming the 670 m and 780 m hill-tops).

Locally two sub-generations which cross each other have been distinguished. The older and younger sub-generations are shown on Plate 10 as MD₂(1) and MD₂(2) respectively. All the MD₂s have chilled contacts with the country rock. The general strike of this swarm is north-east, but local swings to north-north-east or east-north-east often occur. 'En échelon' and 'en bajonette' arrangements have been found sporadically. A peculiar feature of this 'en échelon' structure is that dykes suddenly stop, swarming out in a large number of minor dykes, and begin again some hundred metres to the side. It is apparent from the map that this also happens to the thickest dykes. They are sheared by the south-east and north-south set of faults and fractures but not usually by the north-east ones, although some laminations occur along the strike. Veins of epidote and other hydrothermal veins occur along the south-east fractures; these are described later together with fractures. The dykes of this generation, when large enough, exhibit a zonal structure. From the margins, where the rock has an aphanitic glassy texture, the grain size increases toward the centre. Another feature, which is also present in the MD₃ dykes, is that they become porphyritic along the strike in a discontinuous way. For instance, the thin dykes which extend from the south-western part of Igassortoq and pass a few hundred metres north of mountain 880 m have large plagioclase phenocrysts in only a small part of their total length, while in the remainder they have a normal coarse-grained texture without phenocrysts for no apparent cause. For this reason no porphyritic dyke has been mapped as such.

The mineral texture of MD₂ dykes is characterised by the ophitic intergrowth of plagioclase and clinopyroxene. Plagioclase is zoned. Clinopyroxene is either colourless or pale brown. Some minor amounts of olivine have been found. A mineral zoning occurs in the thicker dykes; olivine may be present towards the contacts together with clinopyroxene and plagioclase but is absent in the centre. This can be explained by the different rate of cooling of the contact and the centre, producing a weak differentiation. Minor amounts of brown biotite are also present. The primary minerals are partially uralitised and consist of aggregates of chlorite, talc, sericite with accessory opaque minerals and apatite.

MD₃ dykes

MD₃ dykes are generally thinner and much less weathered than MD₂s. Their thickness is usually limited to 10–20 m and in only one case, the MD₃ crossing the peninsula Igassortoq and forming the top of mountain 560 m, does it attain a thickness of 80 m. They generally trend south-east, but swings to east-west or even north-east are frequent. The contacts are always chilled. As in the MD₂ dykes, the grain size increases from the contacts to centre, a feature limited to the thickest dykes. The

MD₃s also possess the peculiar 'en échelon' structure, described for the MD₂ dykes although less commonly.

MD₃ dykes are sheared by north-south faulting. Sometimes, as in the case of the thin dyke which crosses the whole area from Nunaqarfia they are sheared by south-east fractures. The mineral composition and texture of these dykes is similar to that of the MD₂s.

TD dykes

Only three dykes of this generation have been found in this area. The first dyke, one metre thick, was found east of Nunaqarfia cutting both an MD₂ and an MD₃. The second is a long, thin dyke crossing the western part of the area from the complex of lakes north-west of mountain 880 m to Qíngua. The third is a dyke 10-20 metres thick crossing the rocks of the eastern part of the present area. They have a general south-south-east strike, but swings towards a north-south direction occur. Their contacts are always chilled. Field examination in other areas suggests that TDs are never affected by shearing but in this area, the TD dyke of the eastern peninsula in the inland ice is strongly sheared along the strike east of mountain 920 m. The sheared dyke looks completely transformed and albitisation phenomena occur. This indicates a relatively recent rejuvenation of the north-south fractures. The mineralogy of the TDs differs a little from that of the preceding generations in that biotite is present in much larger amounts. Clinopyroxene is a pale brownish type which is commonly zoned and twinned.

Primary hornblende may be present, as well as some olivine. Plagioclase is often zoned and presents a subophitic texture with pyroxene. Alteration of these minerals is common. The TD dykes are characterised by the presence of vesicles of up to two centimetres in diameter. They are filled with fibrous zeolites which, according to X-ray determinations, belong to the natrolite group.

Lamprophyres

Only two lamprophyres have been found: one is a very thin dyke (four metres thick) which is traceable only for a few hundred metres in the western part of the area, near mountain 880 m, and the other, a little thicker (5-10 m), near mountain 560 m in the peninsula north of Sermilik avangnardleq. Their age relationships are not well defined; the first was not found to cut any other dyke, while the second was found to intersect an MD₃ but not a TD. The first is an irregular east-west dyke while the second has a definite north-east strike.

The lamprophyre near mountain 880 m is a dark green spessartite presenting grain-size inhomogeneities: coarse-grained roundish pebbles are embedded in a finer grained matrix which nevertheless has the same composition. The texture is porphyritic. The mineral assemblage consists of a large predominance of barkevikitic

zoned amphibole and fairly acid plagioclase. The centre of the amphibole phenocrysts is pleochroic with α = pinkish yellow, β = reddish brown, γ = dark brown, while at the periphery, the colours become darker and greener. Transformations into bluish amphibole and chlorite are common. Small amounts of augite-like, pink clinopyroxene are present. Accessory minerals are represented by sphene, apatite and sagenitic rutile which forms a network in the bluish amphibole and chlorite.

The lamprophyre near mountain 560 m is mineralogically different from that described above. It is thin but it exhibits clear zoning in both grain size and mineralogical composition. Near the chilled contacts it consists of an ultramafic assemblage dominated by secondary serpentine after olivine, and pinkish clinopyroxene with minor amounts of biotite and plagioclase. Half-way between the contacts and the centre olivine decreases in abundance though some crystals are still present. The clinopyroxene content remains more or less unchanged, while plagioclase increases. At the centre a fairly high amount of hornblende is associated with clinopyroxene, and biotite, as well as plagioclase, increases slightly. Opaque minerals are common throughout the dyke. Uralitisation of pyroxene occurs. The mineral assemblage just described is found a little north of mountain 560 m, near the intersection with the MD₃. Southwards this dyke disappears under drift in a deep valley and a little farther on it is replaced by a north-south striking green dyke, in which chlorite and feldspar predominate.

STRUCTURE

Introduction

In spite of the structural complexity of the area, the presence of lichen-free surfaces, polished by glacier activity, and the continuity of the outcrops have enabled us to distinguish several structural events on a mesoscopic scale. The interpretation of the mesoscopic structures and the presence of more or less continuous marker horizons, given by the lithotypes of the concordant layers, provide a key to the study of the large scale geometry. The events summarised below have been distinguished by means of their mutual relationships.

Ductile structures:

S₀—original lithological layering

F₁—rootless intrafolial folds

F₂—isoclinal or tight meso- and macroscopic folds

S₁—original foliation

F₃—plastic syn-migmatitic folding

S₂—foliation associated with F₃

F₄—late migmatitic folding

F₅—post-migmatitic folding

Brittle structures:

NE fractures

SE fractures

N-S to SSE fractures.

Ductile Structures

Mesoscopic scale

S₀ denotes the lithological layering which pre-dates any other structure. Normally it coincides with S₁, because of the isoclinal character of the folds affecting S₀. The discordance is evident in the closures of F₁ and F₂ and sometimes on the limbs of F₁ folds (figs 18 and 19). This old layering is assumed to be of pre-metamorphic origin even though in some cases it may be confused with S-surfaces created by an early metamorphic differentiation. The lithological layering seems in some cases to be accentuated by an old metamorphic differentiation. In the concordant

layers and in the inclusions in the gneiss (fig. 18) thin felsic layers occur as S_0 . They are often surrounded by thin hornblendite rims (fig. 18), which are cut by the S_1 foliation. These felsic layers and mafic rims are considered to be the result of an early metamorphic differentiation.

F_1 . The earliest recognisable deformation is represented by scattered relics of intrafolial folds which occur in amphibolite boudins within the gneisses. Their style varies from isoclinal to tight. The limbs may be parallel to or truncated by the gneiss foliation (fig. 18). Their axial surface is parallel to the gneiss foliation and is often marked by axial plane structures. Their fold axis has a variable orientation depending on the orientation of the gneisses containing the folded schlieren. It was not possible to determine whether all these folds belonged to a single pre-migmatitic deformation or whether they represent several deformations. The variations in their style might be thought to favour the second hypothesis.

F_2 . Most of the folds of this phase have been observed in the amphibolite layers on both a mesoscopic and macroscopic scale. Their style is normally isoclinal; very occasionally it is tight. The axial plane of F_2 folds is sometimes marked by foliation but never by migmatisation and is always parallel to the gneiss foliation (see for instance fig. 19). Normally the fold closures are approximately semicircular, occasionally they assume an angular shape. When the closures are semicircular the gneiss foliation changes its direction locally but is not conformable with the amphibolite and thus there is locally a discordance between S_1 of the gneiss and S_0 of the amphibolite. Not uncommonly an amoeboidal segregation pegmatite occurs in the gneisses at the point of closure, as this point was a low pressure area. When the closure is angular, the amphibolite dies out by thinning in the gneisses and no evident discordance can be seen. The trend of the fold axis is quite variable because of the later refolding. Parasitic isoclinal folds have been found on the limbs of the major F_2 folds.

S_1 consists of a planar orientation of minerals which gives a foliation to the rocks. It can be seen within a single bed; in banded or veined rocks it is parallel with the banding or veining (and to the P_1 pegmatites, p. 27). In homogeneous gneisses this foliation is formed by the planar orientation of micas and hornblende crystals. The S_1 foliation is always parallel to the axial plane of F_2 (and F_1) folds. When a compositional banding is seen in the rocks of the concordant layers, the gneiss foliation is parallel with this banding, except for closures of F_2 (and for closures and sometimes limbs of F_1). As F_2 folds are usually isoclinal, S_1 and S_0 merge on the limbs of these folds and only in the hinges does a discordance

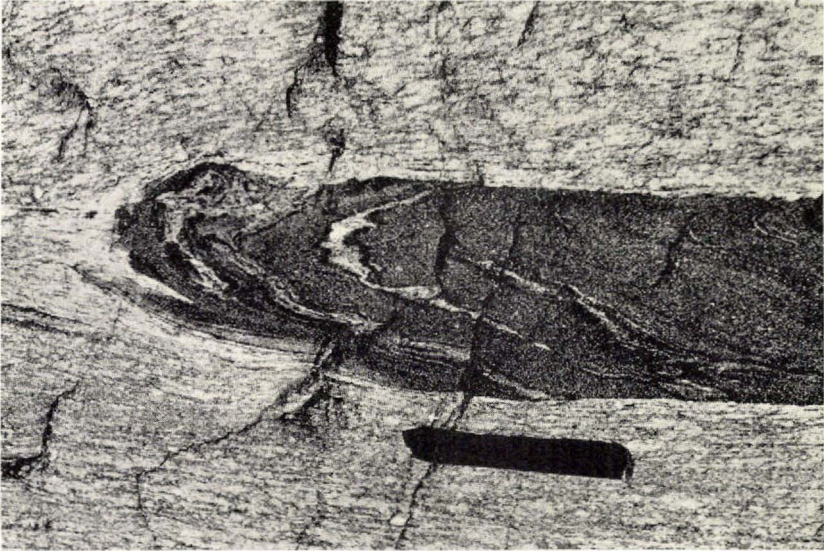


Fig. 18. Rootless intrafolial fold. Note that the felsic layers in the inclusion are surrounded by rims of hornblende which define an S_0 surface cut by S_1 of the gneisses. 2000 m north-west of mountain 880 m.



Fig. 19. Isoclinal F_2 fold of amphibolite. Axial plane parallel to S_1 , 1500 m east-south-east of mountain 760 m.



Fig. 20. Plastic F_3 folding in the gneisses. The axial plane is sometimes curvilinear. At some points limbs are sheared, defining an S_2 . 800 m north-north-east of mountain 880 m.

make the distinction clear. All these features indicate that the S_1 foliation was probably formed by transposition during the F_2 folding. Therefore the P_1 pegmatites, which are always parallel to S_1 and the boudins elongated in the sense of S_1 , were also formed during the F_2 deformation.

F_3 and S_2 . The majority of F_3 folds occur in the small-folded, veined and banded gneisses. They are the commonest mesoscopic folds in the area, and large scale structures are less frequent. Their style is highly plastic (fig. 20). They range from tight, almost isoclinal, to open folds and usually have a similar shape with strongly thickened hinges and slender to sheared limbs. Owing to their peculiar characteristics they fit the description of 'flow' folds (TURNER & WEISS, 1963, p. 481). When layers of different competency were folded together, disharmonic folds were produced. The axial surface is often curvilinear even when not refolded by younger folds, and gives rise locally to conjugate folds. Adjacent curvilinear axial surfaces are not necessarily parallel. The fold axis is marked by lineations which consist of: 1) the orientation of hornblende



Fig. 21. F_1 open fold at the contact between amphibolites and gneisses near lake 650 m.

crystals; 2) the growth of quartz-feldspar porphyroblasts; 3) micro-crenulations of the hinges of parasitic folds. An axial plane foliation, formed by strain-slip cleavage, sometimes occurs. The axial plane structure and the shearing of the limbs may locally create an S_2 foliation which does not seem to be present on a large scale; it occurs on a large scale only in the area 3200 m west-south-west of mountain 880 m in the western part of the area. The orientation of the F_3 folds is variable and is related to the interference with other folds, but a trend of the fold axis toward NE is statistically the most frequent. The axial planes of F_3 folds are associated with a migmatitic neosome which also occurs as thin intrusions, conformable or subconformable with the foliation of the folded

gneisses. The P_2 pegmatites described on p. 27 have partially suffered F_3 deformation (fig. 10) indicating that the formation of these pegmatites is syntectonic with respect to F_3 . These various considerations, i.e. the highly plastic style of F_3 folds and their relationships to the migmatitic neosome, suggest that the F_3 deformation was broadly syn-migmatitic.

F_4 . When unaffected by successive foldings, the folds of this phase have a general orientation NW to NNW or SE to SSE. F_4 folds are found both on a mesoscopic and macroscopic scale. They are normally open to tight folds with a similar style (fig. 24). P_3 pegmatites often occur parallel to axial planes of these folds. Lineations consisting of elongated porphyroblasts of feldspar and quartz emphasise the fold axis direction. A strong lineation of the amphibole described on p. 51 occurs parallel to the fold axis in an F_4 mesoscopic fold, occurring in the rusty schist between lakes 650 m and 745 m in the southern part of the area. This indicates that F_4 too took place during a main phase of metamorphism. The more regular shape of F_4 folds relative to F_3 indicates that the environmental conditions had a lower degree of plasticity.

F_5 folds are open and their profiles approach a concentric form. The fold axis is variable both in trend and in plunge. The trend changes from E-W in the western part of the area to NE or NNE in the eastern and northern parts. The axial plane, marked by a fan-shaped fracturing, is sub-vertical and has an average NE-SW strike. This folding post-dates migmatisation. Its general style and its axial-plane fracturing, indicate that it occurred in relatively brittle conditions with respect to the preceding deformations.

Mesoscopic interference pattern

Some of the commonest interference patterns which have enabled us to recognise the various phases of folding are reported below.

When the axial surfaces of two successive generations are at a high angle to each other and so are the fold axes and the axial planes are roughly perpendicular to the plane containing the fold axes, then a succession of domes and basins is formed (RAMSAY's type 1 interference pattern, 1967, p. 521). This type has been seen in interferences between F_5 and F_4 .

Other simple interference patterns result from the refolding of F_2 by subsequent phases and sometimes from the interference of F_4 with F_3 (Figs 22, 23). This type of structure occurs when the fold axes of the interfering sets are roughly parallel and the axial planes are not (RAMSAY's type 3 interference pattern, 1967, p. 530). When the axial planes and fold plunge directions are at a moderate angle to each other (RAMSAY's type 2 interference pattern, 1967, p. 525) the resulting inter-

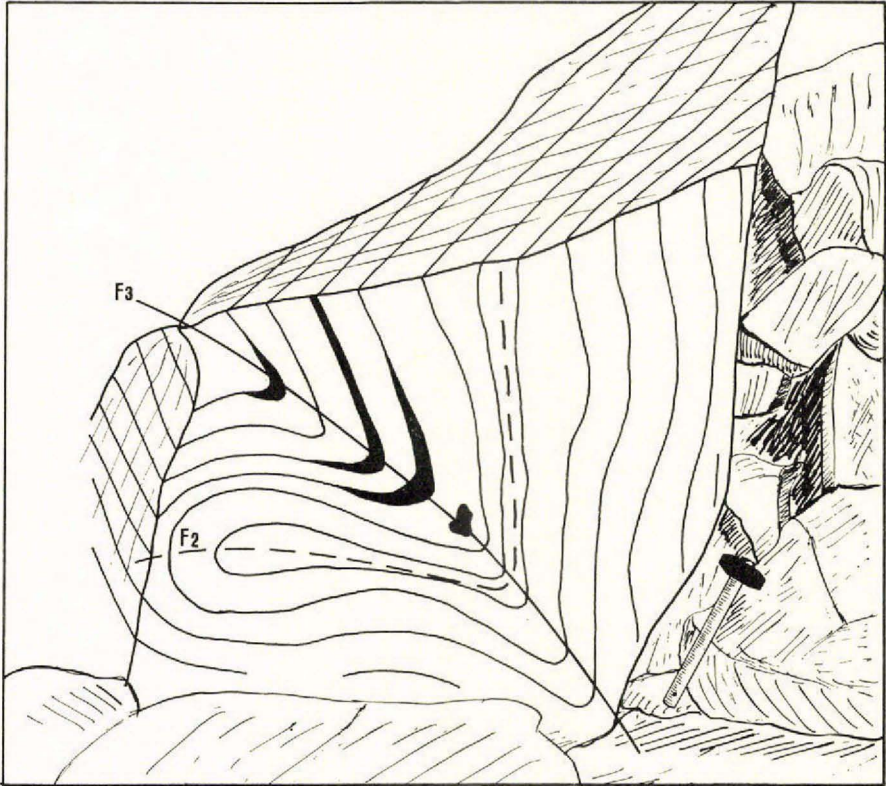


Fig. 22. F_2 refolded by F_3 near the contact between amphibolite and gneisses west of lake 530 m. (Drawn from a photograph).

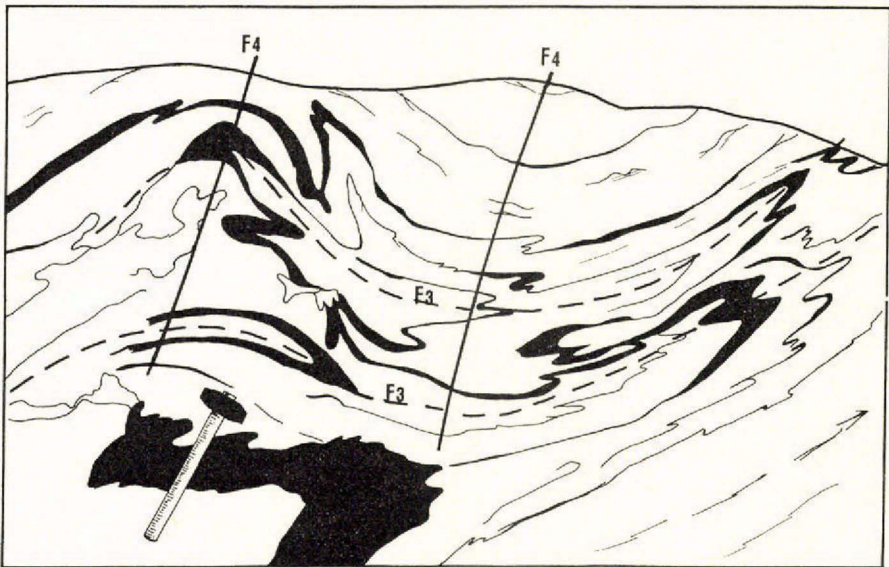


Fig. 23. F_3 refolded by F_4 . 100 m north-east of mountain 933 m. (Drawn from a photograph).

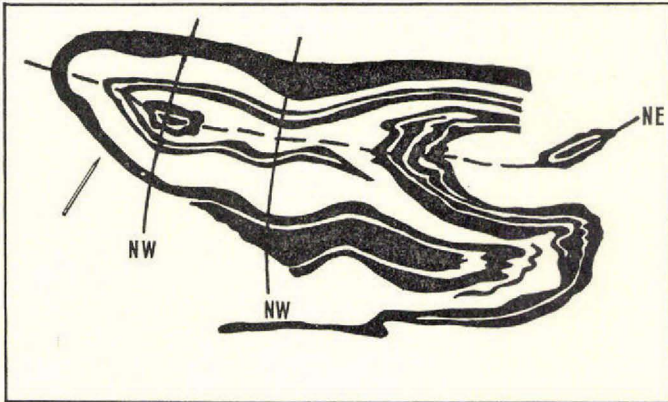


Fig. 24. Interference pattern among three folds. The oldest is an isoclinal folding (F_2), refolded by F_3 , refolded in turn by F_4 . At the contact between amphibolite and gneisses near lake 650 m. (Drawn from a photograph).

ference patterns are much more complicated and the two-dimensional erosion surfaces display mushrooms, crescent- or prong-like figures, which have been found in interferences between F_5 and F_4 or F_3 . The trend of the older hinge can be approximately determined by joining the ends of the prongs (HOLMES & REYNOLDS, 1954). Fig. 24 shows a complicated interference between three folds. The oldest is isoclinal and is clearly refolded in a highly plastic way about a roughly NE axis. It was subsequently refolded by an open fold with a NW axial plane trace (F_2 - F_3 - F_4).

Macroscopic scale

The macroscopic structures are as complicated as the mesoscopic ones. The presence of marker horizons enables one to gain an insight into the general structure. When marker horizons are absent the study is much more problematical although measurements of the systematic changes of the trends of the gneiss foliation help one to understand something of the geometry of the outcrops. The whole area has been divided into 32 sub-areas (plate 8). Normals to foliation planes, minor fold axes and constructed β axes are plotted on an equal area projection, lower hemisphere, from each sub-area (plate 9).

In the following description the area will be divided into an eastern and a western field; this is for simplicity only, because this division does not in fact correspond to any structural boundary, some of the structures of the eastern part continuing in the western part.

Western field

The western field consists of the area limited to the west by the fjord Qagssip kangerdluarssua and to the east by the valley north of

Qíngua. Sub-areas and plots from 1 to 15 (plates 8 & 9) concern this field. In some sub-areas the foliation planes do not form a single great circle, but are spread out. In these cases two or even three great circles have been tentatively traced, but they are of doubtful significance. The constructed β -axis is roughly parallel to the minor fold axes and lineations which have been measured in the field. When they are not parallel, it means either that the β axis is not a real fold axis or, as is commonly the case, that not all the measured axes belong to the same fold generation.

The main structures of the area consist of a succession of antiforms and synforms with almost horizontal fold axis (sometimes plunging towards NE in the north-eastern part of the area. Normally this folding is approximately upright but it is sometimes steeply inclined to the NE. Only the synform passing near mountain 880 m seems to be overturned near lake 620 m (and its axial plane dips to SE), but this cannot be definitely proved. The axial plane is marked by fractures. This fracturing and their general style suggests a probable F_5 age for these folds. The lack of an axial plane migmatisation, as can be seen for instance in the amphibolite synformally folded near lake 670 m, also conforms to the assumption that they are F_5 and not F_3 folds. Apart from the presence of large scale F_4 folds, which occur in the western part of the area and in the garnetiferous gneiss of Nigerdlíp qôrorssua (sub-areas and plots from 1 to 7, plates 8 & 9), an important structure can be seen in the group of amphibolites north-east of lake 530 m. This structure is the result of the interference of three phases of folding which are: 1) an isoclinal F_2 folding, having a roughly horizontal axis and axial plane running along the middle of one of the amphibolites, 2) a tight F_3 folding with NNE plunging axis (the axial surface of this folding is marked by migmatisation), and 3) an F_4 NW open folding, characterised by a swarm of pegmatites along its axial surface, which affects the amphibolites in their south-western part and refolds the F_3 and F_2 axial surfaces.

The amphibolites lying on the southern limb of the synform by mountain 880 m are affected by an old isoclinal folding seen in the amphibolite of the southern of the lakes 615 m. The hinge of the isoclinal folding is strongly thinned. In the field its axial plane is steep. The axial plane trace of the mountain 880 m synform is roughly parallel to that of the F_2 fold.

Eastern field

This field stretches from the valley north of Qíngua as far as the inland ice. In the western part of this field the folding seen in the preceding area and suggested as being of F_5 age, continues with two main structures, the Qíngua antiform (having its NW limb in the preceding field) and the

Aorngo synform, and two less important structures in the northern part: the overturned antiform with SE dipping axial plane and the synform near the glacier (sub-area 17). Sub-areas from 14 to 18, concerning this western part, show NE to NNE trending β axes. Here too, as happened in many sub-areas of the preceding field, some minor fold axes, plot on the projections with a large angle to the β axes, while others lie parallel to it. On the other hand, minor structures of different ages from the main folding are common, and these cause a large spread of the foliation planes when the sub-area considered is large (see, for instance, sub-areas 14 and 16).

The most striking structure characterising the eastern field occurs in its central part and is marked by the long amphibolite horizon which passes north of mountain 993 m. This structure looks like a mushroom closed at the eastern end. The oldest recognisable folding entering this structure is a large scale F_2 isoclinal folding which is particularly evident in the mountain 933 m amphibolite complex, immediately north and west of mountain 933 m. This folding causes clear repetitions in the stratigraphy. As is evident from the map (plate 11), its axial plane is clearly folded by a succession of major F_4 folds which, together with the F_2 folding, are the easier to see at first sight. The major F_4 folds from west to east are:

- 1) An antiform with an almost rectilinear axial plane trace, passing from the south near lake 420 m to the NNW a little west of mountain 933 m. The fold axis generally plunges NNW at angles which vary from sub-area to sub-area (sub-areas 20, 23 and 26). The axis of this antiform probably extends towards lake 460 m, since small, carefully selected sub-areas give NW trending β axes, and minor NW folds are common near lake 460 m. In this case the axial plane appears to be folded and the large antiform immediately west of mountain 933 m dies out southwards.

- 2) A synform having an axial plane trace roughly parallel to the preceding one swinging slightly from NNW to NW. Its fold axis plunges towards the NW near mountain 933 m (sub-areas 24 and 25) and to the SE near lake 650 m. Sub-area 30 refers to this last part and shows that the normal to the foliation planes and minor fold axes plot on a girdle which is probably due to interfering folds. Several minor F_3 folds have been seen in this area.

- 3) An antiform with axial plane trace diverging from the preceding ones. Its fold axis plunges steeply to the NNW near lake 690 m (sub-area 21) and, more gently, to the SSE in the southern part, with a culmination in the area of lake 750 m. Sub-area 31, which refers to the southern part, shows a large spread of data due to the superimposition of folds.

A common characteristic of these NW folds is that they are non-cylindrical. This is evident in the two westernmost F_4 structures, which have clear variations in the plunge of the fold axes, while in the eastern one the variation is smaller.

Other folds belonging to this structure are present in the area of lake 300 m, south of Aorngo. They are a small synform and an antiform with a NE axial surface, probably affecting or affected by other folds, as is indicated by the spread of the foliation planes in their sub-areas (19 and 22). Their axial surface is not traceable with confidence towards the NE although in some sub-areas (27 and 28) a NE plunging β axis is present. These folds exhibit axial plane migmatization, and are therefore F_3 in age.

Minor plastic syn-migmatitic F_3 folds occur all over the area such as the small-folded gneiss areas in the north-eastern and eastern part of this structure.

Towards the glacier the foliation shows some large-scale bucklings defining a NE plunging β axis (sub-areas 29) and believed to be of F_5 age. The description of this structure suggests that its actual shape is the consequence of the interference of several phases of folding.

The following interpretation is proposed. Early F_2 folds were refolded during the F_3 deformation, now recognisable mainly on a mesoscopic scale but also by a few minor large-scale structures. Later on an intense F_4 folding affected the F_3 structures. In the area between mountain 933 m and lake 650 m the F_3 folding was probably represented by an anticline having its axis roughly perpendicular to that of F_4 . This is indicated by the opposing plunges to the north and south of the F_4 axes and by the similarity of these folds with brachiformal structures. The whole picture was later complicated by the F_5 deformation, which caused the bucklings near the glacier. Its effects westwards are doubtful, although F_5 too probably enters the interference pattern, since they occur on a mesoscopic scale.

The structures on the peninsula partly surrounded by the inland ice, east of the area described above, look rather simple. Here the foliation planes have an almost constant NE strike and NW dip. They are thought to form the south-eastern limb of a big synform whose axial plane runs approximately in the area of the rivers bordering the peninsula to the south-west. Unfortunately, the axial zone of this fold is completely hidden, thus it is difficult to establish its relative age. The plot of the normal to foliation planes gives a fairly good great circle girdle and indicates a NE β axis. Possibly, by analogy with what has been seen in the western part of the present area, it represents the last phase of deformation, although the possibility of an F_3 age should not be excluded.

Two other structures are present in the peninsula: an inclined synform, closing near mountain 920 m, and another inclined structured

closing east of lake 680 m. They are tight to isoclinal folds with associated axial plane migmatization. The closure of the fold east of lake 680 m is almost completely hidden by migmatization. These folds do not appear to interfere with other structures, but their tight form, their axial plane migmatization and their general style show them to be of F_3 age.

Brittle Deformations

Not much time has been spent in the field studying the brittle phenomena, but some observations, set out below, may help in further studies. There are three main sets of fractures:

- a) those with a general NE strike, but swings to NNE or ENE are common;
- b) those with a general SE strike, with variations towards a more easterly or southerly strike;
- c) those with a general SSE strike and variations trending N-S or SSW.

All these fractures generally form vertical planes and for the most part do not seem to displace the rocks they cross. A few, minor displacements were found along the dyke crossing the amphibolite synformally folded near lake 670 m, western area, and in the thick MD_2 dyke and amphibolites of the central part of the eastern area.

The first NE fractures are associated with zones of mylonites characterised by large amounts of epidote, albite and chlorite. This fracture probably determined the formation of Qagssip kangerdluarsua and Qíngua fjords. Later shearing of the mylonites, shearing along the MD_2 dykes and the two sets of MD_2 dykes indicate that these fractures were rejuvenated.

The second set of fractures was accompanied by the emplacement of the MD_3 dykes. Its major effects include the formation of the Qagssit fjord, aligned along a fracture, continuing through a zone of rivers and lakes up to the inland ice, and the Nigerdlip qôrorssua valley, whose fracture is traceable up to the easternmost border. These fractures were accompanied by shearing of the rocks, but no large scale displacement is evident. It is possible that vertical movement occurred. The fractures are sometimes accompanied by hydrothermal veins, which mostly consist of almost pure epidote but which sometimes have a more complex composition. For instance, the veins crossing the thick MD_2 dyke near lake 690 m and the other thick MD_2 dyke slightly displaced by a SW fault 1800 m east-south-east of mountain 933 m, are formed by an assemblage of quartz, albite, epidote, sphene, amphibole, chlorite and

some apatite. The MD₃ dykes are sometimes sheared along the strike. This is quite clear in the north-west part of the long, thin MD₃ dyke which runs from Nunaqarfia through the whole area. Therefore the SE fractures have possibly undergone a rejuvenation.

The third set of fractures in the present area is not very important. Nevertheless it again produced shearing and epidotisation. It is worth noting here that the TD dyke of the easternmost peninsula has exceptionally been sheared by a fracture belonging to this set.

Conclusions

The first recognisable event consists of a layering or banding (S₀) which is of pre-metamorphic origin. S-surfaces, which may be confused with S₀, were formed by early metamorphic differentiation. This layering was deformed by ductile flow which formed the now intrafolial folds, of which there might be more than one phase. The first folding (F₂) recognisable on both mesoscopic and a macroscopic scale is isoclinal and caused repetitions of the stratigraphy. The same deformation which produced the isoclinal folding was also responsible for a transposition of the earlier S₀ to a new foliation (S₁) which lies parallel to the axial plane of the isoclinal folds. Metamorphic differentiation (P₁ pegmatites) and boudinage represent other features of this period. This folding is largely obliterated by the subsequent migmatisation and has a relic appearance. The subsequent F₃ folding indicates a highly plastic environment (p. 80) and was syntectonically accompanied by migmatisation. Large scale F₃ structures occur all over the area.

The environmental conditions during the following F₄ phase were characterised by a lower degree of plasticity, as is suggested by the shape of these folds, though the F₄ deformation still has a plastic character. Large scale F₄ folds enter some of the largest structures of the eastern field (p. 86), while they are little represented to the west. In adjacent areas (S. B. JENSEN, private communication) field examination has shown that a significant break, during which sediments were deposited, intervened between the F₃ and F₄ phases.

The F₅ folding took place in relatively brittle conditions, as is shown by the fracturing along the axial plane. The most prominent structures occurring all over the area are thought to be of F₅ age.

Subsequently basic dykes were intruded and fractures formed. These last produced zones of weakness easily eroded by the glacial activity and thus largely influenced the actual topography of the area.

RELATIONSHIPS BETWEEN METAMORPHISM, PETROGENESIS AND STRUCTURE

The correlations thought to exist between metamorphic and structural events are summarised in Table 16.

It has already been stated that the area most probably consisted of a geosynclinal series which at first underwent a period of increasing metamorphism, as shown by a few relic mineral assemblages. This early period of metamorphism, during which an early metamorphic differentiation occurred (p. 78) may possibly be related to the F_1 phase (or phases) of folding, but not enough is known about this period to establish definite relationships.

The effects of the F_2 deformation (transposition of the S_0 to the S_1 gneiss foliation, formation of P_1 pegmatites, boudinage) indicate a possible relationship to the period when migmatisation began, i.e. in a metamorphic grade of the low granulite facies (almandine–cordierite–biotite subfacies, p. 71).

The period of 'quartz (or grano-) dioritisation', where the effects of migmatisation are most marked, is clearly synchronous with the F_3 deformation, as is shown by the relationships between F_3 folds and P_2 pegmatites and by the recrystallisation of hornblende elongated along the F_3 fold axis. Also the increase in the water pressure (p. 71) is in good agreement with the highly plastic style of the F_3 folds. Therefore F_3 must have occurred in the high almandine–amphibolite facies.

Because of its relationships with the P_3 pegmatites (p. 82) the F_4 deformation can be related to the period of microcline porphyroblast formation i.e. with a medium to low amphibolite facies metamorphism. The style of F_4 is less plastic than that of F_3 and this is in agreement with a lower metamorphic grade. The transformation found in a rusty schist with an anorthite–anthophyllite assemblage into a hornblende–plagioclase assemblage, with hornblende aligned along the F_4 fold axis, again indicates that the F_4 deformation occurred with decreasing metamorphic conditions, but within the almandine–amphibole facies.

The F_5 phase does not seem to have been associated with important metamorphism, but some low-grade transformations, quartz mobilisations (with consequent quartz veining) are, however, ascribable to this phase,

Table 16. *Relationships supposed to exist between metamorphic and structural events.*

Metamorphic facies	Petrogenesis	Tectonism	
	intrusion of doleritic dykes	} brittle deformations	
	local retrogression connected with faulting		
metamorphism decreasing	greenschist facies	} F_4 semi-brittle folding.	
	epidote-amphibolite facies		} F_4 folding. P_3 pegmatites parallel to the axial plane
	medium to low almandine-amphibolite facies	} F_3 synmigmatitic folding. Scattered presence of S_1 .	
	high almandine-amphibolite facies (si-al-mu subfacies)		
	migmatisation {		
		P_2 mobilisates	
		quartz (grano-) dioritisation	
		P_1 mobilisates	
	relic assemblages (?anatexis)		F_2 folds. Axial plane structures. Formation of the regional S_1 . Boudinages
metamorphism increasing	?	? early metamorphic differentiation	} F_1 intrafolial folds, including probably more than one phase
	staurolite-almandine subfacies	relic assemblages	
	?	geosynclinal series	} S_0

and its semi-brittle conditions correspond well with a low metamorphic grade. The scattered sericitisation and epidotisation, even of oligoclase, and the chloritisation of the mafics are its most evident effects. The further evolution linked with brittle deformation formed only mylonite zones or local retrogressions associated with laminations and the occurrence of some hydrothermal activity.

Although no absolute age determination has been carried out on the rocks of our area, the metamorphic and tectonic history previously described is considered to be pre-Ketilidian (except for the last swarms of basic dykes, see p. 73).

It is known that the undeformed MD dykes belong to those generations of dykes which in the Ivigtut area, 125 km to the south, were transformed during the Ketilidian deformations. The gneiss complex in the area is therefore pre-Ketilidian and is at least 1800 m.y. but may be even as much as 2500 or 3000 m.y. old, as these ages have been recorded from similar rocks in the Neria and Fiskeneset areas, 80 km to the south and 100 km to the north respectively. (LARSEN, 1966; LARSEN & MØLLER, 1968; LAMBERT & SIMONS, 1969).

ACKNOWLEDGEMENTS

The authors wish to express their gratitude to the Director of Grønlands Geologiske Undersøgelse, mag. scient. K. ELLITSGAARD-RASMUSSEN for his permission to publish this paper, and to cand. mag. S. B. JENSEN, who was the leader of the field parties in the Mellelmygd area.

Thanks are due to Mr. S. B. JENSEN and Mr. T. C. R. PULVERTAFT for their very valuable criticism of the first draft of this paper. Many of their suggestions have been taken into account, but responsibility for the final draft rests with the authors.

It is with pleasure that we extend our thanks to the whole research staff of the 'Istituto di Mineralogia e Petrologia' of Modena University, and in particular to the Director, Professor GLAUCO GOTTARDI, and to Professor BERTOLANI, Dr. SIGHINOLFI and Dr. CAPEDEI for their valuable advice and help.

Mr. S. ENGELSTOFT and Mr. W. THOMSEN, who assisted us during the field work, the helicopter pilots Mr. F. CARDINAUX, Mr. M. BURKHARD and Mr. J. P. FÜLLEMANN, and Mr. L. H. NORRIS who helped with the correction of the English manuscript, are also gratefully acknowledged.

Mrs. M. ALBERTI is thanked for her typing of the manuscript.

Istituto di Mineralogia e Petrologia
Via S. Eufemia 19
41100 Modena
Italia

APPENDIX

Analytical methods of chemical and mineral analyses

The following methods of chemical analyses were used.

Si, Al, Ti were determined by silicate rapid analysis according to the methods of SHAPIRO & BRANNOCK (1956).

Mn, total Fe, Mg, Ca, Na, K were determined by atomic absorption spectroscopy using a Perkin Elmer 303 spectrophotometer. The procedure is described by ALTHAUS (1966).

Fe²⁺ was determined by semi-microanalysis according to MEYROWITZ (1963).

The modal analyses were carried out using a J. S. Swift & Son point counter.

Plagioclase compositions were determined either by means of the universal stage, using the curves published by EMMONS (1959), or by measuring the refractive index by means of an Emmons' stage with monochromatic sodium light and variable temperature.

The optical characters of pyroxenes and amphiboles were determined by means of the universal stage.

Olivine composition was determined by X-ray diffractometry following the method and using the curves published by YODER & SAHAMA (1957).

Sample localities

Maps showing the position of the samples mentioned in the text are available for inspection in the archives of the Geological Survey of Greenland.

REFERENCES

- ALTHAUS, E. 1966: Die Atom-Absorptions-Spektralphotometrie. Ein neues Hilfsmittel zur Mineralanalyse. *Neues Jb. Miner. Mh.*, **1966**, 259–280.
- AOKI, Y. 1961: Biotites in metamorphic rocks. *Jap. J. Geol. Geogr.* **32**, 397–406.
- ATHERTON, M. P. 1965: The chemical significance of isograds. In: PITCHER, W. S. & FLINN, G. W. (edit.) *Controls of metamorphism*. 169–202. Edinburgh: Oliver & Boyd.
- BACKLUND, H. 1953: The granitisation problem. *Estudios geol. Inst. Invest. geol. Lucas Mallada* **17**, 71–112.
- BERTHELSEN, A. 1960: Structural classification of gneisses—as used in team work in SW Greenland. In SØRENSEN, H. (edit.) *Symposium on migmatite nomenclature. Rep. 21st Int. geol. Congr., Norden, 1960*, **26**, 69–71.
- BERTOLANI, M. 1968: La petrografia della Valle Strona, (Alpi occidentali italiane). *Schweiz. miner. petrogr. Mitt.* **48**, 695–732.
- BLACKBURN, W. H. 1968: The spatial extent of chemical equilibrium in some high-grade metamorphic rocks from the Grenville of Southeastern Ontario. *Contr. Miner. Petrol.* **19**, 72–92.
- BOWEN, N. L. & TUTTLE, O. F. 1949: The system MgO–SiO–H₂O. *Bull. geol. Soc. Amer.* **60**, 439.
- BRIDGWATER, D. 1965: Isotopic age determinations from South Greenland and their geological setting. *Bull. Grønlands geol. Unders.* **53**, (also *Meddr Grønland, 1794*), 56 pp.
- BROWN, G. C. & FYFE, W. S. 1970: The production of granitic melts during ultra-metamorphism. *Contr. Miner. Petrol.* **28**, 310–318.
- CAPEDEI, S. 1968: Sulle rocce basiche della formazione Ivrea-Verbanò. 1; Considerazioni petrografiche e petrogenetiche sulla bassa Val Mastallone. *Schweiz. miner. petrogr. Mitt.* **48**, 103–112.
- CHADWICK, B. 1969: Patterns of fracture and dyke intrusion near Frederikshåb, Southwest Greenland. *Tectonophysics* **8**, 247–264.
- DAWES, P. R. 1970: Bedrock geology of the nunataks and semi-nunataks in the Frederikshåbs Isblink area of southern West Greenland. *Rapp. Grønlands geol. Unders.* **29**, 60 pp.
- DEER, W. A., HOWIE, R. A. & ZUSSMAN, J. 1962–1963: *Rock-forming minerals*. 5 vols. London: Longmans.
- DE WAARD, D. 1966: The biotite-cordierite-almandite subfacies of the hornblende-granulite facies. *Can. Miner.* **8**, 481–492.
- EMMONS, R. C. 1959: The universal stage. *Mem. geol. Soc. Amer.* **8**, 204 pp.
- ENGEL, A. E. J. & ENGEL, C. G. 1960: Progressive metamorphism and granitisation of the major paragneiss, northwest Adirondak Mountains. New York, part II. *Bull. geol. Soc. Amer.* **71**, 1–58.
- ESKOLA, P. 1952: On the granulites of Lapland. *Amer. J. Sci.* Bowen vol., 133–189.

- GRANT, J. A. 1968: Partial melting of common rocks as a possible source of cordierite-anthophyllite bearing assemblages. *Amer. J. Sci.* **266**, 908–931.
- GRESENS, R. L. 1967a: Tectonic hydrothermal pegmatites. I. The model. *Contr. Miner. Petrol.* **15**, 345–355.
- 1967b: Tectonic hydrothermal pegmatites. II. An example. *Contr. Miner. Petrol.* **16**, 1–28.
- HENTSCHEL, H. 1943: Die kalksilikatischen Bestandmassen in den Gneisen des Eulengebirges (Schlesien). *Miner. petrogr. Mitt.* **55**, 1–136.
- HINRICHSSEN, TH. 1967: Über den Stabilitätsbereich der Mg–Fe²⁺–Al Mischkristallreihe rhombischer Hornblenden—Teil I: Hydrothermale Untersuchungen der Anthophyllit-Ferro-anthophyllit-Mischkristallreihe. *Neues Jb. Miner. Mh.*, **1967** 257–270.
- HOLMES, A. & REYNOLDS, D. L. 1954: The superposition of Caledonian folds on older fold systems in the Dalradian of Malin Head, Co. Donegal. *Geol. Mag.* **91**, 417–444.
- JAHN, R. H. 1955: The study of pegmatites. *Econ. Geol.* **50**, 1025–1130.
- JAMES, R. S. & HAMILTON, D. L. 1969: Phase relations in the system NaAlSi₃O₈–KAlSi₃O₈–SiO₂ at 1 kilobar water vapour pressure. *Contr. Miner. Petrol.* **21**, 111–141.
- JENSEN, S. B. 1966: Field work in the Frederikshåb area. *Rapp. Grønlands geol. Unders.* **11**, 32–35.
- KALSBECK, F. 1970: The petrography and origin of gneisses, amphibolites and migmatites in the Qasigialik area, South-West Greenland. *Bull. Grønlands geol. Unders.* **83** (also *Meddr Grønland* **189**¹), 70 pp.
- LAL, R. K. & MOORHOUSE, W. W. 1969: Cordierite-gedrite rocks and associated gneisses of Fishtail Lake, Harcourt Township, Ontario. *Can. J. Earth Sci.* **6**, 145–165.
- LAMBERT, R. ST. J. & SIMONS, J. G. 1969: New K/Ar determinations from southern West Greenland. *Rapp. Grønlands geol. Unders.* **19**, 68–71.
- LARSEN, O. 1966: K/Ar determinations from western Greenland. *Rapp. Grønlands geol. Unders.* **11**, 57–67.
- LARSEN, O. & MØLLER, J. 1968: K/Ar age determinations from western Greenland I. Reconnaissance programme. *Rapp. Grønlands geol. Unders.* **15**, 82–86.
- LEAKE, B. E. 1964: The chemical distinction between ortho- and para-amphibolites. *J. Petrology* **5**, 238–254.
- LOSCHI GHITTONI, A. G. 1968: Caratteristiche dell'anfibolo della peridotite di Alpe Campo in valle Strona (Novara). *Rc. Soc. ital. Miner. Petr.* **24**, 271–275.
- MARMO, V. 1967: On granites—a revised study. *Bull. Comm. géol. Finlande* **227**, 1–83.
- MEDARIS, L. G. 1969: Partitioning of Fe²⁺ and Mg²⁺ between coexisting synthetic olivine and orthopyroxene. *Amer. J. Sci.* **267**, 945–968.
- MEHNERT, K. R. 1962: Petrographie und Abfolge der Granitisation im Schwarzwald. III. *Neues Jb. Miner. Abt.* **98**, 208–249.
- 1968: *Migmatites and the origin of granitic rocks*. Amsterdam: Elsevier Publishing Company.
- MEYROWITZ, R. 1963: A semimicro procedure for the determination of ferrous iron in nonrefractory silicate minerals. *Amer. Miner.* **48**, 340–347.
- MÍSAŘ, Z. (in press) Ultramafic rocks in the basement south of Sermilik, Frederikshåb district, South-West Greenland. *Bull. Grønlands geol. Unders.* (also *Meddr Grønland*).
- MIYASHIRO, A. 1953: Calcium-poor garnet in relation to metamorphism. *Geochim. cosmochim. Acta* **4**, 179–208.

- PETTIJOHN, F. J. 1957: *Sedimentary rocks*. (2nd ed.) New York: Harper & Brothers.
- RAMBERG, H. 1952: *The origin of metamorphic and metasomatic rocks*. Univ. Chicago Press.
- 1956: Natural and experimental boudinage and pinch-and-swell structures. *J. Geol.* **63**, 512–526.
- RAMBERG, H. & DEVORE, G. 1951: The distribution of Fe⁺⁺ and Mg⁺⁺ in coexisting olivines and pyroxenes. *J. Geol.* **59**, 193–210.
- RAMSAY, J. G. 1967: *Folding and fracturing of rocks*. London & New York: McGraw-Hill.
- RAST, N. 1965: Nucleation and growth of metamorphic minerals. In: PITCHER, W. S. & FLINN, G. W. (edit.) *Controls of metamorphism*, 73–102, Edinburgh: Oliver & Boyd.
- RIVALENTI, G. 1966: Problema della genesi degli gneiss anfibolici della serie “diortico-kinzigitica” delle Alpi Pennine. *Periodico Miner.* **35**, 933–957.
- 1971: Genetical problems of banded amphibolites in the Frederikshåb district, South West Greenland. *Atti Soc. tosc. Sci. nat.*, **A 77**, 342–357.
- RIVALENTI, G. & SIGHINOLFI, G. P. 1969: Geochemical study of graywackes as a possible starting material of para-amphibolites. *Contr. Miner. Petrol.* **23**, 173–188.
- — 1971: Geochemistry and differentiation phenomena in basic dikes of the Frederikshåb district, South West Greenland. *Atti Soc. tosc. Sci. nat.*, **A 77**, 358–380.
- SHAPIRO, L. & BRANNOCK, W. W. 1956: Rapid analysis of rocks. *Bull. U.S. geol. Surv.* **1036**.
- SHAW, D. M., MOXHAM, R. L., FILBY, R. H. & LAPKOWSKY, W. W. 1962: The petrology and geochemistry of some Grenville skarns—Part I: Geology and petrography. *Can. Miner.* **7**, 420–442.
- SIGHINOLFI, G. P. 1967: Metamorfismo di alto grado: i granati—Part I. *Periodico Miner.* **36**, 485–513.
- 1968: Metamorfismo di alto grado: le biotiti. *Periodico Miner.* **37**, 877–893.
- 1971: Investigations into deep crustal levels: fractionating effects and geochemical trends related to high-grade metamorphism, *Geochim. cosmochim. Acta* **35**, 1005–1021.
- STRECKEISEN, A. L. 1967: Classification and nomenclature of igneous rocks. *Neues Jb. Miner. Abh.* **107**, 144–240.
- SØRENSEN, H. 1953: The ultrabasic rocks at Tovqussaq, West Greenland. A contribution to the peridotite problem. *Bull. Grønlands geol. Unders.* **4** (also *Meddr Grønland* **136**), 86 pp.
- SØRENSEN, P. BRØGGER, 1968: Comment on the zoned calc-silicate lenses in the Frederikshåb area. *Rapp. Grønlands geol. Unders.* **15**, 49–50.
- TRÖGER, E. 1952: *Tabellen zur optischen Bestimmung der gesteinsbildenden Minerale*. Stuttgart: E. Schweizerarbeit, Verlagsbuchhandlung.
- TROMMSDORF, V. & EVANS, B. W. 1969: The stable association enstatite-forsterite-chlorite in the amphibolite facies ultramafics of the Lepontine Alps. *Schweiz. miner. petrogr. Mitt.* **49**, 325–332.
- TURNER, F. J. & VERHOOGEN, J. 1960: *Igneous and metamorphic petrology*. (2nd ed.) New York & London: McGraw-Hill.
- & WEISS, L. E. 1963: *Structural analysis of metamorphic tectonites*. New York & London: McGraw-Hill.
- VUAGNAT, M. 1954: Le rôle des coulées volcaniques sous-marines dans les chaînes des montagnes. *C. r. 19^{me} Congr. géol. int., Alger, 1952*, **15**, 53–59.

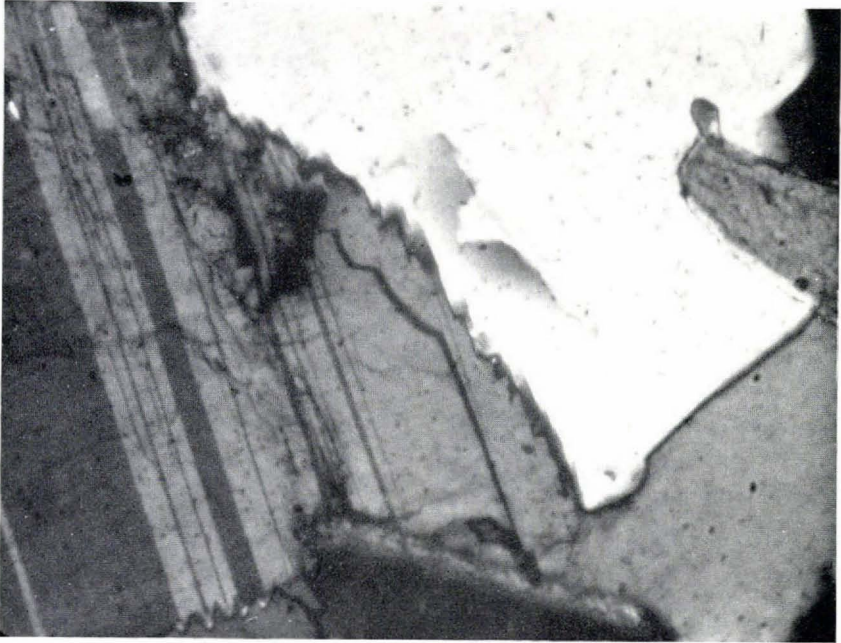
- WALTON, B. J. 1966: The relationship between relic pillow structures and zoned calc-silicate skarns, and the significance of talc balls in gneisses south of Frederikshåb. *Rapp. Grønlands geol. Unders.* **11**, 38–39.
- WATT, W. S. 1969: The coast-parallel dike swarm of southwest Greenland in relation to the opening of the Labrador Sea. *Can. J. Earth Sci.* **6**, 1320–1321.
- WINGHELL, A. N. & WINGHELL, H. 1951: *Elements of optical mineralogy*. Part I, description of minerals. New York: John Wiley & Sons.
- WINKLER, H. G. F. 1965: *Die Genese der metamorphen Gesteine*. Berlin: Springer-Verlag.
- YODER, H. S. & SAHAMA, T. G. 1957: Olivine X-ray determinative curve. *Amer. Miner.* **42**, 475–491.

PLATES

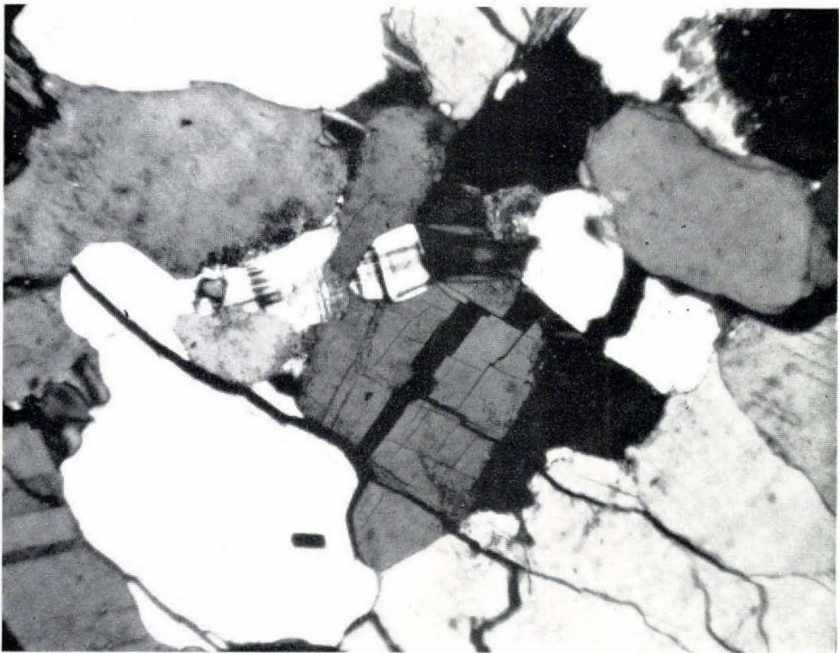
Plate 1

Plate 1 a. Saw-like absorption contacts between quartz and plagioclase (sample 57724),
Crossed nicols, $\times 45$.

Plate 1 b. Substitution of plagioclase by microcline (sample 57873). Crossed nicols,
 $\times 30$.



1 a

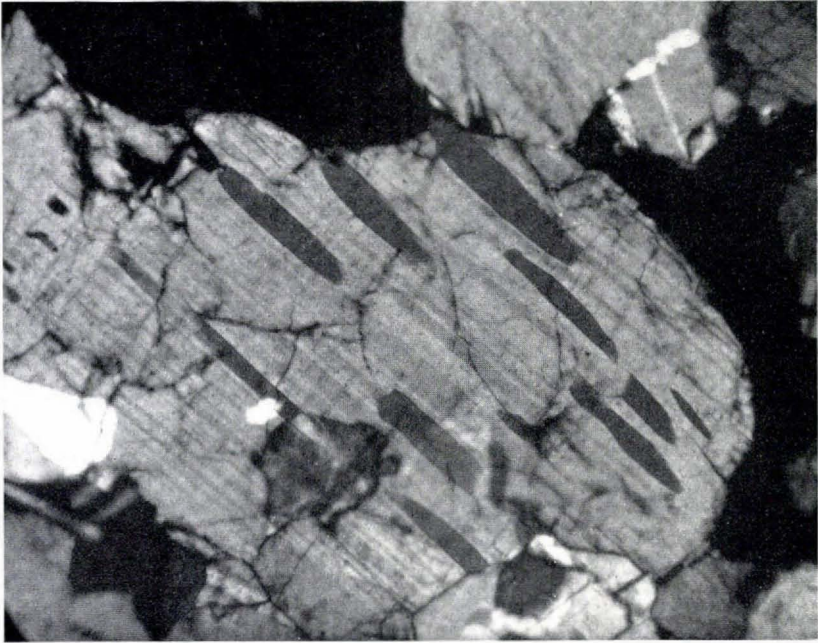


1 b

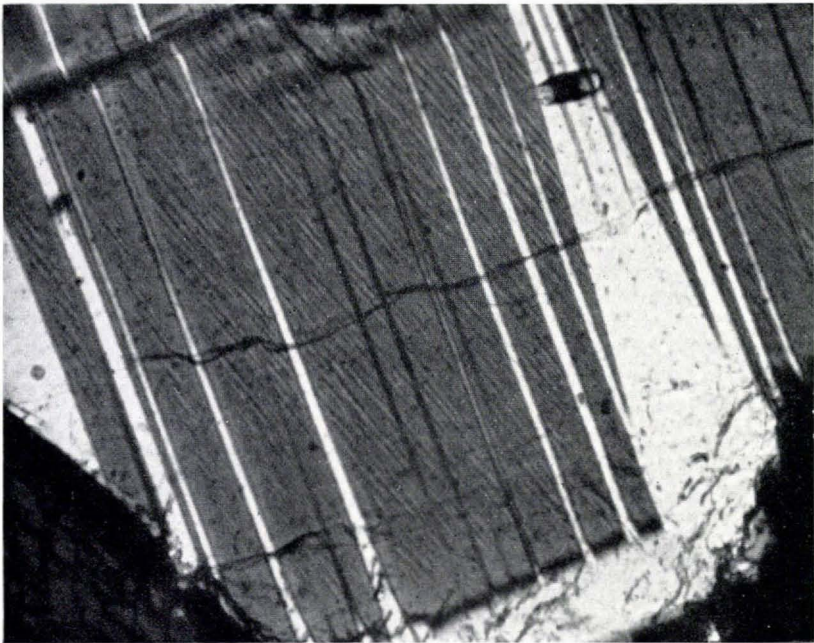
Plate 2

Plate 2 a. Antiperthites in the homogeneous gneiss west of mountain 780 m (sample 57756). Crossed nicols, $\times 45$.

Plate 2 b. Microantiperthites in calcic plagioclase from an amphibolite (sample 73858). Crossed nicols, $\times 120$.



2 a

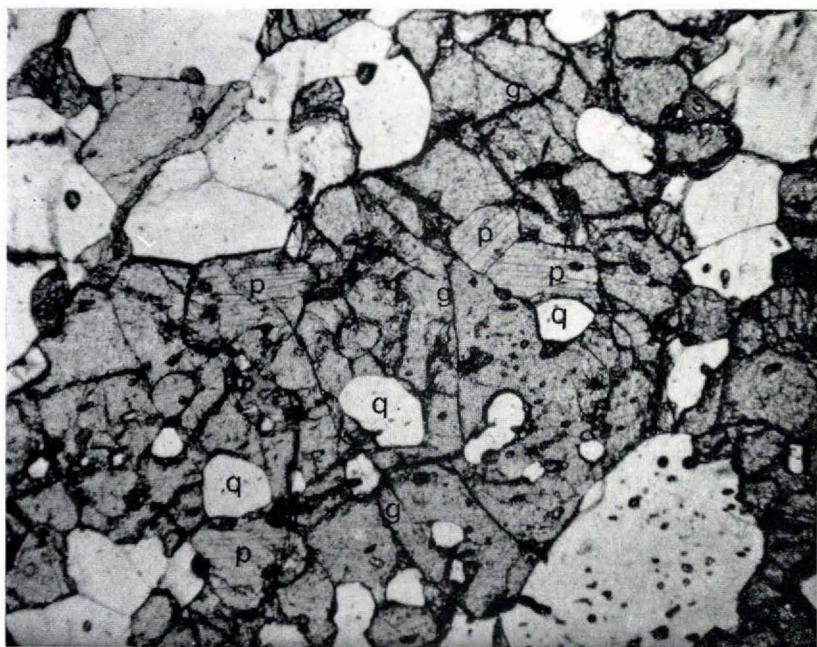


2 b

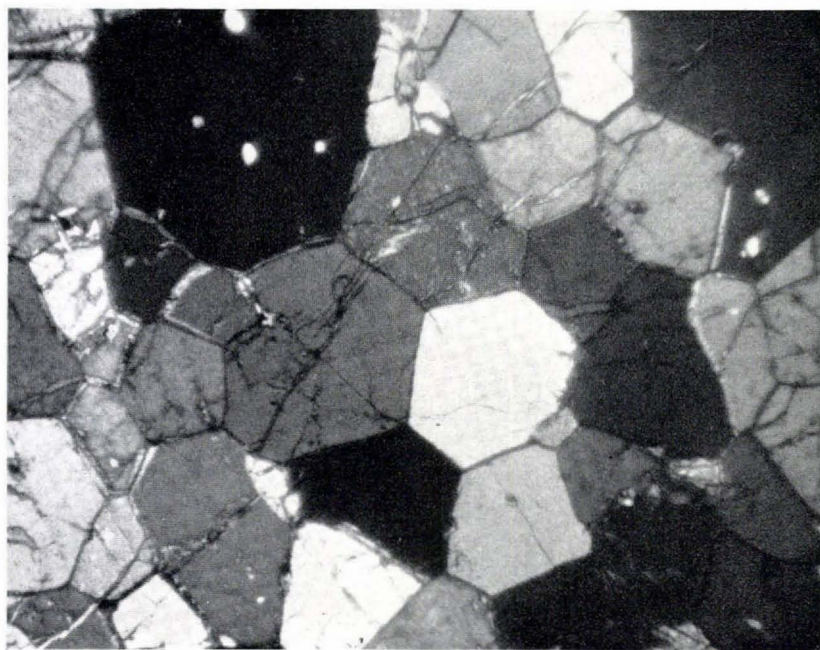
Plate 3

Plate 3a. Garnet (g) replacing clinopyroxene (p). Sphene (s), hornblende (h) and quartz (q) are also formed in the reaction (sample 73819). Plane polarised light, $\times 30$.

Plate 3b. Polygonal equilibrium texture in a peridotite (sample 73566). Crossed nicols, $\times 15$.



3 a



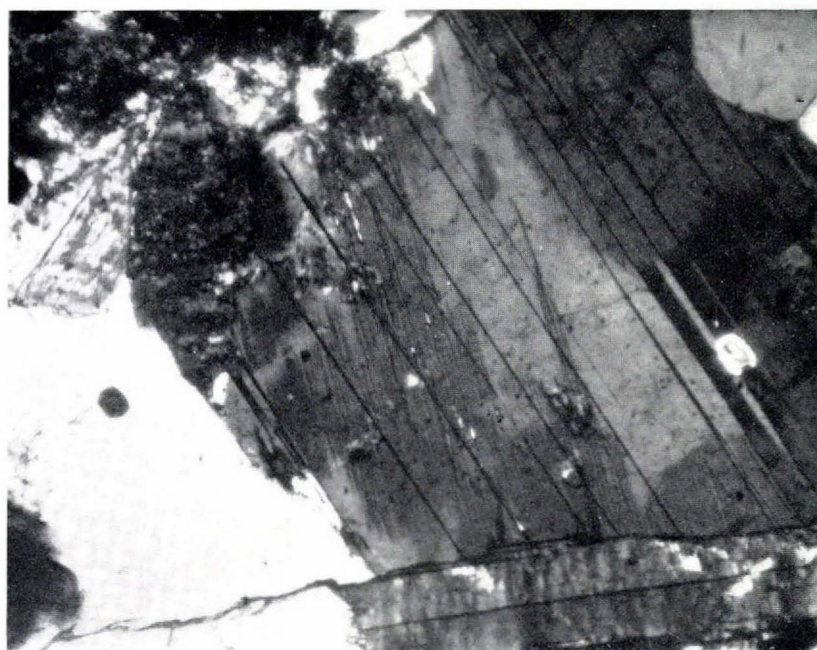
3 b

Plate 4

- Plate 4a. Amphibole partially altered to carbonate in an ultramafic lens (sample 73839). Crossed nicols, $\times 40$.
- Plate 4b. Irregular zoning in a plagioclase from a rusty schist. Some zones are microantiperthitic and have An_{80} , others are not microperthitic and have An_{60} (sample 75898). Crossed nicols, $\times 90$.



4 a

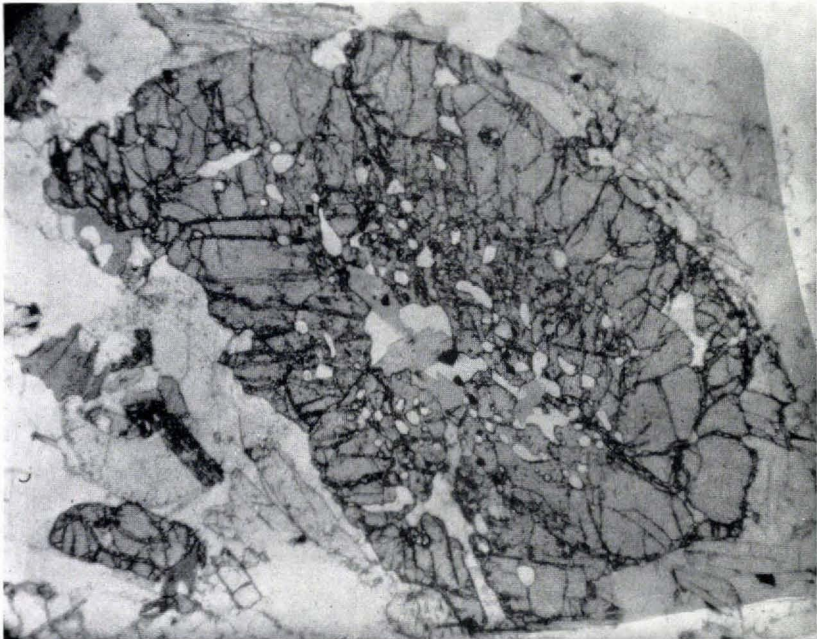


4 b

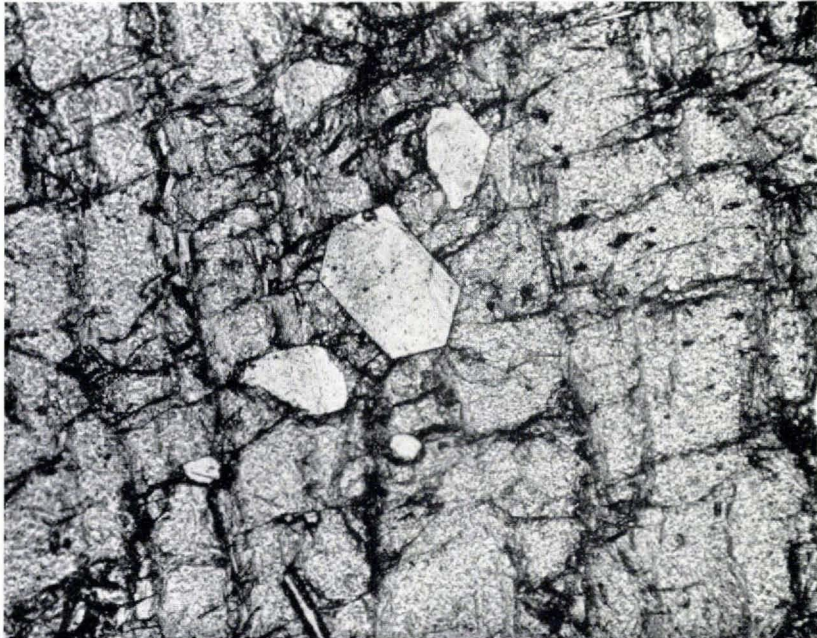
Plate 5

Plate 5 a. Atoll structure in garnet. Note the poikiloblastic centre and the compact outer zone (sample 58884). Plane polarised light, $\times 20$.

Plate 5 b. Pseudo-idioblastic feldspar in garnet (sample 73590). Plane polarised light, $\times 45$.



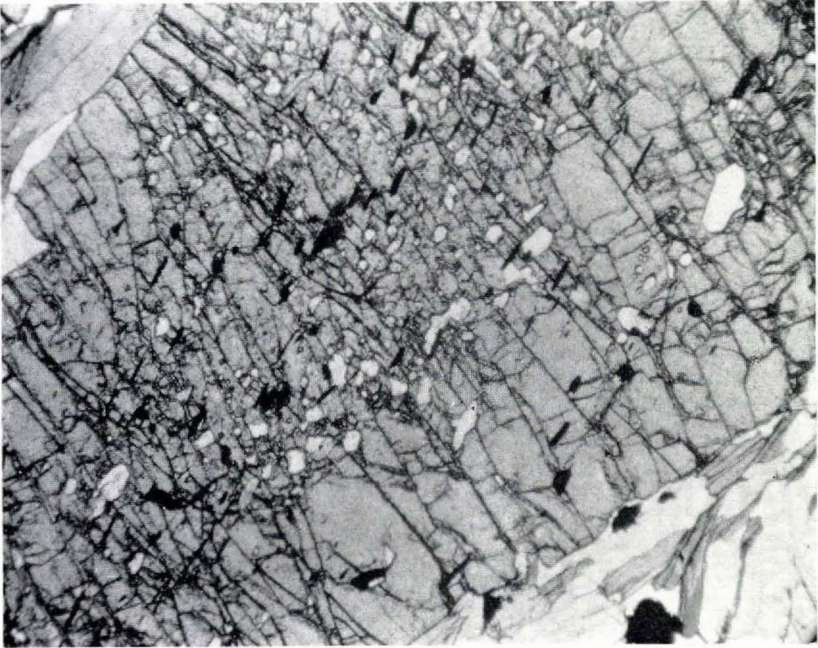
5 a



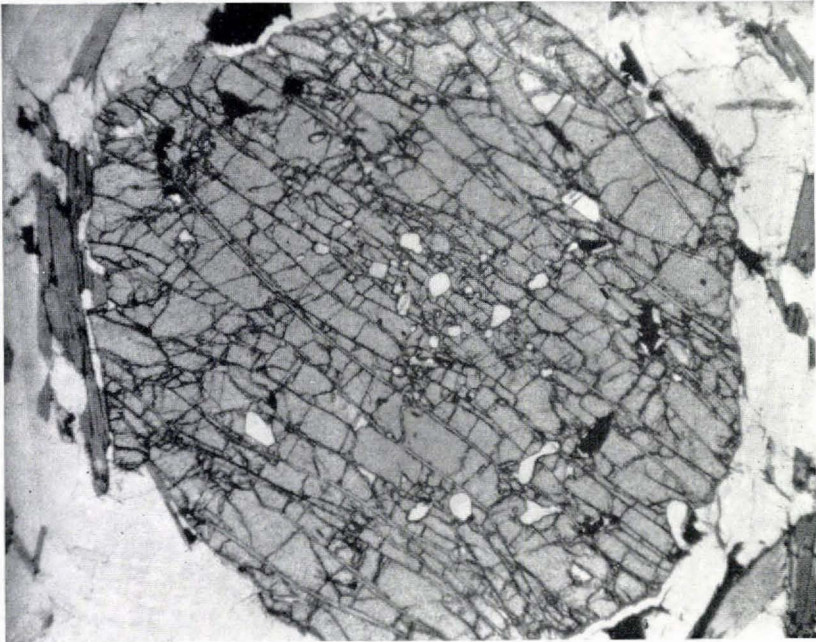
5 b

Plate 6

Plate 6 a & 6 b. Ilmenite in garnet: plate 6a) aligned parallel with the foliation of the rock; plate 6b) with concentric zonal distribution (sample 57820).
Plane polarised light, $\times 30$ and $\times 20$.



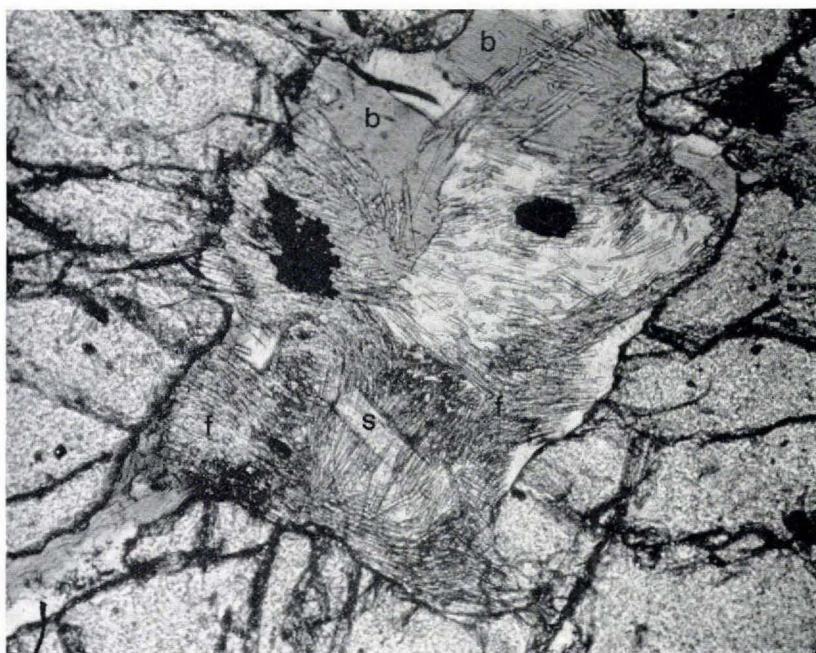
6 a



6 b

Plate 7

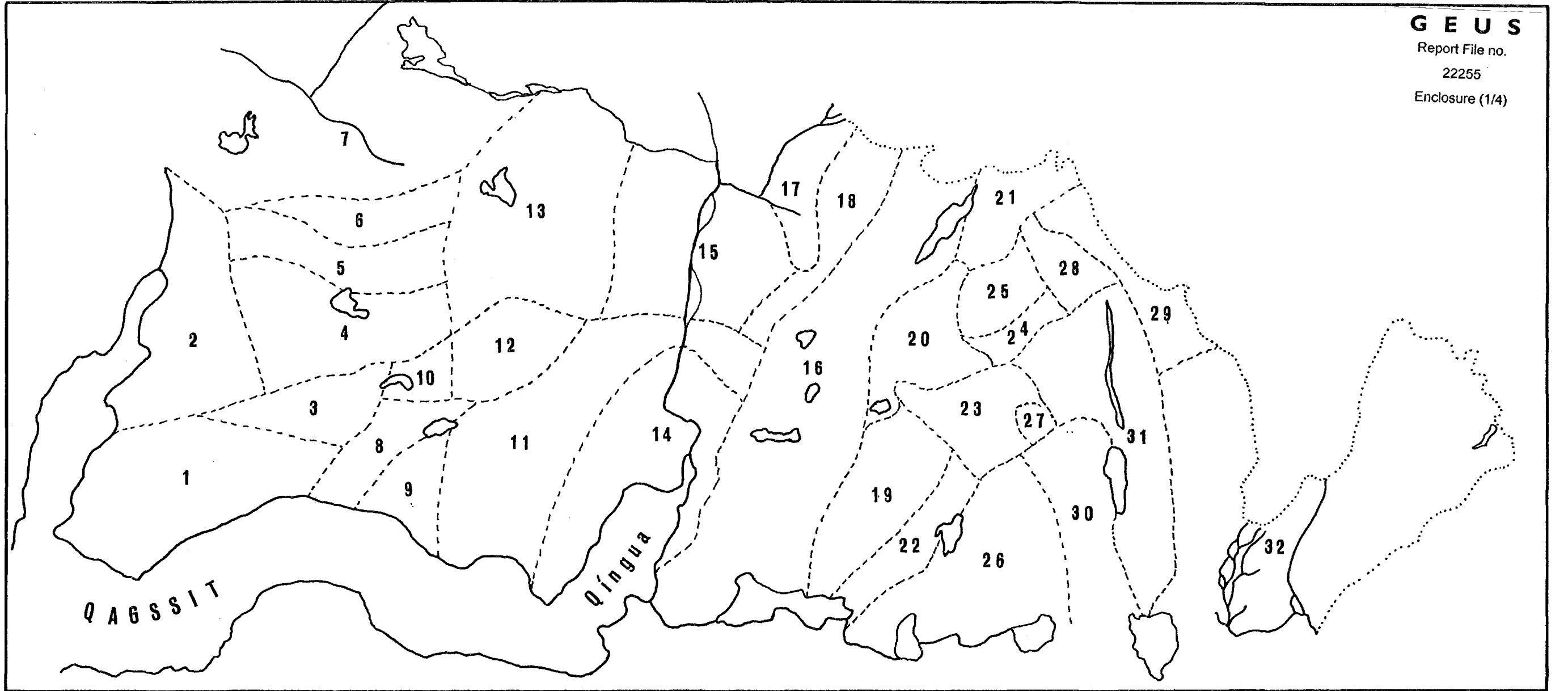
- Plate 7a. Feldspar, sillimanite and fibrolite occurring as the inner part of an atoll garnet. Fibrolite crystallisation post-dates sillimanite. (s = sillimanite, f = fibrolite, b = biotite; sample 73590). Plane polarised light, $\times 45$.
- Plate 7b. Quartz-epidote symplectites at the contact between hornblende and plagioclase in an amphibolite inclusion in the gneisses (sample 57724). Crossed nicols, $\times 20$.



7 a



7 b



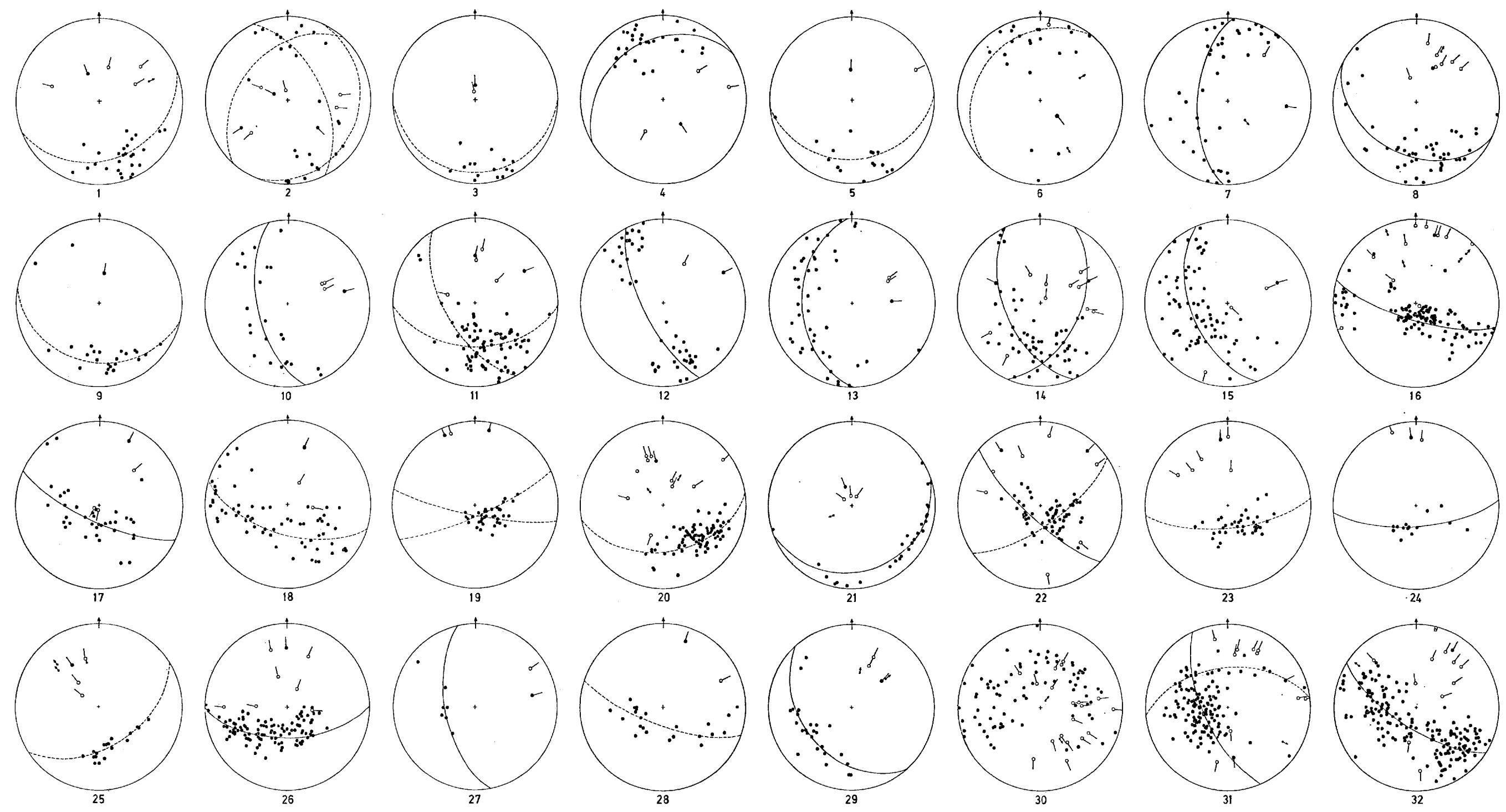
GEUS

Report File no.

22255

Enclosure (1/4)

The sub-area fields into which the area has been divided.








Plots for each sub-area of the normal to foliation planes (dots), lineations (arrows), mesoscopic fold axes (circles with a tail), constructed β axes (dots with a tail).
Lower hemisphere, Lambert's equal-area projection.

GRØNLANDS GEOLOGISKE UNDERSØGELSE
THE GEOLOGICAL SURVEY OF GREENLAND

MEDDELELSER OM GRØNLAND BD. 192, NR. 5 (G. RIVALENTI AND A. ROSSI).

MAP OF THE BASIC DYKES AND FRACTURES

-  MD2 dykes.
The number in parenthesis refers to the sub-generation
-  MD3 dykes
-  TD
-  Lamprophyres
-  Fractures
- 670 Numbers on the dykes are their thickness in metres

